

# Escapement-Based Movements as Positioning Mechanisms: Design and Modelling

THÈSE N° 6851 (2016)

PRÉSENTÉE LE 29 JANVIER 2016

À LA FACULTÉ DES SCIENCES ET TECHNIQUES DE L'INGÉNIEUR  
LABORATOIRE D'ACTIONNEURS INTÉGRÉS  
PROGRAMME DOCTORAL EN SYSTÈMES DE PRODUCTION ET ROBOTIQUE

ÉCOLE POLYTECHNIQUE FÉDÉRALE DE LAUSANNE

POUR L'OBTENTION DU GRADE DE DOCTEUR ÈS SCIENCES

PAR

Romain David BESUCHET

acceptée sur proposition du jury:

Prof. M.-O. Hongler, président du jury  
Prof. Y. Perriard, directeur de thèse  
Prof. B. Dehez, rapporteur  
Dr T. Conus, rapporteur  
Prof. Y. Bellouard, rapporteur



ÉCOLE POLYTECHNIQUE  
FÉDÉRALE DE LAUSANNE

Suisse  
2016



"There is nothing like looking, if you want to find something. You certainly usually find something, if you look, but it is not always quite the something you were after."

***Thorin II Oakenshield**, King under the Mountain*

"You must unlearn what you have learned."

***Yoda**, Grand Master of the Jedi Order*



# Remerciements

Le travail que je présente dans cette thèse n'aurait jamais pu être accompli sans l'aide, l'appui, la présence d'un grand nombre de personnes. Je profite donc de ces quelques lignes pour remercier en premier lieu M. Legrand qui a initié le projet par lequel mon travail a débuté. Je remercie aussi les Prof. Hongler, Bellouard, Dehez et Dr Conus d'avoir accepté de faire partie du jury pour l'examen de cette thèse et de s'être plongé dans mon travail.

Je remercie également tout particulièrement le Prof. Yves Perriard, qui m'a fait confiance dès le début et qui m'a guidé tout au long de ces années de doctorat, tout en me laissant beaucoup d'autonomie. Je tiens aussi à le remercier pour l'atmosphère qu'il arrive à créer dans son laboratoire. Laboratoire qui, d'ailleurs, ne saurait fonctionner correctement sans ses cadres, toujours prêts à échanger des idées, donner des coups de main, relire rapports et articles. Je remercie ainsi très chaleureusement Christian d'avoir partagé son expertise en conversion électromécanique, Paolo pour son incroyable disponibilité et son aide pour les réalisations de toutes sortes, Yoan pour ses conseils tant en rédaction qu'en recherche, Mika de m'avoir suivi au début de mon travail, ainsi que Magda et Myriam pour leur efficacité.

Je remercie aussi bien évidemment tous mes collègues avec qui j'ai passé des moments incroyables, au labo et en dehors. En particulier, je remercie ShiDan, Tophe et Nico qui ont partagé mon bureau, mais aussi tous les autres : Joël, Greg, Pascal, Omar, Chris, Daniel, Jasha, Xinchang, Florian, Cécile, Jonathan et Jiantao. C'était bonnard !

Un tout grand merci aussi à toutes les personnes d'autres laboratoires, des ateliers mécaniques ou de structures externes qui ont participé par leur expertise à ce travail.

Durant un travail de cette envergure, il est aussi important de pouvoir se changer les idées, et pour cela je remercie mes amis de tous les horizons. Finalement, je veux remercier mes parents, qui ont absolument toujours été là pour moi, ma femme, Mei, qui m'a soutenu sans relâche, et toute ma famille.

*Neuchâtel, janvier 2016*

Romain



# Abstract

This work has been triggered by an industrial project targeting the design of a mechatronic injector for the medical field. Injections are usually performed using a syringe, a quite clumsy tool that transforms the injection task in a positioning one. The quality of injections can be enhanced by using devices that help control the injected dose, or the injection rate, but usually at the cost of a slower operation, a reduced manoeuvrability, or a short battery life for electrically-powered devices. The idea was therefore to provide a cordless miniaturised injector capable of managing the dosage as well as injection rate according to the user's desires, with the constraint that it should have a long battery life. This is why escapement-based movements are investigated in this work. Such stepper movements, where a regulator controls the speed at which a stock of mechanical energy is emptied, have been used for centuries in clockwork. Purely mechanical devices, the regulators are designed to work at a given frequency, with the stability of said frequency as the main objective. For the discussed application, the use of an electronic regulator permits variable injection rates and simplifies dosage control.

Being mostly used in clockwork, escapement-based movements are hardly mentioned, let alone studied, outside this field in the literature. This research is aimed at filling this void to provide engineers with the basics for the design of escapement-based movements, using Pahl & Beitz's design methodology. First of all, a general structure of such movements is proposed. Using functional analysis, a canvas for the requirements specification of a movement is given. To ensure an efficient and fast evaluation of the quality of a solution at any stage of the development, modelling and design tools are suggested.

The industrial project is then used as a case study that exemplifies the concepts introduced. The requirements, a selected functioning principle, and the main technical solutions are described. The application of the modelling tools is done in two parts, representing two sub-systems designed concurrently but separately: the purely mechanical part of the movement that includes the escapement, and the mechatronic regulator.

## Remerciements

---

The dynamic and energetic performances of both subsystems are modelled, using relevant techniques. Analytical models characterise the mechanical part of the system, using advantageously the stepper nature of the system. Because they are analytical, the models require very limited computational resources and are thus extremely convenient design tools. They also permit a stochastic study of the influence of manufacturing tolerances on said performance.

Regulators, in particular electronically-controlled ones, are then discussed. An optimisation strategy for highly constrained problems is proposed. It consists in first optimising a set of input parameters towards acceptable values for the constraints. Once one or more sets of parameters respecting the constraints are found, these sets are used as initial points for the actual optimisation of the objectives. The efficacy of this strategy is demonstrated by an example.

Finally, a prototype of the devised escapement-based movement is presented. It is used to establish the validity of the developed models, but also demonstrate the capabilities of the retained functioning principle.

*Keywords: Design methodology, Escapement-based movements, Functional analysis, Linear actuators, Mechatronic design, Modelling, Multi-objective optimisation, Tolerance analysis*



# Résumé

Ce travail de thèse a été effectué sur la base d'un projet industriel visant la conception d'un injecteur mécatronique pour application dans le domaine médical. Dans la plus part des cas, les injections sont faites au moyen d'une seringue, un instrument relativement grossier qui transforme la tâche de dosage en une tâche de positionnement. Il existe des outils permettant d'améliorer la qualité d'injection en contrôlant le dosage ou la vitesse d'injection, mais généralement au prix d'une opération plus lente, une maniabilité réduite ou une faible autonomie dans le cas d'injecteurs électriques. L'objectif industriel était donc de concevoir un injecteur sans fil de petite taille permettant de contrôler le dosage et la vitesse d'injection selon les désirs de l'utilisateur, tout en visant une grande autonomie électrique. C'est pour cet objectif d'autonomie que les mouvements à échappement ont été étudiés dans cette thèse. Ces systèmes pas à pas, dont la vitesse d'avance est contrôlée par un régulateur, sont utilisés dans l'horlogerie depuis de siècles. Purement mécanique, le régulateur est conçu pour fonctionner à une fréquence donnée dont la stabilité est l'objectif principal. Pour l'application médicale mentionnée, un régulateur électronique est envisagé pour permettre la variation de la vitesse d'injection et simplifier le contrôle du dosage.

Étant un mécanisme principalement horloger, le mouvement à échappement est rarement mentionné ailleurs que dans la littérature relative à cet art. Le but de cette étude est de parer à cela et de fournir aux ingénieurs une base pour la conception de mouvements à échappement, en utilisant la méthodologie de conception prônée par Pahl et Beitz. Dans un premier temps, la structure générale d'un mouvement à échappement est définie. L'analyse fonctionnelle de cette structure est utilisée afin de développer un cadre pour l'établissement du cahier des charges pour un mouvement. En outre, pour assurer une évaluation rapide et efficace de la qualité d'une solution à n'importe quelle étape du développement, des outils de modélisation sont proposés.

Dès cette étape, le projet industriel est utilisé comme étude de cas pour démontrer l'application des concepts introduits. Le cahier des charges, un principe de fonctionnement et les principales solutions techniques pour celui-ci sont décrits. L'application des outils de

## Remerciements

---

modélisation est faite en deux parties distinctes, correspondant à deux sous-systèmes conçus en parallèle mais séparément : la partie purement mécanique du mouvement incluant l'échappement, et le régulateur mécatronique.

Les performances dynamiques et énergétiques de chaque sous-système sont modélisées avec des méthodes appropriées. La partie mécanique est principalement modélisée analytiquement en utilisant avantageusement la nature pas à pas du système. Puisqu'ils sont analytiques, ces modèles nécessitent une faible puissance de calcul et sont donc des outils de conception très pratiques. Ils permettent aussi une étude stochastique de l'influence des tolérances d'usinage sur les performances du mécanisme.

Les régulateurs, en particulier électroniques, sont ensuite discutés. Une stratégie d'optimisation pour les problèmes fortement contraints est proposée. Elle consiste en une pré-optimisation des paramètres d'entrée de manière à ce que le système respecte les contraintes. Lorsque l'un ou plusieurs ensembles de paramètres valides sont obtenus, ceux-ci sont utilisés comme points de départ pour l'optimisation du système en regard des véritables objectifs. L'efficacité de cette stratégie est démontrée par des exemples.

Finalement, un prototype du mouvement à échappement conçu est présenté. Il permet de valider les modèles mais aussi de démontrer les capacités du principe de fonctionnement sélectionné.

Mots clés : *Actionneurs linéaires, Analyse de tolérance, Analyse fonctionnelle, Conception mécatronique, Méthode de conception, Mouvements à échappement, Optimisation multiobjectif*

# Contents

<b>Remerciements</b>	<b>v</b>
<b>Abstract (English/Français)</b>	<b>vii</b>
<b>1 Introduction</b>	<b>1</b>
1.1 Medical applications of dosage . . . . .	2
1.2 Tasks of the addressed injector . . . . .	2
1.3 Injectors — a brief history and the state of the art . . . . .	3
1.3.1 Passive injectors . . . . .	4
1.3.2 Motorised injectors . . . . .	5
1.3.3 A hybrid solution . . . . .	7
1.4 Field of research . . . . .	9
1.5 An introduction to escapement-based movements . . . . .	9
1.6 Contents of the thesis . . . . .	12
<b>2 Elements of Design Methodology for Escapement-Based Movements</b>	<b>15</b>
2.1 General design methodology . . . . .	16
2.2 Definition of an escapement-based movement . . . . .	18
2.3 Functional analysis and functional requirements . . . . .	21
2.3.1 Movement . . . . .	22
2.3.2 Sub-functions . . . . .	23
2.4 Evaluation and design tools . . . . .	25
2.4.1 Strategy for efficiency modelling . . . . .	26
2.4.2 Dynamic modelling of a stepper system . . . . .	28
2.5 Conclusion . . . . .	29
<b>3 Conceptual Design of a Linear Movement</b>	<b>31</b>
3.1 Case study: a linear escapement . . . . .	32
3.2 Functioning principle . . . . .	34
3.2.1 Studied movement . . . . .	36
3.2.2 Principles for efficacy . . . . .	37
	xi

## Contents

---

3.3	Transmission & escapement . . . . .	38
3.3.1	Functional requirements . . . . .	38
3.3.2	Teeth . . . . .	38
3.3.3	Leaf spring stage and recoil spring . . . . .	40
3.3.4	Release mechanism . . . . .	42
3.4	Conclusion . . . . .	42
<b>4</b>	<b>Modelling of the Mechanical Performance of a Movement</b>	<b>43</b>
4.1	Dynamic performance . . . . .	44
4.1.1	Methodology . . . . .	44
4.1.2	Application to the linear movement . . . . .	44
4.2	Energetic performance . . . . .	50
4.2.1	Methodology . . . . .	50
4.2.2	Application to the linear movement . . . . .	50
4.2.3	Conclusion . . . . .	60
4.3	In-depth study of the overall performance . . . . .	60
4.3.1	Selected values of the parameters . . . . .	60
4.3.2	Sensitivity analysis . . . . .	62
4.4	Conclusion . . . . .	70
<b>5</b>	<b>Electronically-Controlled Movements</b>	<b>71</b>
5.1	Use of actuators in escapement-based movements . . . . .	72
5.2	Case study: regulating organ for a linear escapement . . . . .	74
5.3	Model of the efficiency and mechanical performance . . . . .	76
5.3.1	Electric model . . . . .	78
5.3.2	Mechanical model . . . . .	82
5.3.3	Global model – Addition of the magnetic model . . . . .	83
5.3.4	Conclusion . . . . .	86
5.4	Multi-objective optimisation . . . . .	86
5.4.1	Optimisation strategy for highly constrained problems . . . . .	87
5.4.2	Implementation . . . . .	88
5.4.3	Discussion . . . . .	93
5.4.4	Optimisation for the studied movement . . . . .	98
5.5	Conclusion . . . . .	100
<b>6</b>	<b>Prototypes &amp; Experiments</b>	<b>101</b>
6.1	Regulating organ – a miniature linear actuator . . . . .	102
6.1.1	Structure and parameters . . . . .	102
6.1.2	Characterisation . . . . .	102
6.1.3	Steady state performance . . . . .	102

6.1.4	Dynamic performance . . . . .	105
6.1.5	Conclusion . . . . .	108
6.2	An electronically-controlled linear movement . . . . .	109
6.2.1	Dynamic performance . . . . .	111
6.2.2	Energetic performance . . . . .	115
6.2.3	Discussion . . . . .	118
6.3	Conclusion . . . . .	119
<b>7</b>	<b>Conclusion</b>	<b>121</b>
7.1	Original contributions . . . . .	122
7.2	Outlook . . . . .	124
<b>A</b>	<b>Alternative functional principles and solutions</b>	<b>127</b>
A.1	Alternative working principles . . . . .	127
A.1.1	Movements ideas . . . . .	130
A.1.2	Conclusion . . . . .	132
A.2	Alternative solutions . . . . .	134
<b>B</b>	<b>Collision-Based Energy Transmission</b>	<b>137</b>
B.1	Modelling . . . . .	138
B.1.1	Single Collision . . . . .	138
B.1.2	Series of Collisions . . . . .	139
B.1.3	Infinite Series of Collisions . . . . .	142
B.1.4	Efficiency of Energy Transmission . . . . .	145
B.2	Conclusion . . . . .	146
<b>C</b>	<b>Estimated Performance of Marshall and Rolfe's Design</b>	<b>147</b>
C.1	Mechanical performance . . . . .	147
C.1.1	Dynamic performance . . . . .	149
C.1.2	Energetic performance . . . . .	149
C.2	Regulating organ . . . . .	150
C.3	Discussion . . . . .	151
	<b>Nomenclature</b>	<b>153</b>
	<b>Bibliography</b>	<b>161</b>
	<b>Curriculum Vitae</b>	<b>167</b>



# 1 Introduction

Escapement-based movements are stepper mechanisms historically associated with clockwork, and rightly so since this industry has been using, developing and reinventing such mechanisms for centuries in order to create innovative timepieces to fulfil ever changing requirements. The escapement, central part of the movement and responsible for the staccato motion of the hands, has extremely peculiar and interesting energy distribution features.

The work achieved in this thesis has been done as part of the development of a medical device. Among other objectives, this dosage device should have a very low electrical energy consumption. This introduction therefore starts with the description of the expected behaviour of the device. After a review of existing devices, the field of research and its targets are defined. Then, the reader will be introduced to the concept of escapement, getting an insight on existing mechanisms, before taking a step back and generalising the concept. From there on, the reader will be invited to think outside the box — or outside the clock — on the way to new applications for escapements. . .

### 1.1 Medical applications of dosage

Dosing is the act of measuring, preparing and delivering a quantity of product. For example, the preparation of a two components adhesive requires a precise amount of each component in order to produce the expected mixture. Similar examples can be found in cooking, where the amount of salt has to be controlled more or less accurately. In the medical field, this notion of dosage is important at different levels. When administering medicine to treat a disease, an error of dosage can make the treatment inefficient and worse, an overdose can be lethal. The accuracy of dosage is also an obvious concern when administering expensive products. An extremely wide variety of products are injected for numerous applications.

In the medical field, the preferred tool for the dosage of fluids is the syringe. A typical syringe (Fig. 1.1) is composed of two main mechanical sets: the barrel and the plunger. The barrel, which contains the product, is nowadays mostly made of plastic, although it might also be made of glass. The needle, made of metal, is attached to it. The fingers rest on the opposite side of the barrel are used for ergonomics. When the user applies pressure on the thumb rest, the plunger pushes the fluid out of the barrel. The plunger tip, made of elastomer, constitutes the interface between the barrel and the plunger. It acts as a joint to ensure that the fluid is expelled from the barrel through the needle and does not leak in the direction of the plunger.

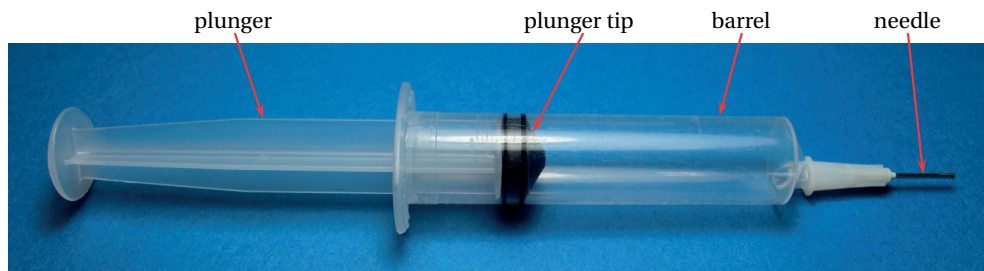


Figure 1.1: Image of a typical plastic syringe.

Syringes vary on most aspects: size, materials, ergonomics, quality, stiffness, etc. Although many syringes are multi-purpose, some are particularly adapted to specific applications. For the user, the choice of a syringe is therefore dependent on the conditions of the injection as well as the product. By design, a syringe is a rather clumsy tool when used to inject only part of its content and dosage can be inaccurate because the control is done visually.

### 1.2 Tasks of the addressed injector

The main objective of the injector is to provide the user with a solution to perform usually complicated and tiring injections more easily, and most importantly effortlessly. To do so,



### 1.3. Injectors — a brief history and the state of the art

---

the injector has to be highly manoeuvrable, that is to say small, light and well balanced. As the presence of a power cord impedes manoeuvrability, the target device has to be cordless. Regarding performance itself, the injector has to provide a given force over a given linear stroke, in a single direction. It is essential for the user that using the injector does not slow the operation down compared to working traditionally by hand. The injection can consist in just a drop (*drop mode*) or a larger volume (*flow mode*, Fig. 1.2) delivered at various speeds.

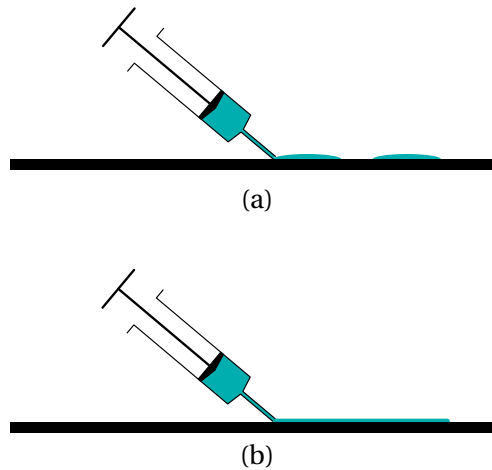


Figure 1.2: Examples of drop (a) and flow mode (b) injections.

The challenges of the design is the numerous conflicting requirements. On the one hand, the mechanism is required to have a good accuracy to deliver small amounts of liquid, but on the other hand, it has to deliver doses rather quickly. The conflict between speed and resolution is illustrated simply: writing a sentence with very small characters takes more time than writing in a normal size. Also, a strong thrust force is necessary but the size of the device should be as small as possible, whereas material resistance indicates the opposite. To make matters worse, the device has to be cordless and yet offer a long battery life (if electrical energy is necessary). The developed solution should therefore provide a satisfying trade-off between all of the above.

The analysis of the state of the art provides interesting information and ideas. The historical evolution of injectors can also be a source of inspiration.

### 1.3 Injectors — a brief history and the state of the art

All the injectors discussed here work on the same principle as a syringe, namely a plunger mounted with a sealing joint pushing the fluid out of a barrel. Slightly different injection principles exist, such as the application of pressure on an elastic tube containing the fluid

## Chapter 1. Introduction

---

(peristaltic pump [All81]), or an impeller (a propeller used to drag fluid rather than propel a submarine [MBC<sup>+</sup> 10]). They will not be analysed because of the device devised has to be compatible with commercial syringes.

### 1.3.1 Passive injectors

The early traces of automatic injectors appear in 1950. In [Tra50], Gerald O. Transue patented the idea of a device designed to house a loaded syringe, and equipped with a spring. When a specific button is pressed, the spring is released and actuates the plunger of the syringe, thus ejecting its content. Fig. 1.3 shows an example of the injector. The key points of the design are that the body is made of two parts that can slide against one another and that they are connected by a spring (24). On the drawing, a syringe (11) is placed inside the device.

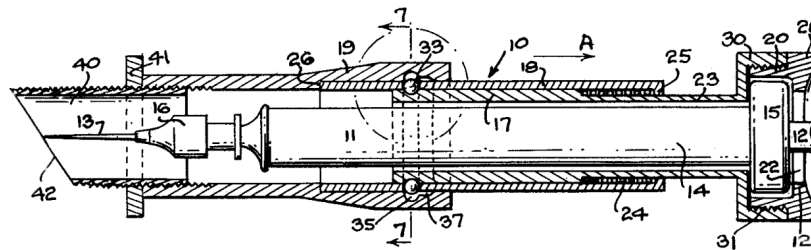


Figure 1.3: An automatic injector as seen by Transue [Tra50].

Automatic injectors then evolved to become extremely popular today, as can be seen by examining the number of different models available on the market. The most widely spread injectors are probably insulin pens used by diabetic patients in case of hyperglycaemia. Typical insulin pens require the user to load an insulin cartridge in the injector. The dose is then selected thanks to a mechanical dial. The user then injects the dose by pushing a button. A spring loaded beforehand pushes on the plunger to expel the product out of the syringe. The functioning is therefore extremely similar to that of Transue's device. With time, enhancements have been added to facilitate the process as well as the tracking of the doses taken during a certain period of time.

More recently the *Restylane Injector* (Fig. 1.4) proposed an interesting principle to control dosage. Before the injection, the practitioner has to spin the part at the end of the injector to load a spiral spring inside the injector. This spring constrains a gear train that ends with a screw-nut mechanism to transform the circular motion to a linear one. During the injection, pushing a button located close to the syringe releases some energy from the spring, thus expelling a drop of product. This way, controlled doses can be injected at will, with the downside that the dose cannot be modified. Another drawback of this solution is that it is

### 1.3. Injectors — a brief history and the state of the art

---

not possible to inject continuously and that the administration of the dose is rather slow.



Figure 1.4: Restylane Injector [Gal15].

The *Preciquant Injector* designed by the Swiss company *Primequal* (Fig. 1.5) is quite similar in that the injection energy is provided by a spring. The main difference is that it is a compression spring, so the system does not have any rotating part. Here again, pushing on the long handle releases one drop of fluid. Several models exist, adapted to the type of fluid to be injected.



Figure 1.5: Primequal injector [Pri15].

#### 1.3.2 Motorised injectors

The purely mechanical injectors presented above can be classified in two categories: one-shot or drop injectors. One-shot injectors, such as insulin pens, provide a user-defined dose at once. This dose is typically large. Drop injectors like the *Restylane* and *Preciquant* injectors

## Chapter 1. Introduction

---

provide much smaller doses (typically an advance of the plunger smaller than 1 mm) and are designed for the administration of several doses in a rather short timespan. Both one-shot and drop injectors are good for certain applications but fail to provide a solution when the injection speed has to be controlled carefully.

The use of electronics permits to address this issue. In 1983, Anders Blomberg patented an injector, shown in Fig. 1.6, for insulin where the thrust force was given by a DC motor (17) [Blo86]. The energy was provided by accumulators and transmitted from the motor to the plunger through a gear set and a screw-nut mechanism.

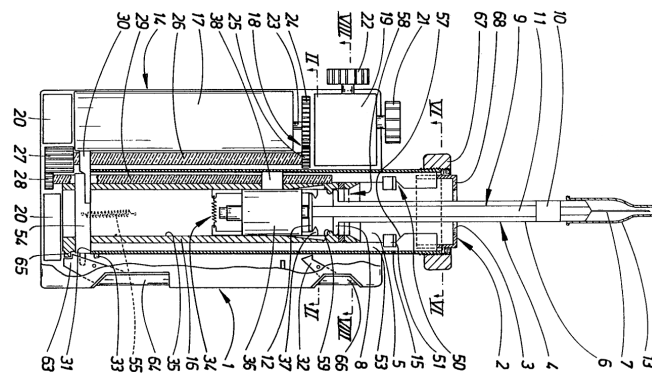


Figure 1.6: An embodiment of Blomberg's invention [Blo86].

With this solution, the control of both speed and dose is made easier for the user, since he is assisted by a microcontroller, typically by selecting the dose and/or injection speed before performing the injection by simply pushing a button. This solution increases the quality of the injection because the user simply focuses on performing the injection rather than having to provide the injection force and visually controlling the amount of product injected. However, this comes at a cost, since a battery-powered injector might fall short of energy during an injection, causing a disruption in the intervention, especially when the thrust force has to be large.

Nowadays, various kinds of motorised injectors based on the same principle can be found with different specifications and for different applications. Some have peculiar ergonomics [AA93], use piezoelectric actuators [SEK97] or use the grid as a power source [Ant15] to avoid battery-life issues. In the field of application of the industrial project, let us mention Juvapulus' *Teosyal Pen* (Fig. 1.7), a quite miniaturised battery-powered injector. Its functioning principle is the same as Blomberg's invention but it provides performances and ergonomics that led it to win awards in its field.



Figure 1.7: Teosyal Pen by Juvaplus [Juv15].

#### 1.3.3 A hybrid solution

The combination of the advantages of both passive and motorised injectors gave birth to a very interesting device. In 2013, Jeremy Marshall and Steven Mark Guy Rolfe patented a new concept [MR13]. In all the earlier injectors, the motor was used to supply the required energy to push the product out of the syringe. In their design, this energy is provided by a spring, just as it is in passive injectors. However, the energy flow between the spring and the plunger is interrupted by an escapement function, in some ways similar to those found in clockwork. An actuator is used to control when the escapement allows the injection of a small dose. Fig. 1.8 shows an example of a device according to their invention.

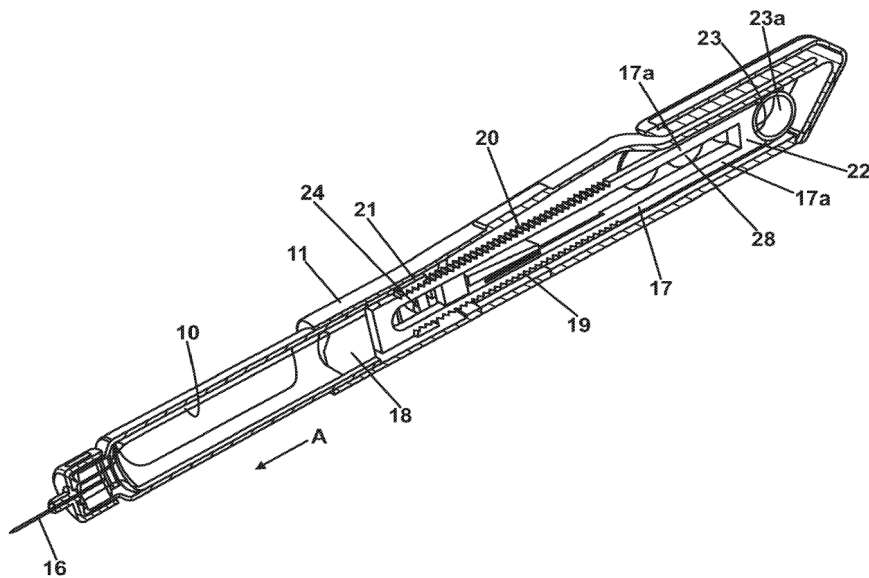


Figure 1.8: An embodiment of the invention of Marshall and Rolfe [MR13].

## Chapter 1. Introduction

---

The working principle of their device is extremely simple. Logically, the syringe (10) is to be emptied by the plunger (17). That part is made of a plunger head (18) and two ratchet surfaces (19, 20). The teeth of the ratchet surfaces are shaped with a vertical face facing the plunger head and a sloped face on the other side. These teeth can be blocked by a collar (24) actuated by a piezoelectric actuator through a lever mechanism. A constant force tension spring (23a) connects the bulk of the injector to the far end of the plunger. In order to place a syringe in the injector, the user has to reload the spring, by pulling the plunger all the way back. By pushing a button, the user chooses when the injector expels the product. Based on Fig. 1.9, let us see how the piston moves.

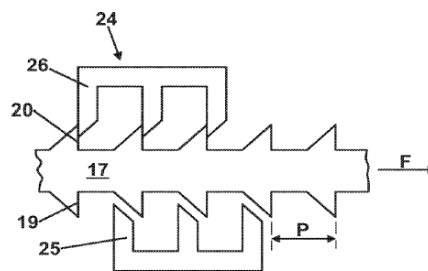


Figure 1.9: Escapement in Marshall and Rolfe's invention [MR13].

The arrow  $F$  indicates the direction of the force applied by the spring on the plunger. In the configuration presented here, it is clear that the piston is blocked and that no product is ejected from the syringe. Let us consider that the piezoelectric motor is actuated such that it moves the collar up. The teeth of the upper ratchet surface are released and the plunger is pulled to the right by the spring. However, the design is such that when the collar moves up, its lower part blocks the teeth of the lower ratchet surface and stops the plunger. During this cycle, a drop of product has been ejected from the syringe. By doing this over and over, it is possible to inject the exact amount of product and, to a certain extent, at the desired speed.

The advantage of this configuration, apart from its simplicity, is that the motor is not used to inject the product, but to allow a spring to do it. It is crucial to realise that the direction of actuation of the motor is perpendicular to that of the movement of the plunger. Through this trick, the energy required for the electric motor is much smaller, since it only has to overcome the friction forces between the collar and the ratchet wheel. The energy consumption and the dimensions of the motor are thus much smaller in such a case. The possible miniaturisation of the whole system is extremely important.

As of 2015, no product has been commercialised using the principle described in this patent. There might be several reasons to this, one of them being the system getting patented really early in the design process. Also, the embodiment presented has several design issues or

imperfections (discussed in appendix C) that might prove serious when trying to prototype or industrialise the product. Nevertheless, the approach to the issues addressed opens interesting perspectives.

### 1.4 Field of research

The state of the art shows that many solutions have been developed for injectors, some of them purely mechanical, some using electrical energy as injection energy, and finally a solution where the injection energy is provided mechanically but the advance is controlled electrically. The focus of the thesis is set on mechanisms similar to the latter because this solution, not yet commercialised, offers interesting prospects in terms of battery life as well as mechanical performance. Rather than discussing dosage systems, escapement-based movements will be addressed regardless of their final application. Because of the highly optimised and application-specific nature of escapements, a multi-purpose escapement-based movement does not exist. Therefore, these systems offer researchers and designers alike a very wide playground. In addition to being at least partly powered by the user's energy (by way of a simple operation such as loading a spring), the discussed escapements have to work without any sensor.

The main objectives of this thesis are to:

- awaken the interest of the reader for escapement-based movements as a mean to enhance the battery life of cordless mechanisms;
- provide the reader the basics for the development of escapement-based applications.

Let us briefly recount the history of escapements in clockwork and start generalising the concept of escapement.

### 1.5 An introduction to escapement-based movements

In clockwork, a movement is composed of four main elements: a mechanical energy stock, a regulating organ that provides timing, an escapement, and a transmission. The latter connects the energy stock, the escapement and the hands of the clock together. The escapement is at the interface between the regulating organ and the transmission. Numerous types of escapement-based movements exist, all particular in their own ways. Some of them are monostable, some are bistable; some are driven by gravity induced forces, others by hair-springs; some are based on elastic elements. Nevertheless, all modern escapements regroup the same basic functions, the most important of which are:

## Chapter 1. Introduction

---

- transferring energy from the energy source to the oscillator;
- synchronising the speed of rotation of the gear train with the movement of the oscillator.

Let us investigate briefly on two particular escapements: one being among the oldest clockwork escapements, the other because it is widely used nowadays.

Escapements appeared as early as the 13<sup>th</sup> century [Hea02], via a mechanism called *verge and foliot*, represented in Fig. 1.10. This rudimentary mechanism was used in tower clocks as a way to convert the potential energy stored in driving weights to kinetic energy in the foliot – timekeeping element, a mechanical oscillator – and the hand (clocks from that era did not comprise seconds, nor minutes hands). The name escapement derives from the fact that the mechanism blocks the energy flow between the energy source and the load, only to let it escape periodically.

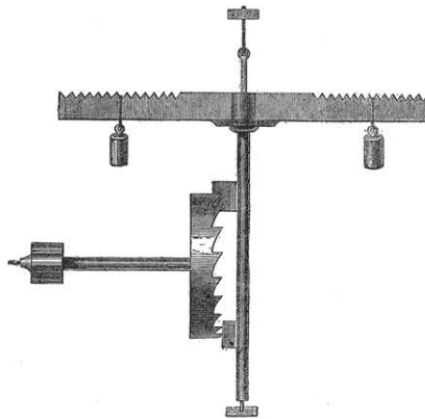


Figure 1.10: Sketch of a verge and foliot mechanism [Mil47].

Since then, clocks enormously evolved, eventually leading way to pocket watches and wrist-watches, thanks to evolutions such as the discovery of the properties of leaf springs. Let us examine more carefully the *Swiss lever escapement*, a game-changer in the field of horology around 1860, shown in Fig. 1.11. Its main features are an increased energetic efficiency and better timekeeping performance. The Swiss lever escapement consists in three main parts:

- the *escapement wheel*, which consists in a cogwheel comprised in the gear train between the main spring (source of mechanical energy) and the hands of the watch;
- the oscillating timekeeping element, known as the *balance wheel* or oscillator;
- the *anchor* whose role is to link the balance and escapement wheels.



## 1.5. An introduction to escapement-based movements

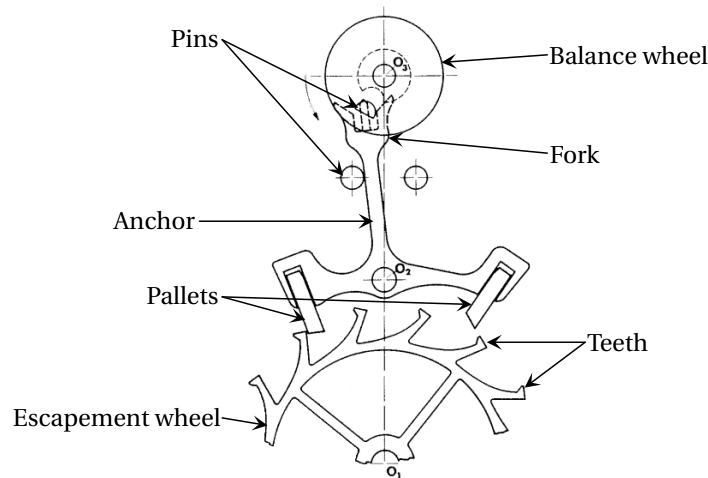


Figure 1.11: Sketch of a Swiss lever escapement [HGG74].

The main spring creates a torque on the escapement wheel so as to drive it clockwise. However, in a stable position, motion is prevented by one of the *pallets* of the anchor that is itself blocked by a *pin*. In Fig. 1.11, the anchor and the escapement wheel are stable on the left pallet, but the balance wheel is rotating counter-clockwise. When the pin on the balance wheel hits the *fork* at the end of the anchor, the impact initiates a rotation of the anchor around its axis ( $O_2$ ), thus liberating the tooth and the pallet. A clever system based on inclined planes ensures that the acceleration of the escapement wheel transmits energy to the balance wheel through the anchor, so as to maintain its movement. Meanwhile, the other pallet gets in the way of one of the escapement wheel's teeth so as to bring the anchor and the escapement wheel in a stable state. The balance wheel continues its movement freely except for the force of the spiral spring on which it is mounted, which generates the oscillating motion. On its way back, a very similar chain of events happens, initiating yet another step of the hands. These escapements typically function at a frequency of 4 Hz.

The technical and historical literature about clockwork is wide. Enthusiastic readers are invited to discover watchmaker George Daniels' books [CD65, Dan81], or from other authors [Bar98, Bru04]. Technical textbooks are also available in French [HGG74, VBP<sup>+</sup> 11].

Escapements are also commonly found in radically different products: typewriters. The issue is to ensure that two consecutive characters are not typed on the same spot. The retained solution consists in moving the sheet of paper laterally relative to the rack of type bars. This displacement is obtained by a rather simple mechanism made of cogwheels and a ratchet rail. Much as is the case in clockwork escapements, the system is constrained by a loaded spring. Hitting a key on the keyboard triggers a series of coordinated mechanical motions that print

## Chapter 1. Introduction

---

the desired character on the sheet of paper before displacing a part similar to a pallet to liberate the escapement wheel that generates a displacement of the sheet of paper. There again, a variety of escapements exist, but to a lesser extent than for clockwork escapements, during the short product life of typewriters.

There are obvious differences between clockwork and typewriter escapements, starting with the output motion: circular versus linear. Secondly, typewriter escapements are actuated by the user, at a frequency that he defines. In addition, the tiny dimensions and loads of modern clockwork escapements are very different from the ones of typewriters. Last but not least, typewriter escapements do not play any role in distributing the input energy, which renders them much simpler.

### Conclusion

This analysis of the role of escapement is very interesting for the development of our mechanism. The conceptual differences between these three mechanisms is very small, although the nature of the application, the energy and power involved as well as type of motion are radically different. A supply of mechanical energy always provides energy to the movement, which conveys it to the output via transmission gears. A regulating organ supplies the timing information; in other words, it triggers the steps, a process that requires energy. Between clockwork and typewriter escapements, the difference lies in the regulating organ. In clockwork, it is an oscillator that collects energy from the energy supply through the escapement before giving it back to trigger steps. Energetically speaking, the system is stand-alone. In typewriters, the regulating organ is the user who chooses when to trigger steps and provides energy by pushing on a key. The mechanical energy supply is not sufficient in itself and the timebase needs its own energy supply.

The movement discussed for the injector takes from both types of movements, with a stronger bond with typewriter escapements. Indeed, regulating organ should not consist in a simple oscillator because the advance has to be performed at the user's will. However, it is not defined whether the regulating organ should use energy from the mechanical energy supply, via the escapement or not, or have its own energy supply.

## 1.6 Contents of the thesis

The ambition of this thesis is to familiarise the reader with escapement mechanisms and stimulate him or her on the way to developing new applications based on this principle. In this scope, providing the reader with tools to facilitate the design of an escapement-based movement is a cornerstone. Chapter 2 proposes a general functional analysis of an

escapement-based movement. It is performed so as to be as application independent as possible. The resulting functional requirements are a canvas for the definition of application dependent requirements. In addition, a modelling strategy for escapement-based movements is proposed.

In chapter 3, a case study, used as an example throughout the thesis, is introduced and its functional requirements specified. This case study is intended to demonstrate one particular escapement-based movement and is used to give the reader a concrete development. The studied solutions for the example are introduced and key design issues are discussed.

The performance, dynamic as well as energetic, of the studied movement is modelled in chapter 4, with a focus on the escapement itself. Each subpart of the movement is modelled either analytically or numerically, with a preference for the former. These models are used to study the influence of manufacturing tolerances on the movement performance.

Chapter 5 discusses electronically-controlled movements. After an introduction describing this class of escapement-based movements, the case study is again used as an example of such a mechanism. A model is proposed that describes the dynamic and energetic performance of the electronic part of the movement. This model, combined to the models defined earlier, permits an evaluation of the overall performance of the studied movement.

Prototypes are used to validate the various models used throughout the thesis. In chapter 6, all relevant information regarding the prototypes and the experiments conducted for the validations is given. In addition to their academic interest, these prototypes show a practical example of an electronically-controlled escapement-based movement devised using the proposed methodology.

### **Context of the research**

The academic research presented in this thesis has been motivated by an industrial collaboration between the company Juvaplus\* and the Integrated Actuators Laboratory (LAI)<sup>†</sup> from the Swiss Federal Institute of Technology in Lausanne (EPFL), in Switzerland. Industrial aspects of the design such as the user interface or packaging are not discussed in this thesis. For the same reason, miniaturisation and integration are discussed to a certain extent only.

---

\*<http://www.juvaplus.com/>

<sup>†</sup><http://lai.epfl.ch/>



## **2 Elements of Design Methodology for Escapement-Based Movements**

The aim of this chapter is to guide the reader in the process of devising an escapement-based movement. Instead of focusing on clockwork, this chapter widens the field of applications of the escapement principle by defining a very general structure applicable to any escapement-based movement. To do so, Pahl and Beitz's design methodology is briefly explained. The following discussion is centred on the application of this methodology to the design of escapement-based movements.

Firstly, the definition of movements such as considered in this thesis is stated. Secondly, a functional block diagram is used to perform the functional analysis and help establish the requirements of a movement. The very general nature of the analysis makes it relevant to a large number of applications, far beyond the field of clockwork. Finally, quantifying and design tools are proposed for the dynamics and the energy flows in escapement-based movements. These tools provide a direct link between the devised movement at any stage of development and the requirements.

### 2.1 General design methodology

Numerous design processes can be found in the literature. Among others, Pahl and Beitz [PBF07] or Roozenburg and Eekels [RE95] are celebrated authors. Pahl and Beitz propose a general methodology (Fig. 2.1) that leads the designer through the steps of the resolution of a task. Without entering into too much detail, their methodology consists in four main steps described below.

- The **clarification of the task** consists in understanding what is expected of the device and compiling all these needs in the requirements.
- The objective of the **conceptual design** stage is to decide the working principle, or *concept*, of the task. This is usually achieved using functional analysis. This stage demands rigour and creativity.
- Throughout the **embodiment design** stage, a demonstration prototype is gradually constructed and enhanced.
- Finally, the **detail design** stage, as its name indicates, focuses on the detailed design of all the parts of the product. It is common that issues arise during this stage that necessitate a return to one of the previous stages. The final outcome is the complete documentation on the design.

Permanent challenging of the solutions, by confronting them to the requirements or by always trying to identify their weaknesses, is necessary to obtain a viable result. This constant feedback breaks the monotony of the design process to make it iterative. A wise choice of these tools is crucial for a good design, because they are the interface between the requirements and the solutions being developed. The strength of this methodology is that it can be applied to different levels. It can be applied to the design of a product, but also to the design of a subpart of said product.

This methodology is quite general and can be tweaked to particularly fit one field or the other. The reader interested in an application of Pahl & Beitz's methodology to mechatronic (or multidisciplinary) design can refer to [Deh04]. Slightly different approaches to the design of mechatronic devices can be found in [Flu10, Ber11].

The content of this chapter is centred on the clarification of the task of *designing a positioning mechanism using an escapement* and the beginning of the conceptual design stage. This task can be seen as one of the functions of the task *create an injector* discussed in introduction. Later chapters discuss specific topics of the embodiment design. Because of its industrial purpose, the detail design is not discussed.

## 2.1. General design methodology

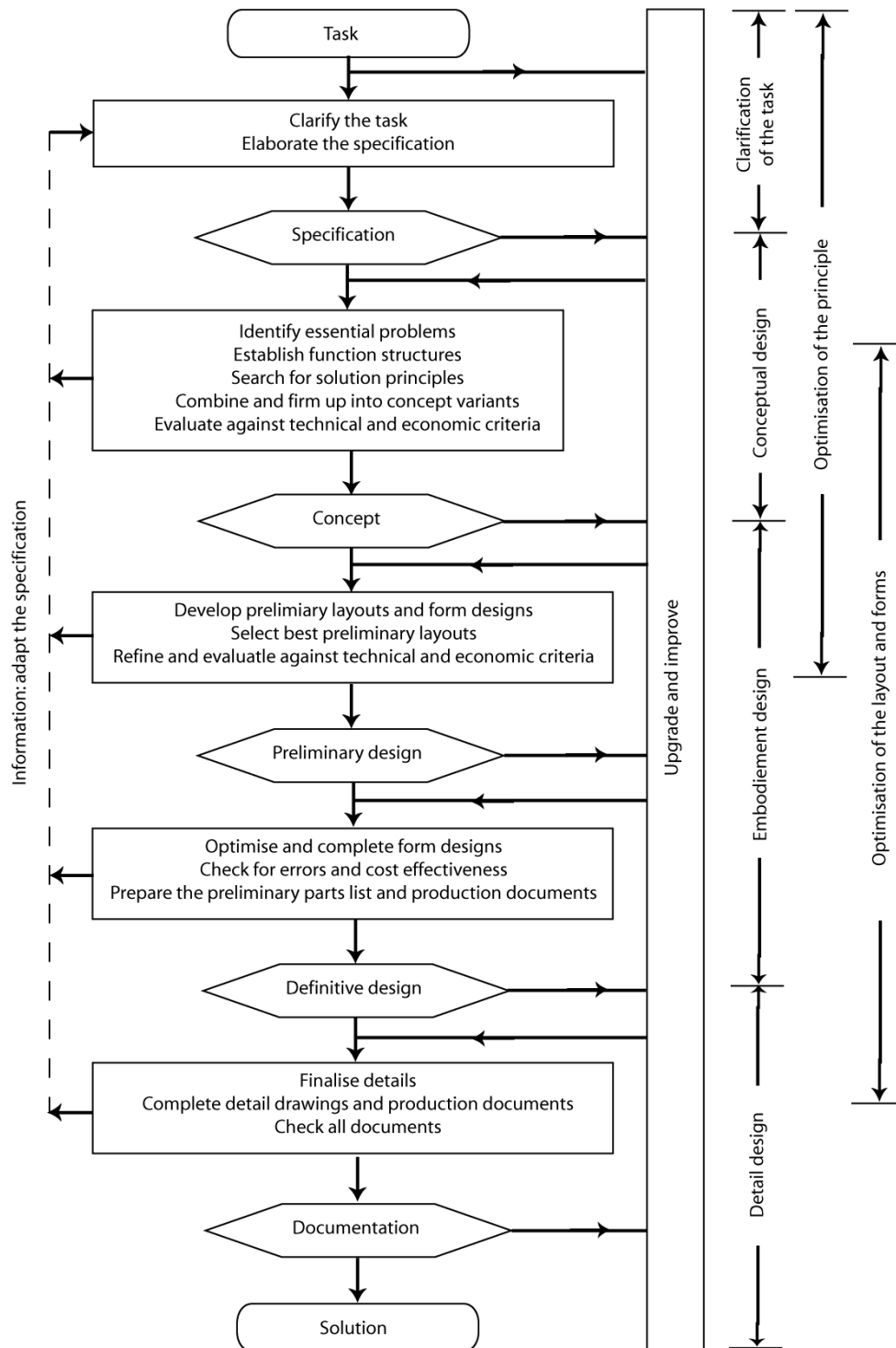


Figure 2.1: Process flow of the design methodology proposed by Pahl & Beitz [tIDEW15b].

### 2.2 Definition of an escapement-based movement

A general yet specific methodology suitable for any design cannot exist. Therefore, a precise formulation of the subject studied in this thesis is necessary. Let us consider the following:

*An escapement-based movement is a uniaxial and unidirectional stepper mechanism whose energy management is such that most or all of its output energy is provided by a manually rechargeable energy stock so as to be as energetically autonomous as possible.*

This definition describes the importance of the energetic behaviour of the movement. Of course, the exact performance is application dependent yet the idea that the mechanism has to work for a long duration without other maintenance than what can be done by hand is important. Typically, purely electrically-driven systems are not discussed in this dissertation. The stepper nature of the system highlights that its mechanical structure has a finite number of stable positions, therefore implicitly primarily meant for position control. The distance (linear or circular) between two consecutive positions is generally constant and yields the resolution of the mechanism. It is also clearly mentioned that an escapement-based movement is made to work in a single direction along a single axis of freedom.

Fig. 2.2 shows a general block diagram of an escapement-based movement as described above. The idea of energetic independence is materialised by the presence of an energy supply which plays a dominant role in the functioning of the escapement. The energy is of course not created, but it is acquired or harvested from the environment, which is why the supplied energy's nature and availability should be clearly defined. This energy supply provides energy to a stock that in turns forwards it to the transmission. The energy can be supplied directly to the stock, or through the transmission. Until this point the energy can be of any nature, but it consists in mechanical energy when it reaches the load after the transmission, who might thus also be a converter. The escapement is often a part of the transmission but performs the task of interfacing it with the regulating organ and creating the stepper motion. It is therefore represented as strongly coupled with the transmission but yet separated to highlight its specific role. The regulating organ is the control centre of the mechanism as it defines when energy can be transmitted to the load. It produces a data flow that goes through the escapement and to the load. Importantly, the regulating organ has its own energy stock. In the mechanisms discussed here, it is acceptable that this energy be non-renewable so long as it represents a small fraction of the total energy in the system. Other solutions include a supply directly from the energy supply, from the energy stock or through the escapement, represented by the 'hypothetical' links in the diagram. In any case, a lower energy consumption from the regulating organ is preferable. The user, who is part of



## 2.2. Definition of an escapement-based movement

the environment, can also interact with the timebase in order to define the way the advance should be performed. In some applications, it might also be necessary to give the user a way to interact directly with the transmission so as to change the position of the output of the transmission by hand.

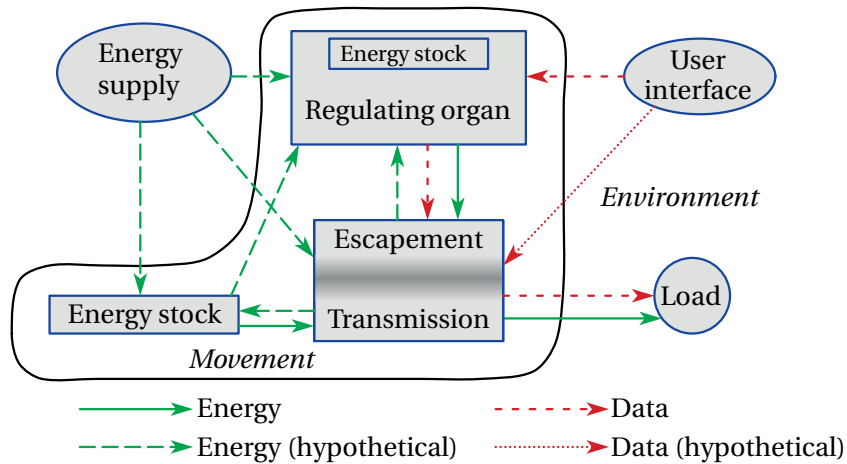


Figure 2.2: Block diagram of an escapement mechanism. The arrows show energy and data flows.

The many hypothetical flows represented in the diagram show that numerous possibilities exist. Their presence as well as the precise energy flows are up to the designer who should carefully study the available options. For example, a wise selection of the principle to recharge the energy stock from the energy supply permits a limitation of the number of mechanical parts.

Because energy is a crucial theme when discussing escapements, let us define here that:

- the energy coming from the mentioned energy supply, referred to as *rechargeable energy*, is considered ‘free’ and infinite in the limitations of the defined availability (arrows from the energy supply in Fig. 2.2);
- any energy coming from another source, *disposable energy*, necessitates a costly operation from the user (not represented in Fig. 2.2 because it is not part of the normal functioning of an escapement).

In other words, a system working purely on rechargeable energy is considered highly efficient, whereas one that works with disposable energy is less efficient. The definition of ‘costly’ is application dependent and an important specification of the product.

### Identification with clockwork movements

Because of the abundance of clockwork movements based on escapements, it is crucial that the diagram above thoroughly describes them. Let us focus on the case of a movement comprising a Swiss lever escapement in an automatic wristwatch. The *energy supply* is a combination of the accelerations applied on the watch by the user as well as the change of orientation of the watch in the gravity field. It is acquired thanks to the free rotor and the click. Its motion loads the mainspring that plays the role of the *energy stock*. In this case, the system obviously purely works on rechargeable energy. If it was not automatic, it would require rewinding, an operation that might or not be considered costly (disposable or rechargeable energy) depending on the type of product desired by the manufacturer. The mainspring is connected to a set of cogwheels that drive the different hands of the watch (*transmission*). The hands can either be considered as the *load* of the movement, or as part of the transmission. Indeed, if the exact set of hands is already defined, it is legitimate to consider them (and their interaction with the medium in which they operate) as part of the transmission and setting the load as null. However, the design of the hands might be separated from the design of the movement, in which case the hands can be considered as the load. The *escapement* is attached to the same set of cogwheels through the escapement wheel that rotates synchronously with the rest of the set. The escapement is connected with the balance wheel (*regulating organ*), to which it provides energy. The latter is mounted on the balance-spring that participates in controlling the advance of the hands, through the escapement. Mechanics show that an oscillating system composed of a spring and a mass accumulates mechanical energy (*regulating organ energy stock*), either as potential or kinetic energy. Of course, the system has losses due to friction, but also because of the unlocking of the escapement that requires the moving of mechanical parts. For this reason, the escapement receives energy from the regulating organ yet also transmits some to it. The energy flow is thus as described in Fig. 2.2, without the hypothetical energy transfers from the energy supply and stock to the regulating organ, but with the energy transfer from the escapement. The data flow is exactly as described, since the oscillations of the regulating organ control the escapement that in turn controls the advance of the hands. The watchmaker can adjust the running of the watch by adjusting the settings of the balance-wheel. And finally, the crown, through which the user sets the time, allows the user to adjust the position of the output of the transmission.

In the case of the Swiss lever escapement, the proposed block diagram is fitting. The same analysis can be performed successfully on most escapement-based clockwork movements. Thanks to its general formulation, it can serve as a guide to the design of different applications. To further work towards this target, let us perform the functional analysis of this movement architecture in order to generate the requirements.

### 2.3 Functional analysis and functional requirements

Defining the requirements is a complicated task. It is usually iterative, as shortcomings in the requirements arise during the solutions searching process. Functional analysis [VCFS12, tIDEW15a], mentioned as part of the conceptual design stage of the development, is a widely used tool to express the technical (*functional*) requirements for a task. It consists in trying to express all the functions that the designed object should be able to perform. In addition, it helps the designer truly understand the nature of his task.

In design terms, a function is a task that has to be performed. A function is described by an identification number (ID), a label, a level of performance. A tolerance level is usually given. The label is a short but accurate description of the task to be performed. Functions commonly have more than one level of performance, typically the torque and the speed are both requirements for 'create a rotating motion' for a motor. In that case, each level of performance is given an ID. The tolerance on the performance can be a range of acceptable values, such as a difference in percent with the level of performance, or stating it as a minimum or maximum. Some functions can also be evaluated by a simple 'yes' or 'no'. Finally, the necessity of a function can be given, typically by making a function a demand (D) or a wish (W), the latter being less strong than the former. For example, if a wish is costly, it might not be included in the system.

Among the many ways to organise functions, it was chosen to organise them in terms of *external*, *internal* and *constraint* functions. External functions are interaction functions. In the block diagram, they correspond to the flow lines between the movement and its environment or between subsystems and represent the way they communicate. They also include bulk, weight, shape, stiffness and all relevant mechanical properties. Put another way, they are functions that the user (or adjoining subsystems) needs or needs to be aware of. By opposition, internal functions are needed to ensure the correct functioning of a subsystem. Finally, constraint functions are unavoidable. They gather regulations and norms, be they imposed by law or by the company's capabilities and rules, that affect the design process. Furthermore, the cost limitations of a task are often stated here. Because of their nature, they are not discussed here.

The functional requirements are given in two separate parts: the movement and the subsystems. As Bernhard's work [Ber11] very nicely shows, a system can be finely described through functional analysis. Most importantly, his analysis shows that a system's functions can themselves be split in functions of lower level. Therefore, the internal functions can be seen as those sub-functions. Depending on the complexity, this can go on and on, which is why, in our case, the system is split in the four functions shown in the block diagram, to whom the classification of external, internal and constraint functions are applied. Hence,

only external functions are stated for the movement.

With a view towards a generalised definition of the functions of an escapement-based movement, the functions are listed with a very general vocabulary, so as to open doors to as many potential applications as possible. This functional analysis is largely based on the work of Conus [Con07], who performed a similar analysis on clockwork escapements. The ID of each function is composed of letters and a number. The first letter designates the concerned system or subsystem, the second one indicates if the function is external (E) or internal (I), and each function is assigned a number.

### 2.3.1 Movement

The functional requirements for the movement are mostly user-oriented, since they specify the level of performance of what the user sees as a black box. Since the behaviour of the system has already been discussed, the functions are given rather naturally as the expression of the interactions between the system and its environment. However, some practical functions cannot simply be expressed as an interaction between the system and its environment, such as the lifespan of the product, parts replacement and user expectations. As cannot be stated enough, the main strength of escapement-based movements is their energy management, therefore the amounts of handled energy need to be specified as well as functioning duration of the device with a given amount of rechargeable and disposable energy. To describe these energy-related functions, called *energy budget*, quantifiers are introduced in Sec. 2.4.1. The functions are summarised in Table 2.1, in which functions typeset in italics are hypothetical, necessary only in some movements.

ID	Function
M.E.1	Create the unidirectional motion of a load
M.E.2	Control the displacement
M.E.3	Be energetically efficient
M.E.4	Comprise at least one energy stock rechargeable <i>in situ</i>
M.E.5	<i>Provide a mean to recharge the energy stock of the regulating organ</i>
M.E.6	Lifespan of the movement
M.E.7	Be compact
M.E.8	Permit user setting
M.E.9	Resist to external perturbations

Table 2.1: Requirements of an escapement-based movement

### 2.3.2 Sub-functions

#### Energy stock

The stock has to acquire energy from the energy supply and store it before it can perform its main functionality: providing energy to the transmission. Although the energy could be of any kind, mechanical energy is a convenient alternative. The way the energy is received or provided, in particular the instantaneous power and force ratings, should be clearly defined for a coherent movement. In the case of mechanical energy, transferring it through a linear or circular motion is a major decision. Because of the prominence of the energetic performance in an escapement-based movement, it is natural that the efficiency of the energy transfer is specified in some way.

ID	Function
S.E.1	Receive energy – <i>from the energy supply</i> – <i>from the transmission &amp; escapement</i>
S.E.2	Store energy
S.E.3	Provide energy – to the transmission & escapement – <i>to the timebase</i>
S.E.4	Mass, volume and shape

Table 2.2: External functions of the energy stock.

#### Transmission & escapement

The intimate relation between the transmission and the escapement results in a common functional analysis. The transmission is an energy conveyor that transports it from the energy stock to the load, but that can also deal it to the regulating organ through the escapement, whose role is to interrupt or allow the energy flow to the load. Through this function, it acts as a data conveyor between the regulating organ and the load, and to perform it, the escapement receives energy, although usually little, from the regulating organ. The external functions of this system (later abusively referred to as the ‘escapement’) are thus rather straightforward, since it consists in receiving energy from the energy stock and the regulating organ, and providing energy to the load and hypothetically to the regulating organ. As previously seen, the way the energy is transferred is of importance. The energy transmission to the load includes the description of the resolution of the displacement, the speed and the stroke. Unlike the energy stock and the regulating organ, the escapement does not store significant amounts energy. In some applications, it is possible that the escapement is required to redirect energy from the supply to the stock. In addition to the energy and data related

functions, volumetric and mass specificities are external functions.

ID	Function
E.E.1	Receive energy – from the energy stock – from the regulating organ – <i>from the energy supply</i>
E.E.2	Transmit energy – to the load – <i>to the regulating organ</i> – <i>to the stock</i>
E.E.3	Transfer data from the regulating organ to the load
E.E.4	Mass, volume and shape

Table 2.3: External functions of the transmission & escapement.

The list of internal functions is more interesting. Primarily, the escapement is responsible for creating the stepper behaviour of the movement. To do so, there needs to be a series of stable positions, the repetition of which can be regular or not. The stability of the steps should also be quantified by stating what conditions a step should be able to withhold without damage. A way to interpret the instructions sent from the regulating organ is required, so as to generate the desired motion. In case the energy received is not mechanical, the escapement has to transform it. Also, the adaptation of the energy flow – Where does the energy come from and where does it go? – inside the escapement has to be determined.

ID	Function
E.I.1	Discretise the advance by creating steps
E.I.2	Trigger steps according to the regulating organ
E.I.3	Manage the repartition and nature of the energy

Table 2.4: Internal functions of the transmission & escapement.

### Regulating organ

The regulating organ's role is to generate the steps by sending energy and data to the escapement according to the settings given by the user. The definition of the settings is complicated and application dependent. For a watch, the settings is the oscillation frequency, and the user is not the watch bearer but the watchmaker. In a different positioning application, the settings can be a number of steps at a certain cadence at a predefined moment or when the user pushes a button. Part of the settings is also the behaviour of the escapement at rest, or in other words: should it always generate steps (like a watch), or wait for a user intervention

to do so (like a typewriter)? Therefore, the interpretation of the data sent through the user interface (UI) is one of the external functions. Of course, so are storing energy and managing it. If the regulating organ's internal energy supply is rechargeable, it has to receive energy and process it so as to store it. If not, it has to offer a way of replacing the energy stock by a charged one or recharge it.

ID	Function
R.E.1	Receive information from the user interface
R.E.2	Initiate steps
R.E.4	Receive energy – <i>from another part of the movement</i> – <i>by an external action from the user</i>
R.E.5	Store energy
R.E.6	Provide energy to the escapement
R.E.7	Mass, volume and shape

Table 2.5: External functions of the regulating organ.

The internal functions are very close from those of the escapement in that it also mostly consists in the handling of the available energy. One big difference is that the energy source is also controlling the timing to define when the steps should take place. This timing might be purely user defined — the user pushes a button every time a step is required — or based on a timer, or oscillator — typically the case for a watch — or a combination of both. In the latter case, the regulating organ might also be asked to count the number of steps.

ID	Function
R.I.1	Interpret the settings and trigger steps accordingly
R.I.2	Manage the repartition and nature of the energy
R.I.3	<i>Provide timing and counting capabilities</i>

Table 2.6: Internal functions of the regulating organ.

## 2.4 Evaluation and design tools

With the target of designing highly efficient devices, evaluation tools are strongly needed. These tools are used during the whole design process because they enable a clear definition of the requirements as well as a way to compare theoretical and experimental results with them. In the development of escapement-based movements, evaluation tools can be given for many functions but let us focus on the energetic efficiency of the system and the modelling of the evolution of the position of the output of the transmission. Watchmakers would probably spend more time on the timekeeping capabilities of the movement.

These tools are integrated in the design process as described in Sec. 2.1. They are first used in the specification of the requirements. During the solutions searching process, it provides a rapid comparison with the requirements and offers a selection criterion. Later on, for the detail design, a more accurate model can be devised to verify at all times the validity of the selected solution. Functional prototypes can be used to enhance the model so as to optimise the design.

### 2.4.1 Strategy for efficiency modelling

Expressing the energy budget in technical terms requires *quantifiers*. Commonly, the efficiency  $\eta$  serves exactly that purpose. It is defined as the ratio (2.1) between the useful output and the total input energy (or power), respectively  $E_{out}$  and  $E_{in}$ . For systems combining two or more sources of energy, this definition can be applied if  $E_{in}$  is the sum of the energy provided by all sources, in which case  $\eta$  could be called *overall efficiency*.

$$\eta = \frac{E_{out}}{E_{in}} \quad (2.1)$$

The complexity of the energy flows in escapement-based movements makes the task slightly more complicated. The proposed method is to model the overall energetic behaviour of the movement with respect to the rechargeable and disposable energy. Let us call *rechargeable energy factor* the ratio  $\eta_a^*$  (the index  $a$  indicates energy that can be accumulated) between the output energy and the rechargeable energy ( $E_{in,a}$ ), given in (2.2). Similarly,  $\eta_d^*$  (2.3) is called the *disposable energy factor* (hence the index  $d$ ) and represents the amount of output energy that can be obtained per unit of disposable energy ( $E_{in,d}$ ).

$$\eta_a^* = \frac{E_{out}}{E_{in,a}} \quad (2.2)$$

$$\eta_d^* = \frac{E_{out}}{E_{in,d}} \quad (2.3)$$

These quantifiers are called energy factors rather than efficiency for the simple reason that they are mathematically not bounded by 0 and 1. Indeed, since  $E_{in} = E_{in,a} + E_{in,d}$ , we have:

$$\frac{1}{\eta} = \frac{1}{\eta_a^*} + \frac{1}{\eta_d^*}. \quad (2.4)$$

Therefore, it is possible to maximise one or the other of the energy factors largely over 1, but it has to be done at the expense of the other factor. A third factor, which is a composition



of the previous two can also be handy. The *relative energy factor* (index  $r$ ) directly links the rechargeable and disposable input energy:

$$\eta_r^* = \frac{E_{in,a}}{E_{in,d}} = \frac{\eta_d^*}{\eta_a^*}. \quad (2.5)$$

Very similar to the disposable energy factor, this factor is a representation of the importance and abundance of rechargeable and disposable energy, and should be maximised for enhanced energetic independence. Although less interesting for the user, the relative energy factor is more natural for the designer. Using it instead of the disposable energy factor yields:

$$\eta = \frac{\eta_a^*}{1 + \frac{1}{\eta_r^*}}. \quad (2.6)$$

These factors are especially well-suited for applications where the output of energy is the main objective of the movement.  $\eta_a^*$  and  $\eta_d^*$  can be linked even more strongly to the requirements if they are calculated based on the actual output energy desired  ${}^t E_{out}$ . The *rechargeable* and *disposable true energy factor*, respectively  ${}^t \eta_a^*$  (2.7) and  ${}^t \eta_d^*$  (2.8), do just that. Such quantifiers are for example justified in cases when the output force (and thus energy as soon as there is displacement) of the mechanism is larger than the force in the requirements. The true energy factors are lower than the energy factors, because  $E_{out}$  has to be larger or equal to  ${}^t E_{out}$ . Similarly,  ${}^t E_{in,a}$  and  ${}^t E_{in,d}$  might differ from  $E_{in,a}$  and  $E_{in,d}$  for example if slightly more energy is provided to ensure that each step is initiated successfully or that the output energy is large enough. The true energy factor is discussed further in a study case in chapters 4 to 6.

$${}^t \eta_a^* = \frac{{}^t E_{out}}{{}^t E_{in,a}} \quad (2.7)$$

$${}^t \eta_d^* = \frac{{}^t E_{out}}{{}^t E_{in,d}} \quad (2.8)$$

The *relative true energy factor*  ${}^t \eta_r^*$  is slightly different because it compares the disposable energy and an estimation of the rechargeable energy required to obtain the desired output energy  ${}^t E_{out}$ . It therefore cannot be directly measured on a prototype.

This methodology can of course be used to describe any energy flow in the system. In clockwork, it would for example be preferred to express the energy factor between the rechargeable energy and the energy transferred to the regulating organ.

### 2.4.2 Dynamic modelling of a stepper system

Alongside the energy management, the dynamic behaviour of the escapement is extremely important. Stepper systems create a discretised motion, where a displacement is performed through an addition of steps. Since the displacement is discrete, it is sufficient to model the behaviour of the mechanism during one step to model its overall dynamic performance. Clearly, steps might differ, be it because of a different load or a varying parameter in the driving mechanism. It is thus necessary to model a step in the least favourable conditions.

The modelling of the system is achieved by splitting the mechanism in blocks of moving parts that move together called *subgroups*. The sequence of motion of each subgroup to achieve a step is then explicitly stated, especially as far as interactions between subgroups are concerned. Afterwards, special timing informations, later called *specific durations*, are defined for each subgroup. Once all specific durations have been identified, it is required to model them, analytically, empirically or numerically. Based on the sequence of motions, rules can be defined on the specific durations to ensure the correct functioning of the system and the respect of the requirements. This allows to use the model as a design tool. The last step is then to design all the subgroups in a way that ensures that the set of enacted rules is respected.

This dynamic model is based on two parameters that directly yield the performance of the mechanism: the length of a step  $r_o$  and the number of steps per second  $f_{steps}$ . Of course,  $r_o$  is the resolution of the output position. Used with  $f_{steps}$ , it trivially gives the speed  $v_o$  (2.9).

$$v_o = r_o \cdot f_{steps} \quad (2.9)$$

The advantage of such a model is thus that it permits a rather fast and efficient evaluation of the performance of a given solution. In addition, analysing the relative motion of each part of the mechanism separately is extremely convenient in terms of design, as it highlights the requirements for each subgroup.

## 2.5 Conclusion

In this chapter, a synthesis of escapement-based movements has been performed. The structure given is as general as possible so as to provide a basis for the development of various applications. The functional analysis yields helpful guidelines towards the definition of the requirements for such movements, be they for clockwork or not.

Finally, some tools are introduced for the quantification of the desired performance of the movement, in particular its energy management. These quantifiers are useful for the definition of the requirements, as well as all along the design process in order to estimate and later validate the selected solutions.

---

Publications related to this chapter:

- Romain Besuchet, Yoan Civet, and Yves Perriard. Study of the Efficiency of an Electronically-Controlled Linear Escapement. In *Advanced Intelligent Mechatronics (AIM 2015), IEEE/ASME International Conference on*, 2015.
- Romain Besuchet, Yoan Civet, and Yves Perriard. A Novel Electronically-Controlled Linear Escapement Mechanism. In *Electrical Machines and Systems (ICEMS), 2014 17th International Conference on*, page: 2197 – 2203, 2014.



## **3 Conceptual Design of a Linear Movement**

This chapter gives an example of conceptual design. It is centred on the design of a linear movement for the injection device mentioned in introduction. The difference between movement and device is that the device is an industrial product, with packaging, interface, and so. The movement only describes the elements that participate in the task of positioning the output. The definition of the requirements for the movement, as well as the requirements for the subsystems is documented. It also introduces a study case that is used all along this dissertation to illustrate the concepts introduced. The iterative nature of the design process being impossible to reproduce on paper, only the results of the reflections are given.

Because of the highly challenging nature of the design of the escapement, most of this chapter discusses it, setting aside the design of the energy stock and the regulating organ, that is discussed in chapter 5. The most important design points for the escapement are discussed.

### 3.1 Case study: a linear escapement

This example is a movement for the injector mentioned in introduction. Let us here establish the requirements of the movement using the previous functional analysis.

#### Requirements

As already explained in Sec. 1.4, two different injection modes should be provided, the drop mode consisting in injecting a drop of fluid, and the flow mode being the injection of fluid at a given speed. For the movement, this corresponds to two different advance modes. Yet, since the movement is a stepper mechanism, both modes are performed in exactly the same manner, with only the number of steps of a sequence differentiating the modes.

The device does not need to be fully energetically independent. A quick recharge manipulation by the user before each injection is not considered 'costly' for the user, so the energy supply consists in the user's mechanical energy. On the other hand, it is also tolerable that some of the energy is disposable, but there are limitations on the frequency at which the disposable energy stock has to be replaced or recharged. The nature of the rechargeable and disposable energy is not pre-defined, yet for the sake of simplicity, energy conversion should be as limited as possible. With the same idea, some parts of the device can be expendable if replacing them is fast and easy. Because the targeted movement should be compact, simple solutions are preferred, even though they might not be the best from the point of view of the performance.

In particular, the regulating organ will be electrically-powered. Indeed, electric power allows the use of electronics, whose control performance is extremely interesting thanks to its flexibility. Structurally, it however requires a converter to transform the electrical energy to mechanical energy in order to trigger steps. More is given on this topic in chapter 5.

The requirements for the case study are summarised in Table 3.1. Requirements related to functions classified as wishes have not been listed in this table. In addition to the very standards size and volume requirements, the energetic performance is clearly stated. This list of requirements consists in values that the user can measure. They are not solution dependent.

### 3.1. Case study: a linear escapement

ID	Function	Parameter	Value
M.E.1	Displace a load along one axis		
M.E.1.1	– mass of the load	$m_l$ (g)	5
M.E.1.2	– friction force	$F_l$ (N)	40
M.E.1.3	– load profile	Constant	
M.E.2	Control the displacement		
M.E.2.1	– at rest, the displacement is blocked		
M.E.2.2	– position resolution	$r_o$ (mm)	$0.4 \pm 0.05$
M.E.2.3	– stroke	$s_o$ (mm)	50
M.E.2.4	– maximal average speed	$v_o^{max}$ (mm·s <sup>-1</sup> )	10
M.E.2.5	– average speed resolution	$v_o^{res}$ (mm·s <sup>-1</sup> )	1
M.E.3	Energetic performance		
M.E.3.1	– work with normalised batteries or accumulators		
M.E.3.2	– minimal disposable true energy factor	${}^t\eta_d^*$ (—)	5
M.E.3.3	– minimal rechargeable true energy factor	${}^t\eta_a^*$ (—)	0.1
M.E.4	Have a mechanical energy stock rechargeable by hand		
M.E.4.1	– can be recharged for the whole stroke in a single motion		
M.E.4.2	– disposable energy not necessary for recharge		
M.E.4.3	– maximal necessary recharge force	$F_{rec}$ (N)	60
M.E.4.4	– recharge time	$T_{rec}$ (s)	3
M.E.5	Provide a mean to recharge or change the disposable energy stock		
M.E.6	Lifespan of the movement		
M.E.6.1	– parts (expendables) can be replaced every cycle if it is quick enough		
M.E.6.2	– maximal total time to replace expendables	$T_{rep}$ (s)	2
M.E.6.3	– minimal number of cycles of non-expendables	(—)	10000
M.E.7	Be compact		
M.E.7.1	– weight	$m_{tot}$ (g)	50
M.E.7.2	– volume	$V_{tot}$ (mm <sup>3</sup> )	120x40x20
M.E.8	Permit user setting		
M.E.8.1	– drop or flow mode		
M.E.8.2	– drop size and speed selection		
M.E.8.3	– select moment of start of the advance		
M.E.9	Resist to external perturbations		
M.E.9.1	– drop tests		
M.E.9.2	– be undisturbed by external accelerations up to 10g		

Table 3.1: Requirements for the studied movement.

### 3.2 Functioning principle

The search for solution principles is not described here, but there is more information in appendix A. Working towards miniaturisation, one of the design paradigms is to use as little mechanical parts as possible. Similarly, the energy and data flows should be as simplified as possible. In that scope, the studied functional diagram is shown in Fig. 3.1. Three separate modes are introduced: *working*, *recharge* and *maintenance* modes. The working mode (Fig. 3.1a) is when the movement is used to provide energy to the load. In this mode, the energy stock is being discharged. When in recharge mode (Fig. 3.1b), the energy stock receives energy from the supply and hypothetical expendables can be changed. Finally, in the maintenance mode (not represented), the movement is at standstill but the energy stock of the regulating organ is replaced or recharged. The requirements for the external functions of the energy stock, transmission & escapement and regulating organ (Tables 3.2 to 3.4) can be clarified.

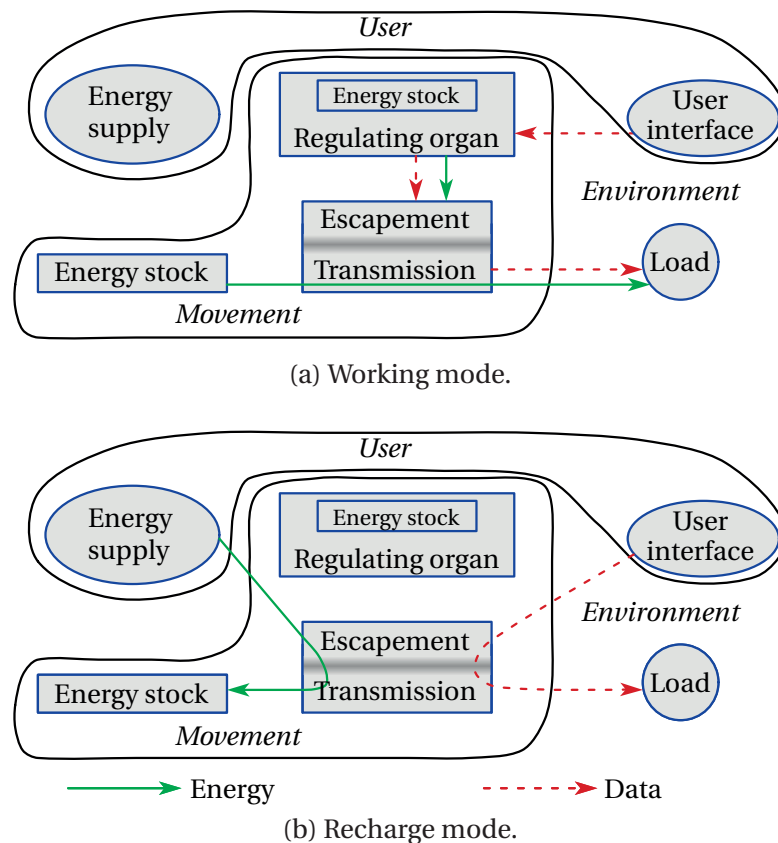


Figure 3.1: Studied functional diagram.



### 3.2. Functioning principle

ID	Function
S.E.1	Receive energy from the transmission & escapement in recharge mode – Extreme instantaneous power – Type of motion (linear or circular)
S.E.2	Store mechanical energy – Minimal quantity of energy – Maximal losses in a given amount of time
S.E.3	Provide energy to the transmission & escapement in working mode – Minimal thrust force or torque – Type of motion (linear or circular)
S.E.4	Mass, volume and shape

Table 3.2: External functions of the energy stock.

ID	Function
E.E.1	Receive mechanical energy from the energy stock in working mode – Extreme force or torque – Type of motion (linear or circular)
E.E.2	Receive mechanical energy from the regulating organ in working mode – Extreme force or torque – Type of motion (linear or circular)
E.E.3	Receive mechanical energy from the energy supply in recharge mode – Extreme force or torque – Type of motion (linear or circular)
E.E.4	Transmit mechanical energy to the load in working mode – Extreme force – Linear motion – Efficiency
E.E.5	Transmit mechanical energy to the regulating organ in recharge mode – Extreme force or torque – Type of motion (linear or circular) – Efficiency
E.E.6	Generate a step when required by the regulating organ
E.E.7	Mass, volume and shape

Table 3.3: External functions of the transmission & escapement.

ID	Function
R.E.1	Receive information from the user interface
R.E.2	Initiate steps
R.E.4	Receive energy by an external action from the user
R.E.5	Provide energy to the escapement <ul style="list-style-type: none"> <li>– Minimal energy, power, force or torque</li> <li>– Type of motion (linear or circular)</li> </ul>
R.E.6	Mass, volume and shape

Table 3.4: External functions of the regulating organ.

### 3.2.1 Studied movement

The functioning principle of the movement studied in the remainder of the thesis is sketched in Fig. 3.2. The energy stock consists in a linear *spring*. It constrains the *rail*, guided linearly along the  $x$ -axis, whose other extremity is used as the positioning reference. This rail is part of a set of three similarly toothed rails that discretise the output displacement and create the stepper motion. The other two shorter rails — the *blockers* — are identical and have a degree of freedom along the  $z$ -axis. Their teeth interlock with those of the rail to block the advance of the output. The distance between the first tooth of each blocker is equal to several times the distance between consecutive teeth (pitch) added with half of it, thus creating a symmetrical stepper motion. Indeed, when one of the blockers is active (*i.e.* its teeth are interlocked with those of the rail), the other one is passive, as can be shown on Fig. 3.2a. Through a release mechanism, represented by two L-shaped parts — the  $\mathcal{L}$  — pivoting around a pin, the mover of the regulating organ can lift one or the other blocker, but one and only one at a time. For fabrication, assembly, and miniaturisation purposes, the mover of the blocker is not connected to the release mechanism, but provides the energy to initiate a step by colliding with it, using the same principle as a hammer, accumulating kinetic energy to then deliver it over a very short period of time. The nature of the regulating organ is discussed in chapter 5. Each blocker is constrained by a recoil spring whose function is to ensure that the standstill position of the blockers is against the rail. That way, when the regulating organ is inactive, both blockers are in a locking position, which is a good protection against unwanted motion. It will be shown later on that they also serve the dynamic behaviour of the movement. As a representative rule, in all schemes and pictures of the movement, the main spring is located on the left and the working mode consists in a displacement from left to right.

The idea for the recharge of the energy stock is that the user, by hand, pushes on the output of the rail, be it through a handle or directly on the rail, in order to compress the spring. So as to make this operation easy and fast, the teeth have to be designed in a way that the blockers slide on the teeth instead of getting blocked by them in this direction. Discussing

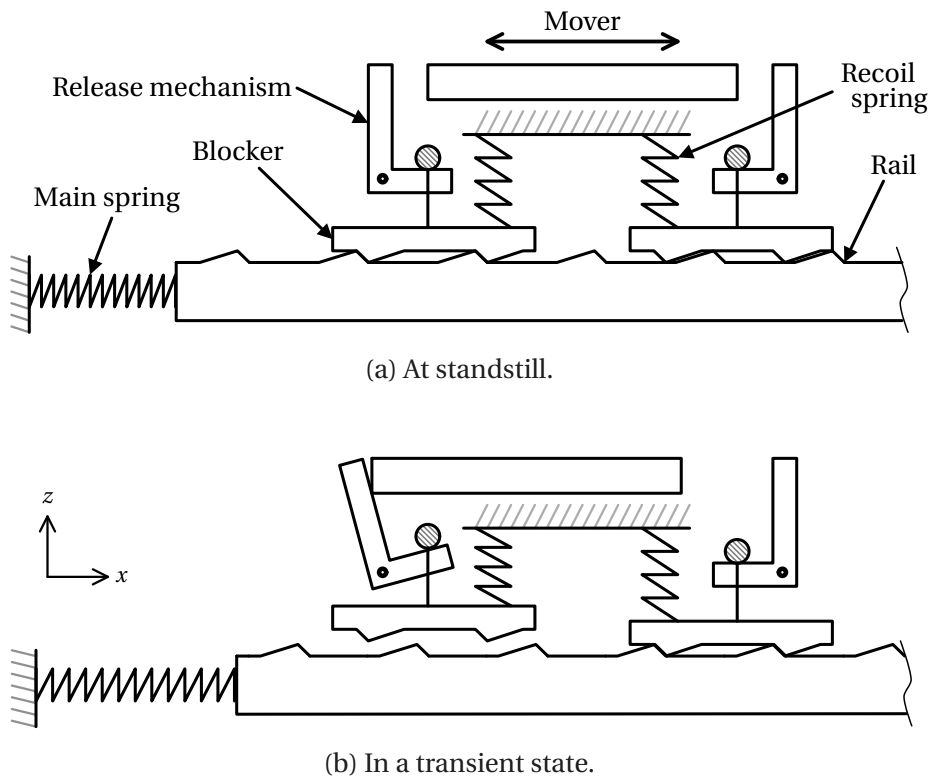


Figure 3.2: Studied functioning principle for the linear escapement-based movement.

the maintenance mode is not relevant, as it is more of a finalisation task.

When confronted with the requirements, the behaviour of the movement is qualitatively satisfactory. Indeed, in the working mode, it provides the motion required in functions M.E.1 and M.E.2. It also fulfils M.E.4 by having a spring capable of storing mechanical energy that can be reloaded by hand. Similarly, the recharge mode is qualitatively satisfactory. The conceptual and embodiment design tasks will allow to define whether the principle also fulfils the requirements quantitatively.

#### 3.2.2 Principles for efficacy

The main concern being disposable energy consumption, some guidelines for the design are suggested:

1. motion of a part other than the output is a source of losses;
2. changes of potential energy also result in losses;
3. mechanical requirements should be satisfied, yet not go too much beyond expectations

because high dynamics and low energy consumption are antagonised.

These guidelines provide useful selection criteria, but are not the be-all and end-all. Let us also remember that the number of parts should be kept low. Indeed, the stakes are much more complex, in particular because the solution should yield a miniaturised mechanism that could be sold at a target price, with a given reliability and lifespan. There are thus many other selection criteria.

### 3.3 Transmission & escapement

The design of the transmission & escapement is particularly interesting because it is the actual core of the movement, both in terms of energy management and dynamic performance. Its complexity and the numerous challenges make it special. This section describes and justifies the solutions retained for the major functions of the escapement.

#### 3.3.1 Functional requirements

A functioning principle being selected, it is possible to write down a relevant list of internal requirements based on the functional analysis (Table 3.5). The conditions in which these requirements need to be satisfied are defined in the requirements for the movement. In particular, external accelerations up to 10g can happen at any time during use. The external requirements can be likewise refined, but it is not of particular interest for the purpose of the thesis. As already explained, the refinement into sub-functions could go on until every single part of the mechanism.

#### 3.3.2 Teeth

The teeth are involved in many functions. In particular, the creation of the steps is their main role. The relation between the number of blockers  $n_{block}$ , the pitch of the repetition of the teeth  $p_t$  and the resulting step length  $l_s$  if the blockers are distributed regularly is:

$$l_s = \frac{p_t}{n_{block}}. \quad (3.1)$$

Since two blockers are used, the pitch has to respect  $p_t = l_s/2 \leq r_o$ , where  $r_o$  is the required resolution of the movement (E.I.1.1). Functionally, each tooth has three main parts: two angled faces and its bulk. One of the angled faces is used in working and the other in recharge mode. For the first one, it is necessary that the advance is blocked by the interaction of the teeth of the rail and those of the active blocker to create the steps (E.I.2.4). In the other

### 3.3. Transmission & escapement

ID	Function	Parameter	Value
E.I.1	Create steps by using toothed rails		
E.I.1.1	– Step length	$l_s$ (mm)	$r_o = 0.4$
E.I.1.2	– Total number of steps	$n_{steps}$ (—)	$s_o/l_s = 150$
E.I.1.3	– Number of blockers	$n_{block}$ (—)	2
E.I.1.4	– Distance between the blockers	$d_{block}$ (mm)	{1, 1.4, 1.8, ...}
E.I.1.5	– Maximal size of the rail	$w \times h \times l$ (mm <sup>3</sup> )	3x3x100
E.I.1.6	– Maximal size of the blockers	$w \times h \times l$ (mm <sup>3</sup> )	3x5x5
E.I.2	Trigger steps according to the regulating organ		
E.I.2.1	– Working actuation frequency	$f_{steps}$ (Hz)	[0, 25]
E.I.2.2	– Unlock the active blocker		
E.I.2.3	– Displace only one blocker at a time		
E.I.2.4	– Advance blocked when at standstill		
E.I.3	Manage the repartition and nature of the energy		
E.I.3.1	– Force to block along $x$ -axis	$F_s$ (N)	[0, 100]
E.I.3.2	– Friction force along $x$ -axis	$F_f$ (N)	Minimised
E.I.3.3	– Minimal static locking force along $y$ -axis		
		$F_{ul}$ (N)	1
E.I.3.4	– Unlocking energy	$E_{k,trig}$ (μJ)	Minimised
E.I.3.5	– Guide the rail		
E.I.3.6	– Guide the blockers		
E.I.3.7	– Be controlled by the regulating organ in working mode		
E.I.3.8	– Be independent from the regulating organ in recharge mode		

Table 3.5: Internal requirements of the transmission & escapement.

direction, this interaction should not be blocking (E.I.3.9). Finally, the bulk of each tooth provides its mechanical resistance (E.I.3.1). To satisfy the requirements, triangular teeth are used, with the parameters as shown in Fig. 3.3. The face with the angle  $\alpha$ , called *locking* face, is used in working mode and the one with the angle  $\beta$ , the *recharge* face, is used in recharge mode.

Basic mechanics show that a locking force  $F_{lock}$  appears at the interface of two interlocked teeth when one of them is subject to a thrust force  $F_s$ , according to the following rule:

$$F_{lock} = \frac{\mu_s \cdot \tan(\alpha) - 1}{\mu_s + \tan(\alpha)} \cdot F_s, \quad \alpha \in [0^\circ, 90^\circ[, \quad (3.2)$$

where  $\mu_s \in [0, +\infty[$  is the friction factor between the two surfaces and  $\alpha$  the angle of the inclined plane. As intuition suggests, for high values of  $\alpha$ , the locking force is high and it decreases with the angle, until a point where it becomes null and even negative. When it is the case, the system is unstable and a holding force  $F_h$  is necessary to stabilise the system.

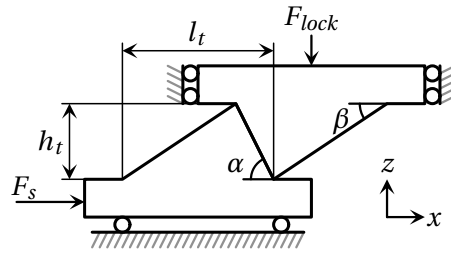


Figure 3.3: Section of the interlocking of a tooth of the rail and the blocker.

Of course, the friction factor also influences the behaviour. Functionally, the locking angle  $\alpha$  has to yield a positive locking force and the recharge angle  $\beta$  a negative one. The critical angle  $\alpha_c$ , defined in (3.3) is the limit of stability and is interesting from the point of view of energy, as will be discussed in Sec. 4.2.2.

$$\alpha_c = \arctan\left(\frac{1}{\mu_s}\right) \quad (3.3)$$

The mechanical resistance of the teeth is not discussed in this thesis. However, many commercial programs permit the evaluation of the stress due to the load. The designer should pay attention, in addition to the static stress, to the maximal stress induced by the impact between the teeth when the rail hits a blocker at the end of a step. Also, wear is to be considered carefully in the selected design where friction plays an important role. The number of teeth on a blocker can be increased to reduce the load on each tooth, but the load will in practice never be evenly distributed between the teeth.

### 3.3.3 Leaf spring stage and recoil spring

On short strokes, leaf spring guides offer interesting perspectives because they are frictionless (no wear) and very accurate. However, they induce a recoil force that may be bothersome, but in the selected functioning principle this force is necessary for dynamic reasons but also to ensure that the system remains locked in case of external accelerations. Therefore, using a leaf spring stage for the blockers tackles two issues at once (functions E.I.2.4 and E.I.3.6). The book from Henein [Hen01] defines the theory necessary to develop leaf spring guides.

Among common structures, the *overconstrained rectilinear parallel spring stage* (Fig. 3.4a) produces a perfectly linear displacement over a very short stroke because of its high recoil force induced by its hyperstatic nature. It is, in terms of energy, beneficial to not have a recoil force too high because it increases the amount of energy required to initiate each step.

By design, the thrust force is applied under the spring stage, therefore, a modified stage is proposed (Fig. 3.4b).

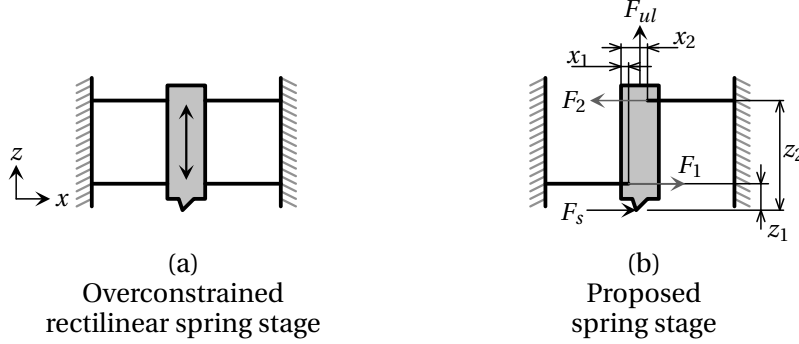


Figure 3.4: Two linear spring stages.

The structure of the proposed stage is particularly designed for this application. Indeed, it is known that a force  $F_s$  can, in a normal situation, only be applied on the teeth in a single direction, and that the unlocking force  $F_{ul}$  is applied vertically. The non-symmetrical load is an opportunity to alter the overconstrained rectilinear parallel spring stage for the best. In terms of complexity and recoil force, keeping only two leaf springs is favourable. The location of the leaf springs should be chosen so as to prevent leaf springs from being under compressive stress, which can yield buckling and the destruction of the springs. Let us assume that the springs have a large spring constant along  $x$  and are attached to the blocker and the bulk by ideal hinges. The reaction forces  $F_1$  and  $F_2$  on the two leaf spring guides when  $F_s$  is applied on the teeth and  $F_{ul}$  is null, are calculated as:

$$F_1 = \frac{z_2}{z_2 - z_1} \cdot F_s \quad \text{and} \quad (3.4)$$

$$F_2 = \frac{z_1}{z_2 - z_1} \cdot F_s, \quad (3.5)$$

where  $F_1$ ,  $F_2$ ,  $z_1$  and  $z_2$  are graphically defined in Fig. 3.4b.

In order to respect the condition that the leaf springs are under tensile stress,  $z_2 > z_1$  has to be respected. Since both  $z_1$  and  $z_2$  are positive and greater than 0,  $F_1$  is larger than  $F_s$  in any case. Its module is however defined by both  $z_1$  and  $z_2$ , with a value of  $F_1$  decreasing as the difference between them increases. A trade-off between the footprint of the proposed spring stage and  $F_1$  is inevitable. On the other hand, under the current hypotheses,  $x_1$  and  $x_2$  do not have influence on the behaviour of the system and can be chosen freely.

The finite value of the spring constant along the  $x$ -axis implies that the stage has a rotational

degree of freedom in the  $xz$ -plane. However, this degree of freedom is limited because of the large value of the spring constant. In opposition, the spring constant is much lower when a vertical force such as  $F_{ul}$  is applied on the blocker, as it bends the leaf springs. So long as the springs are similar in terms of length and spring constant, the mover will be vertically displaced. Analytically calculating recoil force values is complicated because of the nature of the mechanism. Yet, results can be obtained using the finite element method (FEM).

In recharge mode, a force is applied on the blocker along the  $x$ -axis in the other direction, however the teeth have to be designed so that this force creates a force along  $z$  on the blocker. Therefore, the weakness of the spring stage in this direction is not an issue because the leaf spring will bend and separate the blocker from the rail before the leaf springs buckle.

### 3.3.4 Release mechanism

The interface between the regulating organ and the blockers is done through the release mechanism whose tasks include the sporadic linkage of the regulating organ and each blocker alternatively as well as the transmission of sufficient energy to initiate a step. The selected solution is of course strongly related with the retained principle for the regulating organ. Here, the steps are triggered by a horizontal motion along  $x$  in one direction or the other to lift one or the other blocker. Using two symmetrical L-shaped parts — the  $\mathcal{L}$ s — pivoting around pins is extremely simple yet functionally satisfying. There are few defining design options other than the length of each leg of the  $\mathcal{L}$  which defines how the kinetic energy acquired by the part is distributed between the stroke and the force. The exact shape of the  $\mathcal{L}$ , thanks to the addition or subtraction of volume in different places permits to significantly change the moment of inertia of this part, which has its importance in the resulting dynamics. The release mechanism being only temporarily in contact with the mover of the regulating organ to initiate a step is a convenient solution to satisfy functions E.I.3.7 and E.I.3.8.

## 3.4 Conclusion

This chapter shows a practical example of the conceptual design of a movement. The requirements of the movement have been determined, thus providing a basis for the solutions searching process. Once a functional principle was defined, the internal requirements could be expressed and solutions were proposed.

In following chapters, the transmission & escapement and the regulating organ are discussed separately for the sake of clarity, and because the selected modelling strategies for each case differ. Yet, it is crucial to understand that the development of those two subsystems has to be done concurrently to obtain a good overall performance.



## **4 Modelling of the Mechanical Performance of a Movement**

In this chapter, the focus is set on the mechanical performance of the movement. First, a general modelling strategy for the dynamics of a movement is proposed, based on the analysis of the sequential motion of the mobile parts. This strategy is applied to model the case study and its use as a design tool is demonstrated. Later, a similar approach is used to evaluate the energetic performance of the movement. The losses in the energy transmission process are identified and modelled, if possible analytically. In particular, a model for the transmission of kinetic energy by collisions is developed. These two models are finally used to evaluate the impact of machining tolerance on the overall performance of the movement.

### 4.1 Dynamic performance

The displacement of the load is a main objective of any escapement. Therefore, its dynamic behaviour — the evolution along time of the position of the output and all other moving parts of the movement — has to be modelled to verify the conformity of the retained principle with the requirements.

#### 4.1.1 Methodology

Because of the stepper nature of the movement, the dynamic model is a succession of elementary steps, as explained in Sec. 2.4.2. Although each of these steps has its own initial conditions, they all have a similar sequence of events. These sequences are modelled by describing the motion of each mobile subsystem of the movement separately. The specific durations attributed to each subsystem are modelled and functional constraints are defined on their respective values to ensure the correct behaviour of the movement. Obviously, these constraints have to be defined under extreme functioning conditions that are more restrictive. As much as a model, this methodology also provides a precious design tools for the sizing of the different elements of the movement because the external requirements of the movement are translated in terms compatible with the model.

#### 4.1.2 Application to the linear movement

Let us now use this methodology to model the linear movement previously described. The movement's structure is constituted of three mobile groups:

1. the **rail's** displacement is the output displacement;
2. the **blockers** — describing the assembly composed by the release mechanism, a blocker and a leaf spring stage — are responsible for the liberation of the rail;
3. the **mover** of the regulating organ provides the information and energy necessary to initiate steps.

The motion of these groups is summarised in Fig. 4.1 and specific durations are assigned. Their full description is given below.

By design, the advance of the rail is composed of an *advance* and a *waiting* phase. The sum of those two durations yields the *main cycle duration*  $T_a$  to which all specific durations will relate. The main cycle duration, along with the step length  $l_s$ , defines the average output speed  $v_a$ , with respect to (4.1).

$$l_s = v_a \cdot T_a \tag{4.1}$$

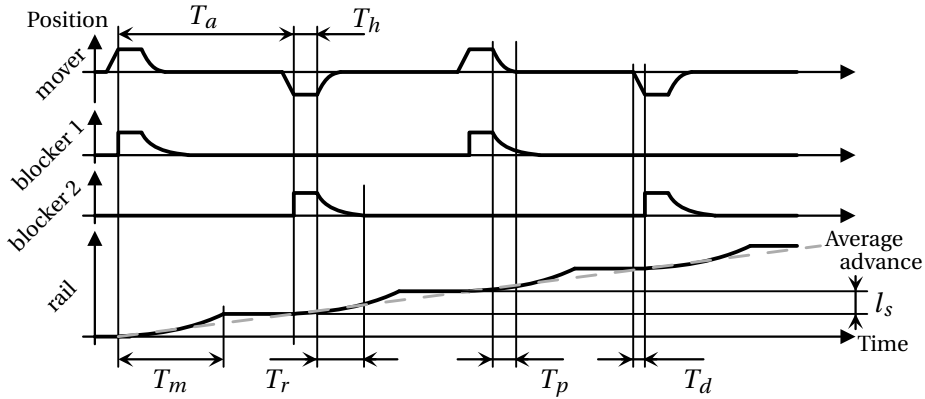


Figure 4.1: Motion of the mobile groups during a sequence of steps and assigned specific durations.

Let us now dissect the run of a step. The advance phase starts as soon as the blocker releases the rail, with a rectilinear accelerated motion, until the second blocker stops it. Then, the rail is idly in wait for the next step to be initiated, with the position remaining constant. The motion model developed here is only valid during one step. In other words, the time variable  $t_* = t - t_{ini}$  is local and always set as 0 when the step starts and so is  $w = x - x_{ini}$ , the displacement of the output.  $t_{ini}$  and  $x_{ini}$  are the time and displacement of the output at the beginning of the step, and  $t$  and  $x$  are the time and displacement of the output initialised at the very first step. A model of the motion over several steps can be analytically obtained by assembling those elementary functions by parts. The variable  $T_m$  ( $m$  stands for main) is assigned to the duration of the advance phase. The motion is ruled by Newton's second law. The displaced mass is composed of the mass of the rail  $m_r$  and that of the load  $m_l$ . This set is under a thrust force  $F_s$ , that depends on the deformation of the spring, and resistive forces because of the linear guiding system  $F_f$  and the load  $F_l$ . Gravitational forces are neglected due to the lightness of the moving parts and the forces at stake. The relation between the time and the position is thus:

$$(m_r + m_l) \cdot \ddot{w}(t_*) = F_s - F_l. \quad (4.2)$$

As a first approximation, the profile of  $F_s$  is not known, therefore, the evolution of the position during one step can be calculated with  $F_s$  constant at its lowest possible value. In the same way, the force of the load  $F_l$  is considered as a worst case, where it is at its maximal value. This provides a margin on the safe side, as the actual acceleration on the rail will be larger.

## Chapter 4. Modelling of the Mechanical Performance of a Movement

---

Evaluated this way, the rail's displacement  $w$  is given in (4.3).

$$w(t_*) = \frac{F_s^{\min} - F_l}{2 \cdot (m_r + m_l)} \cdot t_*^2 \quad (4.3)$$

The overestimated duration of the rail moving phase  $T_m^s$  is the solution to the equation  $w(T_m^s) - x_{ini} = l_s$ , given in (4.4).  $x_{ini}$  can be subtracted because the forces are independent from the position along the stroke; if either of those forces varies, the following is not true.

$$T_m^s = \sqrt{\frac{2 \cdot (m_r + m_l)}{F_s^{\min} - F_l}} \cdot l_s \quad (4.4)$$

Because  $F_s$  is provided by a spring of spring constant  $k_s$ ,  $F_s$  depends on  $x_{ini}$  and a more accurate model can be given.  $F_s$  is expressed as:

$$F_s = k_s (l_{s,f} - l_{s,p} - x_{ini} - w(t_*)), \quad (4.5)$$

with  $l_{s,f}$  and  $l_{s,p}$  respectively the free and prestressed length of the main spring, and  $x_{ini}$  the displacement of the rail at the beginning of the step. In other words,  $(l_{s,f} - l_{s,p} - x_{ini})$  is the initial deformation of the spring. This second-order differential equation (4.2) is easily solved as a function of  $w(t_*)$  (4.6). As expected, the position evolves as a cosine.

$$w(t_*) = - \left( l_{s,f} - \frac{F_l}{k_s} - l_{s,p} - x_{ini} \right) \cos \left( \sqrt{\frac{k_s}{m_r + m_l}} \cdot t_* \right) + l_{s,f} - \frac{F_l}{k_s} - l_{s,p} \quad (4.6)$$

The rail moving phase duration with a thrust spring  $T_m^f$  is calculated by solving  $w(T_m^f) = l_s + x_{ini}$ , for the value of  $x_{ini}$  on the stroke that yields the weakest thrust force. In other words, for the last step of the stroke  $s_o$ , where  $x_{ini} = s_o - l_s$ :

$$\begin{aligned} T_m^f &= \sqrt{\frac{m_r + m_l}{k_s}} \cdot \arccos \left( \frac{l_{s,f} - F_l/k_s - l_{s,p} - x_{ini} - l_s}{l_{s,f} - F_l/k_s - l_{s,p} - x_{ini}} \right) \\ &= \sqrt{\frac{m_r + m_l}{k_s}} \cdot \arccos \left( \frac{l_{s,f} - F_l/k_s - l_{s,p} - s_o}{l_{s,f} - F_l/k_s - l_{s,p} - s_o + l_s} \right). \end{aligned} \quad (4.7)$$

Let us now focus on the blockers. The motion of a blocker is made of four different phases. During the *release* phase, the blocker is lifted by the mover so that its teeth lose contact with those of the rail to initiate a step. Then follows an *active idle* phase during which the blocker

is kept away from the rail. Later, the blocker is liberated and is driven against the rail by the recoil spring; this is the *return* phase. Finally, a *passive idle* phase takes place while the blocker rests against the rail.

The release phase is tightly bonded with the motion of the mover and is not modelled. It is comprised in the motion of the mover of the regulating organ and discussed at the end of this section. In the same manner, the active idle phase is completely dependent on the regulating organ. The modelling of the return phase, on the other hand, is very similar to what was done earlier, with the displacement of the blocker  $x_b$  given by parts (valid for  $t \in [0, T_r]$ ,  $T_r$  being the return duration). The mass of the blocker  $m_b$  is only subject to the recoil force  $F_r$ . The total displaced mass  $m_{b,e}$  also includes the pivoting of the  $\mathcal{L}$  of the release mechanism. To ensure the blocking behaviour of the escapement, at standstill, the blockers should be constrained against the rail by a certain force. Thus, the idle value of  $x_b$  is  $x_{b,0} > 0$ . The return duration  $T_r$  being the time for the blocker to reach that position from its furthestmost position  $x_{b,m} > x_{b,0}$  depends on the magnitude of  $F_r$ . With a margin on the safe side,  $T_r^s$  can be calculated using the lowest value of  $F_r$  along the stroke of the blocker, as follows:

$$T_r^s = \sqrt{\frac{2 \cdot m_{b,e}}{F_r^{min}} \cdot (x_{b,m} - x_{b,0})}. \quad (4.8)$$

With the assumption that  $F_r$  depends linearly on the displacement of the blocker with a spring constant  $k_r$ , the evolution of the blocker position  $x_b$  is given by (4.9), very similarly to previously. For other force profiles, there might not be analytical solutions.

$$x_b(t_*) = x_{b,m} \cdot \cos\left(\sqrt{\frac{k_r}{m_{b,e}}} \cdot t_*\right) \quad (4.9)$$

The newly calculated blocker return duration  $T_r^f$  is thus calculated as:

$$T_r^f = \sqrt{\frac{m_{b,e}}{k_r}} \cdot \arccos\left(\frac{x_{b,0}}{x_{b,m}}\right). \quad (4.10)$$

Last, the displacement of the mover of the actuator is modelled using three specific durations to describe the mover rising  $T_d$ , holding  $T_h$  and return  $T_p$  durations. The mover rising duration is thus the delay between the moment when the signal is given to initiate a step and the moment when the mover finishes separating the blocker and the rail. The mover holding duration  $T_h$  is a parameter that the regulating organ can control and corresponds to the time during which the mover holds the blocker away from the rail. This value should be as short as

possible in terms of energy consumption of the regulating organ, yet it might be necessary to introduce this dead time in order to ensure that the steps are initiated correctly. Finally, the mover return duration describes the time necessary to the mover to retrieve its idle position.

The mover rising  $T_d$  and return  $T_p$  durations are dependent on the regulating organ of the movement. Because of this, they are not modelled here, but they represent requirements for the latter. With experience, the designer can choose reasonable values. This however once again shows the importance of an iterative design process. In the particular case studied here, the regulating organ comprises an electric actuator whose modelling is done using the FEM. The integration of these specific durations in the design process will be shown in chapter 5.

All considered together, these definitions of the motion of the different parts of the system provide an insight into the global behaviour of the movement. The advantage of this model is that it can be transformed into a powerful design tool.

### The model as a design tool

The same division of the movement as before is used, with the motion of the rail, the blockers and the mover of the actuator considered separately. In order to obtain the output mechanical performance stated in the requirements, the approach is to impose conditions — or functional constraints — on the duration of each phase of the motion.

The first constraint regards the size of the steps  $l_s$ . Since  $l_s$  is also the resolution of the output, it has to be lower or equal to the required resolution  $r_o$ . This constraint is more static than dynamic. It nevertheless has an impact on the dynamics because of (4.1). Indeed, it permits to calculate the shortest main cycle time required by the specifications as:

$$T_a^{lim} = \frac{l_s}{v_o}. \quad (4.11)$$

This highlights the importance of the balance between the desired maximal speed  $v_o$  and the displacement resolution given by the step length  $l_s$ . The trade-off between a small resolution and a reasonable actuation frequency (inverse of  $T_a^{lim}$ ) is a design choice. To ensure that the output speed can be reached in all conditions, every single step along the stroke should be feasible in a shorter time than  $T_a^{lim}$ .

From the point of view of the rail, the only phase that matters is the moving phase, whose duration is  $T_m$ . Therefore, the functional constraint is simply  $T_m < T_a^{lim}$ .

The case of the blockers is slightly more complicated. Since the blockers are used alternatively,

the maximal duration of the combination of the blocker release, active idle and return phases can be as long as the addition of the main cycle and rail moving durations. However, it is safer to still consider that at the beginning of the following step, the blocker should be back into place, with the possibility to increase the maximal actuation frequency of the system later on by relaxing this constraint. Also, the release phase as modelled above is instantaneous and coupled with the mover rising phase. The functional constraint on the blockers is thus  $T_d + T_h + T_r < T_a^{lim}$ .

The relaxed constraint is obtained by overlapping the end of a step with the beginning of the next,  $T_a^{lim}$  could be replaced by  $T_a^{lim} + T_m$ . In this case, given that  $T_m \geq T_d$ , which can often be the case, the functional constraint becomes  $T_h + T_r < T_a^{lim}$ . When  $T_a^{lim}$  is extremely short, the latter formulation leaves only very little safety margin.

Finally, the functional constraint of the mover is straightforward. The duration of the combination of the rising, holding and return phases should be shorter than the limit main cycle time:  $T_d + T_h + T_p < T_a^{lim}$ .

Since no realisation is perfect and because of environmental changes (machining tolerance, temperature, humidity, wear, etc.),  $T_a^{lim}$  is slightly modified as follows:

$$T_a^* = S \cdot T_a^{lim}, \quad (4.12)$$

with a safety factor  $S > 1$  given in the requirements. This factor further enhances the certainty of success of the design, but at the cost at reduced performance. Equations 4.13 to 4.16 summarise the functional constraints on the movement.

$$l_s \leq r_o \quad (4.13)$$

$$T_m < T_a^* \quad (4.14)$$

$$(T_h + T_r) < T_a^* \quad (4.15)$$

$$(T_d + T_h + T_p) < T_a^* \quad (4.16)$$

Finally, the maximal speed of advance  $v_a$  of the movement can be calculated using the specific durations above. Knowing the length of a step  $l_s = p_t/2$ , the speed is given as the product between the latter and the inverse of the limiting specific duration:

$$v_a^{max} = l_s \cdot \frac{1}{\max(T_m, T_h + T_r, T_d + T_h + T_p)} = \frac{p_t}{2 \cdot \max(T_m, T_h + T_r, T_d + T_h + T_p)}. \quad (4.17)$$

### 4.2 Energetic performance

The other major aspect of the performance of an escapement-based movement is its energy management. In particular, the way the transmission & escapement subsystem distributes the energy in the movement is interesting.

#### 4.2.1 Methodology

The model is based on the dissection of the working of the movement in steps, as previously done. Over the course of the step, the input and output energy in certain parts in the movement is analysed. With these values, energy factors as introduced in Sec. 2.4.1 are defined and calculated. Their values are then used to compare the theoretical performance of a movement with the requirements.

The evaluation of the energy can be done in several ways, typically following the energy flow downstream (calculating the output energy with respect to the input energy) or upstream (evaluating the required input energy for a certain output energy). The first solution is favoured in cases where the data of the energy stocks are given or for the analysis of an existing system. In opposition, when the energy stocks have to be sized, it is preferable to start with the required output energy as a starting point. The energy losses are modelled all the way up to the energy stock which can then be sized correctly. Both approach yield the same result but require a different way of thinking from the designer.

#### 4.2.2 Application to the linear movement

Let us model the energy flows in the studied linear movement. To do so, the transmission & escapement plays a central role. The input energy comes from the main energy stock ( $E_{in,a}$ ) as well as the energy stock in the regulating organ ( $E_{in,d}$ ). The previous directly goes to the output ( $E_{out}$ ) through the transmission, whereas the latter is mostly used for control purposes. Let us apply the upstream methodology to define the required quantity of input energy to provide the output energy for one step. As a reminder, the energy flows in the escapement are shown in Fig. 4.2. The *thrust* energy comes from the main energy stock and the load, and the *control* energy is provided by the energy stock of the regulating organ.

#### Rechargeable energy

The energy transfer from the main energy stock and the output energy is extremely simple, since the main spring simply pushes the rail. The only losses therefore consist in the work



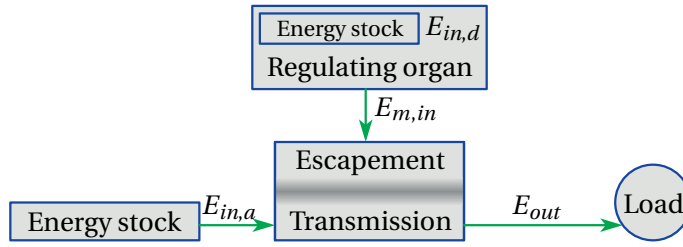


Figure 4.2: Energy flows in the linear movement.

$W_{F_{b,r}}$  of the parasitic forces of the bearings of the rail. We can therefore define  $E_{in,a}$  as:

$$E_{in,a} = E_{out} + W_{F_{b,r}}. \quad (4.18)$$

The model for the evaluation of  $W_{F_{b,r}}$  is of course dependent on the implementation choices. Plain bearings create a friction force where ball bearings create mostly negligible friction but are more expensive, more fragile and slightly less good dynamically.

Let us denote  ${}^t E_{out}$  the desired output energy, as given in the requirements. In many cases,  ${}^t E_{out} \neq E_{out}$ , in particular if the  $E_{in,a}$  is provided by a spring. In this case, the energy factors and true energy factors differ. Since this is academically not particularly interesting, it is not discussed any further in this chapter.

### Disposable energy

Since the disposable energy  $E_{in,d}$  is used for control purposes, it is supposed to be small — in fact, as small as possible — compared to the rechargeable energy. In a way,  $E_{in,d}$  can be considered as pure energy losses in the systemic approach. Yet, its data conveying role makes it essential. Let us therefore start the evaluation of  $E_{in,d}$  from the interaction between thrust and control energy and identify where energy is consumed from there on. Using the upstream methodology, we can identify that energy (Fig. 4.3) is sequentially consumed in:

1. the bending of the recoil spring for the displacement of the blocker ( ${}_L E_{rs}$ );
2. the friction between the blocker and the rail ( ${}_L E_l$ );
3. the displacement of the release mechanism ( ${}_L E_{rm}$ );
4. the collision-based energy transmission (energy transmission between the regulating organ and the release mechanism,  ${}_L E_c$ );
5. the regulating organ ( ${}_L E_{ro}$ ).
6. The residual kinetic energy is not consumed, but corresponds to the excess motion energy stored in the mover of the regulating organ.

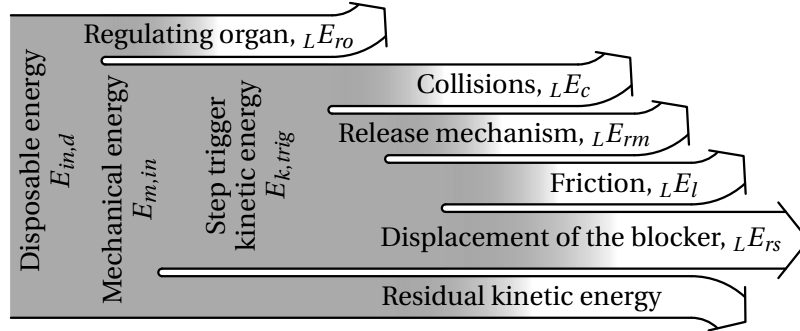


Figure 4.3: Distribution of the control energy.

In this section, only escapement-related energy will be modelled, leaving the regulating organ out of the problem because of its specificities. It will be further discussed in chapters 5 and 6. The energy modelled here, called the *step trigger kinetic* energy  $E_{k,trig}$ , is transferred from the mover of the regulating organ to the escapement and is independent from the regulating organ. This energy is mechanical and transferred as a force over a given linear displacement. The model predicts the theoretical minimal kinetic energy to initiate a step, no safety factor is therefore taken into account.

#### Step 1: Displacing the blocker

We want to calculate the amount of input energy necessary to let through — or escape — a certain amount of mechanical energy  $E_{m,ad}$ . This energy is of course dispensed by a force applied on a certain distance. When the movement is in idle, this force,  $F_s$ , is sustained by a blocker. The blocker has to be displaced to release the energy. To displace the blocker, the recoil spring has to be compressed. The exact force profile of the recoil spring may vary, because it is, in the discussed implementation, a feature of the linear guide. It can easily be modelled using the FEM if it cannot be analytically. Let us nevertheless work under the assumption that the recoil force  $F_r$  is proportional to the displacement, with a spring constant  $k_r$ . The deformation of the spring in idle being  $x_{b,0}$  and the travelled distance to release the teeth  $h_t$ , the work of the recoil force is:

$${}_L E_{rs} = W_{f,r} = \frac{1}{2} \cdot k_r \cdot h_t (2x_{b,0} + h_t). \quad (4.19)$$

#### Step 2: Unlocking the rail

Friction is also opposed to the motion of the blocker. It was shown in Sec. 3.3.2 that  $F_s$  applied on an inclined plane of angle  $\alpha$  with a friction factor  $\mu$  results in a locking force  $F_{lock}$ :

$$F_{lock} = \frac{\mu \cdot \tan(\alpha) - 1}{\mu + \tan(\alpha)} \cdot F_s, \quad \alpha \in [0^\circ, 90^\circ]. \quad (4.20)$$

Let us assume that  $F_{lock} \geq 0$ , or in other words that the system is naturally locking. This is energetically better since it only requires energy to trigger a step, and not to maintain the position. Friction models show that the friction factor differs if the two surfaces in contact have a relative displacement (dynamic) or not (static). The dynamic friction factor  $\mu_d$  for a pair of materials is usually lower than the static friction factor  $\mu_s$ . It is clear that the static locking force  $F_{lock,s}$  is greater than the dynamic locking force  $F_{lock,d}$ . Thus, when the escapement is at rest, the locking force is  $F_{lock,s}$ . An unlocking force  $F_{ul}$  larger than this has to be applied in order for the blocker to start moving away from the rail. However, as soon as the blocker starts moving, the dynamic friction factor is applied, which means that the static locking force does not produce any work. Therefore, the losses generated by the locking force correspond to the work  $W_{F,lock}$  of the dynamic locking force  $F_{lock,d}$ :

$${}_L E_l = W_{F,lock} = F_{lock,d} \cdot h_t, \quad (4.21)$$

where  $h_t$  is the height of a tooth. Indeed, this force is present until the rail and the blocker lose contact.

### ***Step 3: Displacing the release mechanism***

Motion is always subject to losses, be they from friction or changes in potential energy. The case of the release mechanism is rather straightforward. In the discussed embodiment, the release mechanism consists in a small part pivoting for a small angle around a pin. There is thus friction around the pin, as well as a likely change of potential energy of the centre of mass of the rotating part. Since the movement is to be embedded in a hand-held device, the change of potential energy should be as limited as possible so as to provide a behaviour independent of the attitude of the device. The very light weight as well as short displacement of the part points towards the validity of this hypothesis. On the other hand, the light weight of the part also yields negligible friction forces. It therefore yields  ${}_L E_{rm} = 0$ . This should nevertheless be verified with the numerical application.

### ***Step 4: Collision-based energy transmission***

Last but not least, let us analyse the losses due to the energy transmission from the regulating organ to the release mechanism. It was decided that this transmission is done by the collision of a part of the regulating organ and an  $\mathcal{L}$  of the release mechanism. In a collision, the kinetic energy of the impacting particle is transferred, more or less efficiently, to the impacted particle. In the discussed movement, the collision-based energy transmission has two roles. Firstly, the first collision has to be such that it creates a large enough force to overcome the static locking force. Secondly, the hypothetical subsequent collisions should permit to transfer enough energy to release the rail. The model developed is inspired by the work of Conus [Con07]. The exhaustive mathematical development is given in appendix B.

## Chapter 4. Modelling of the Mechanical Performance of a Movement

Let us define a model by reducing the problem to that of the collision of two free particles in a unidimensional space without friction. The *provider* is a particle of mass  $m$ , animated right before the collision by a speed  $v$ . It transmits energy to a slower moving particle — the *receiver* — of mass  $m'$  and speed  $v'$ . After the collision, the provider and the receiver have speeds  $\tilde{v}$  and  $\tilde{v}'$  respectively. As a rule, all variables with an apostrophe concern the receiver. The position is denoted by the variable  $x$ . In the application, the provider is the mover of the regulating organ, and the receiver is the blocker through the release mechanism.

Let us start by calculating the efficiency of the first collision. Collision theories and the law of conservation of momentum yield the equations system (4.22), where  $\epsilon \in [0, 1]$  is the coefficient of restitution. However, for the development, we will consider  $\epsilon \in ]0, 1[$  because of mathematical issues that arise because of 0 and 1, which are ideal cases that cannot be physically encountered.

$$\begin{cases} m\tilde{v} + m'\tilde{v}' = mv + m'v' \\ \tilde{v}' - \tilde{v} = \epsilon(v - v') \end{cases} \quad (4.22)$$

The efficiency of a collision  $\eta_{fc}$  can be defined as the increase of kinetic energy of the receiver after the collision divided by the kinetic energy of the provider:

$$\eta_{fc} = \frac{m'}{m} \cdot \frac{\tilde{v}'^2 - v'^2}{v^2} = k_m \cdot \frac{(1 + \epsilon)(1 + \epsilon + 2u + 2uk_m)}{(1 + k_m)^2(1 + u)^2}, \quad (4.23)$$

where  $k_m = m'/m$  and  $u = v'/(v - v')$ .

If the two particles are subject to external forces  $f$  and  $f'$  respectively, they will be under an acceleration  $a = f/m$  and  $a' = f'/m'$ . If the condition  $a > a'$  is respected, a series of collisions will occur because the provider will accelerate faster than the receiver and eventually always catch up with it (Fig. 4.4).

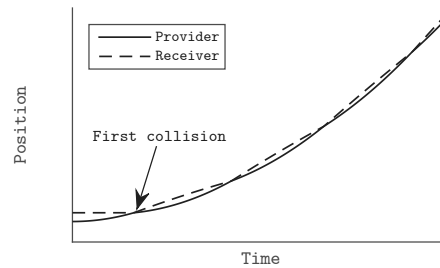


Figure 4.4: Example of a series of collisions between two particles under accelerations  $a$  and  $a'$ , with  $a > a'$ , and  $v'_0 = 0$ .

Tedious calculations permit to evaluate the time and position of each collision in the series. The model assumes that the two particles are under constant forces, and thus accelerations. Between two collisions, the particles follow their own trajectory under the influence of their respective external forces. Each collision is governed by (4.22), which gives the value of the speed of the particles after the collision. The time and position of the  $(n + 1)^{\text{st}}$  collision can therefore be written:

$$\begin{aligned} t_n &= t_0 + \sum_{i=0}^n \frac{2(\tilde{v}'_i - \tilde{v}_i)}{(a - a')} = t_0 + \sum_{i=0}^n \frac{2\epsilon(v_i - v'_i)}{(a - a')} t_0 + \sum_{i=0}^n \frac{2\epsilon(v_0 - v'_0)\epsilon^i}{(a - a')} \\ &= t_0 + \frac{2\epsilon(v_0 - v'_0)}{(a - a')} \sum_{i=0}^n \epsilon^i = t_0 + \frac{2\epsilon(v_0 - v'_0)}{(a - a')} \frac{1 - \epsilon^{n+1}}{1 - \epsilon}, \end{aligned} \quad (4.24)$$

and

$$x_n = x(t_0) + 2a' \frac{(v_0 - v'_0)^2}{(a - a')^2} \frac{\epsilon^2(1 - \epsilon^{2n})}{1 - \epsilon^2} + 2\epsilon \frac{(v_0 - v'_0)}{(a - a')^2} \frac{(K_1 v_0 + K_2 v'_0)(1 - \epsilon^n)}{(m + m')(1 - \epsilon^2)(1 - \epsilon)}, \quad (4.25)$$

where

$$K_1 = (a - a')(1 + \epsilon)m + 2\epsilon^2(m + m')a' \quad (4.26)$$

$$K_2 = (a - a')(m' - \epsilon m) - \epsilon^2(m + m')(a + a'). \quad (4.27)$$

Interestingly, (4.24) and (4.25) converge when  $n \rightarrow \infty$ . The values of  $t_\infty$  and  $x_\infty$  are:

$$t_\infty = t_0 + \frac{2\epsilon(v_0 - v'_0)}{(1 - \epsilon)(a - a')} \quad (4.28)$$

and

$$x_\infty = x(t_0) + 2a' \frac{(v_0 - v'_0)^2}{(a - a')^2} \frac{\epsilon^2}{1 - \epsilon^2} + 2\epsilon \frac{(v_0 - v'_0)}{(a - a')^2} \frac{K_1 v_0 + K_2 v'_0}{(m + m')(1 - \epsilon^2)(1 - \epsilon)}. \quad (4.29)$$

The implication is that for a time  $t > t_\infty$ , the two particles behave as a single particle of mass  $m + m'$  and subject to the two forces  $f$  and  $f'$ . It can then be proved that the speed of the combined particle is:

$$v|_{t > t_\infty} = \frac{f + f'}{(m + m')} t + \frac{m v_0 + m' v'_0}{(m + m')}. \quad (4.30)$$

## Chapter 4. Modelling of the Mechanical Performance of a Movement

---

The speed  $v_\infty$  at the moment  $t = t_\infty$  is expressed as:

$$v_\infty = \frac{a((1+\epsilon)mv_0 + ((1-\epsilon)m' - 2\epsilon m)v'_0) - a'(((1-\epsilon)m - 2\epsilon m')v_0 + (1+\epsilon)m'v'_0)}{(1-\epsilon)(a-a')(m+m')}. \quad (4.31)$$

As demonstrated in appendix, the exact same result can be obtained by considering that the coefficient of restitution is null. In other words, at the time of the first impact, the two particles immediately merge as a single particle which is then accelerated by the two external forces. That way, it is however impossible to evaluate the position of the two particles for  $t < t_\infty$ .

Let us finally analyse the losses incumbent to the infinite series of collisions. The factor  ${}^R_L E_c$  (4.32) represents the relative losses: the difference between the initial and the final total kinetic energy in the system, divided by the initial kinetic energy of the provider.

$${}^R_L E_c = \frac{\frac{1}{2}mv_0^2 + \frac{1}{2}m'v_0'^2 - \frac{1}{2}(m+m')v_\infty^2}{\frac{1}{2}mv_0^2} \quad (4.32)$$

Because the speed reached at the time  $t = t_\infty$  is the same as if a single collision with  $\epsilon = 0$  had happened, the loss of kinetic energy of the whole system is the same whatever the value of  $\epsilon$ . Let us therefore consider  $\epsilon = 0$ . Replacing  $v_\infty$  by its value and simplifying reduces the result to:

$${}^R_L E_c = \frac{k_m}{1+k_m} \frac{(v_0 - v_0')^2}{v_0^2}. \quad (4.33)$$

It is observed that the losses heavily depend on the speed difference between the two particles at the beginning of the series of collisions. The closer the speed, the lower the losses. In addition, the losses decrease as the provider becomes heavier.

Let us now apply this model to the linear movement. The provider corresponds to the mover of the regulating organ and the receiver is the group of parts composed of the mobile parts of the release mechanism and the blocker. The features of the mover are not known beforehand, but can be given as requirements for the regulating organ. The model only requires the mass of the mover  $m_a$  and the material of the interface between the mover and the release mechanism, which defines  $\epsilon$ . On the other hand, the receiver's equivalent mass  $m_{\mathcal{L},e}$  is a composition of the geometric and mass properties of the release mechanism and the blocker:

$$m_{\mathcal{L},e} = \frac{I_{\mathcal{L}} + m_b \cdot l_{\mathcal{L},b}^2}{l_{\mathcal{L},m}^2}, \quad (4.34)$$

where  $I_{\mathcal{L}}$  is the moment of inertia of the  $\mathcal{L}$ , calculated numerically,  $m_b$  the mass of the blocker,  $l_{\mathcal{L},b}$  the distance between the pivot of the  $\mathcal{L}$  and the point of contact with the blocker, and  $l_{\mathcal{L},m}$  the distance between the pivot and the point of contact with the mover (both are shown in Fig. 4.6).

The other influential parameters are the respective speeds of the provider and receiver at the time of the first collision. The structure of the escapement is such that the receiver is at rest at the moment of the impact, which transforms the equation of the losses as:

$${}^R_L E_c |_{v'_0=0} = \frac{k_m}{1 + k_m}. \quad (4.35)$$

$k_m \in ]0, \infty[$ , therefore losses are inevitable. Nevertheless, the function is monotonous so in order to minimise the losses,  $k_m$  should be minimised.

If  $t_{\infty}$  and  $x_{\infty}$  are really small (how small exactly is application dependent), it is guaranteed that all collisions in the series happen. Under this condition, the relative losses  ${}^L E_c$  can be translated into the efficiency  $\eta_{sc}$  of a series of collisions:

$$\eta_{sc} = 1 - \frac{k_m}{1 + k_m}. \quad (4.36)$$

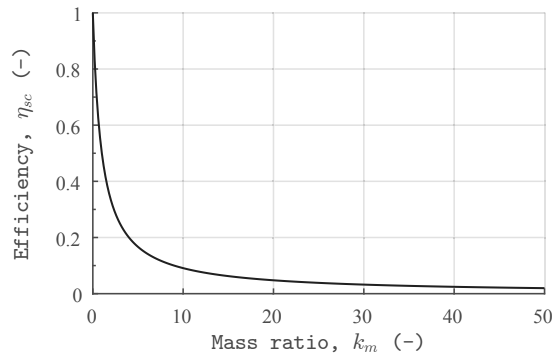


Figure 4.5: Evolution of the efficiency  $\eta_{sc}$  of a series of collisions with respect to the mass ratio  $k_m$ .

### **Global: Triggering a step**

To finalise this model, let us relate the different parts analysed above to the behaviour of the escapement. The mover of the regulating organ, used as a hammer hits the release mechanism. This collision has to produce a force large enough to overcome the static locking force and the recoil force at rest. Evaluating the force on the blocker consecutive to the collision is done using the elasticity of the release mechanism. Fig. 4.6 shows more detail of

the  $\mathcal{L}$  of the release mechanism.

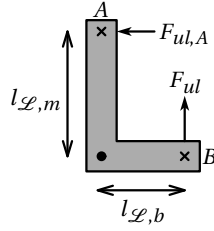


Figure 4.6: Scheme of the release mechanism.

It is given that the input energy is transmitted to the  $\mathcal{L}$  at point  $A$ . So long as the unlocking force  $F_{ul}$  is low ( $F_{ul} \leq F_{lock} + F_{r,ini}$ ), the point  $B$  cannot move. Therefore, let us assume that the point  $B$  is fixed and that the pivot is ideal. The input energy deforms the  $\mathcal{L}$ . If the relation between the displacement  $x_{\mathcal{L},A}$  of  $A$  and the force applied at this point is linear, the deformation energy  $E_{\mathcal{L},def}$  is similar to that of a spring:

$$E_{\mathcal{L},def} = \frac{1}{2} k_{\mathcal{L}} \cdot x_{\mathcal{L},A}^2, \quad (4.37)$$

with  $k_{\mathcal{L}}$  the spring constant of the  $\mathcal{L}$  in these conditions.

Of course, since an elastic part is deformed, a force is created in point  $B$ . Because the two legs of the  $\mathcal{L}$  are of different lengths, the force in  $B$ ,  $F_{ul,b}$ , created by the force in  $A$ ,  $F_{ul,A}$ , follows:

$$F_{ul,b} = \frac{l_{\mathcal{L},m}}{l_{\mathcal{L},b}} F_{ul,A} = l_{\mathcal{L}}^* F_{ul,A}. \quad (4.38)$$

Thus, if  $F_{ul,b} > F_{lock} + F_{r,ini}$ , the point  $B$  is no longer locked and the  $\mathcal{L}$  starts pivoting around its axis. The minimal value of the unlocking force  $F_{ul}^{min}$  is equivalent to a force in  $A$   $F_{ul,A}^{min} = F_{ul}^{min} / l_{\mathcal{L}}^*$ . The corresponding displacement of the point  $A$  is thus:

$$x_{\mathcal{L},A} = \frac{F_{ul,A}^{min}}{k_{\mathcal{L}}} = \frac{F_{ul}^{min}}{k_{\mathcal{L}} \cdot l_{\mathcal{L}}^*}. \quad (4.39)$$

Merging (4.37) and (4.39), we obtain:

$$E_{ul,b} = \frac{1}{2} k_{\mathcal{L}} \left( \frac{F_{ul}^{min}}{k_{\mathcal{L}} \cdot l_{\mathcal{L}}^*} \right)^2, \quad (4.40)$$

where  $E_{ul,b}$  is the mechanical energy required to initiate a motion of the blocker.



This energy has to be provided by the first collision between the mover and the release mechanism because later collisions will be less energetic. Therefore, let us recall (4.23) that gives the efficiency of a single collision in terms of increasing the kinetic energy of the receiver. Since the  $\mathcal{L}$  is at rest before the first collision, we have  $u = 0$ , which gives:

$$\eta_{fc|u=0} = k_m \cdot \left( \frac{1 + \epsilon}{1 + k_m} \right)^2 \quad (4.41)$$

We finally obtain the minimal kinetic energy of the mover to unlock the blocker  $E_{k,ul}$ :

$$E_{k,ul} = \frac{E_{ul,b}}{\eta_{fc}} = \frac{1}{2} \cdot \frac{1}{k_m \cdot k_{\mathcal{L}}} \cdot \left( \frac{F_{ul}^{min} (1 + k_m)}{l_{\mathcal{L}}^* (1 + \epsilon)} \right)^2. \quad (4.42)$$

This condition is required but not necessarily sufficient. Indeed, it is necessary to unlock the blocker, but the work of the recoil and dynamic holding forces have to be taken into account. Let us call the displacement energy  $E_d$  the sum of those two works. Two scenarios may happen: either the first collision provides enough energy to the receiver to displace the blocker and release the rail, or a series of collisions takes place. The displacement energy  $E_d$  is the energy required from the mover to displace the blocker. It is given as:

$$E_d = \frac{W_{f,r} + W_{E,lock}}{\max(\eta_{sc}, \eta_{fc})}. \quad (4.43)$$

Therefore, the minimal step trigger kinetic energy  $E_{k,trig}$  is calculated as follows:

$$E_{k,trig} = \max(E_d, E_{k,ul}) \quad (4.44)$$

The kinetic energy of the mover of the regulating organ  $E_{m,in}$  should therefore be greater than  $E_{k,trig}$ .

### Evaluation of the energy factors

With the input and output energy identified and modelled, it is possible to actually compute the energy factors as suggested in Sec. 2.4.1. Let us introduce the *mechanical relative energy factor*  $\eta_{r,m}^*$  that relates the admitted mechanical energy to the step trigger kinetic energy:

$$\eta_{r,m}^* = \frac{E_{m,ad}}{E_{k,trig}}. \quad (4.45)$$

This factor can be computed directly by using the equations above, giving the energy factor for a single step. However, over the whole stroke of the movement, the calculation of the energy factor is slightly altered because the mechanism is designed to work without any sensor. Therefore, it is necessary that the step trigger energy is sufficient to initiate steps in the toughest conditions, in other words, when the thrust force is maximal. The relative energy factor over the stroke  ${}_s\eta_{r,m}^*$  is:

$${}_s\eta_{r,m}^* = \frac{{}_sE_{m,ad}}{{}_sE_{k,trig}} = \frac{{}_sE_{m,ad}}{n_{steps} \cdot \max(E_{k,trig})}, \quad (4.46)$$

with  $n_{steps}$  the number of steps on the stroke, and  ${}_sE_{m,ad}$  the total escaped energy. The latter is equal to  $E_{in,a}$  that was introduced earlier.

Since the losses between the energy stock and the load are solely due to friction, the required energy  ${}^tE_{out}$  can be linked to the necessary rechargeable energy  ${}^tE_{in,a}$  by adding the work of the friction force to the previous. If the exact friction profile is known, the profile of the thrust force can be adapted accordingly. The true relative energy factor over the stroke  ${}^t\eta_{r,m}^*$  will also be used.

### 4.2.3 Conclusion

An analytical model of the energetic performance of the discussed linear escapement has been developed. It predicts the amount of energy required to trigger a step. Its formulation is of course based on the technical solutions retained for the embodiment of the movement but the methodology can be applied to other movements.

## 4.3 In-depth study of the overall performance

Models are interesting in the perspective of understanding the importance of design parameters in the performance of the device. The models being analytical, they can be studied analytically as mathematical functions or numerically using a computer. The large number of parameters (15) makes a complete analysis tedious. Therefore, we shall inspect the impact on the performance in the neighbourhood of a given set of parameter values.

### 4.3.1 Selected values of the parameters

The values given in Table 4.1 correspond to a movement for the study case discussed in chapter 3. The thrust force has to be larger than the sum of the resistive force of the load and the friction force on the rail anywhere along the stroke, to ensure that the output is displaced

### 4.3. In-depth study of the overall performance

Parameter	Description	Reference value	Dynamic model	Energy model
Requirements				
$s_o$	Stroke (mm)	50		✓
$r_o$	Resolution (mm)	0.4	✓	✓
$F_l$	Force of the load (N)	40		✓
$F_f$	Friction force on the rail (N)	1		✓
Modelled information				
$v_a^{th}$	Theoretical advance speed (mm·s <sup>-1</sup> )	67.4	✓	
$t_s^* \eta_{d,m}^*$	True mechanical disposable energy factor (—)	20.9		✓
$t_s^* \eta_{r,m}^*$	True mechanical relative energy factor (—)	22.0		✓
Free parameters				
$k_s$	Main spring constant (N·m <sup>-1</sup> )	400		✓
$l_{s,f}$	Free length of the main spring (mm)	240		✓
$l_{s,p}$	Preload length of the main spring (mm)	85		✓
$p_t$	Pitch of the teeth (mm)	0.8	✓	✓
$\alpha$	Angle of the locking face (°)	87		✓
$h_t$	Height of the teeth (mm)	0.2		✓
$m_b$	Mass of a blocker (g)	0.5	✓	✓
$\mu_s$	Static friction factor (—)	0.4		✓
$\mu_d$	Dynamic friction factor (—)	0.1		✓
$l_{\mathcal{L},b}$	Distance between the pivot of the $\mathcal{L}$ and the blocker (mm)	7.2		✓
$l_{\mathcal{L},m}$	Distance between the pivot of the $\mathcal{L}$ and the mover (mm)	12.2		✓
$I_{\mathcal{L}}$	Moment of inertia of the $\mathcal{L}$ (g·mm <sup>2</sup> )	6.6		✓
$k_{\mathcal{L}}$	Stiffness of the $\mathcal{L}$ (N·m <sup>-1</sup> )	$450 \cdot 10^3$		✓
$k_r$	Recoil spring constant (N·m <sup>-1</sup> )	1000	✓	✓
$x_{b,0}$	Standstill deformation of the recoil spring (mm)	0.1	✓	✓
$x_{b,m}$	Maximal deformation of the recoil spring (mm)	0.4	✓	
$\epsilon$	Coefficient of restitution (—)	0.9		✓
$m_a$	Mass of the mover (g)	1		✓
$T_d$	Mover rising duration (ms)	} 5	✓	
$T_h$	Mover hold duration (ms)		✓	

Table 4.1: List of parameters of the dynamic and energy models of the escapement

## Chapter 4. Modelling of the Mechanical Performance of a Movement

---

fast enough. The other values have been defined based on mechanical models, analytical or numerical (that are not relevant for this research), to ensure the resistance of the parts and their feasibility. Experimental results, obtained on a prototype having mostly similar parameters values, are given and discussed in chapter 6.

### Comments on the dynamic performance

The theoretical advance speed  $v_a^{th}$  is the maximal speed that can be attained by the escapement. This value is evaluated independently from the regulating organ and the load and its associated dynamics. In other words, it is considered that the dynamics of the advance of the rail and the output (advance duration,  $T_m$ ) are not the limiting factor in terms of maximal speed of advance. Thus, (4.47) permits to evaluate  $v_a^{th}$ .

$$v_a^{th} = \frac{p_t}{2 \cdot (T_d + T_h + T_r)} \quad (4.47)$$

The values  $T_d$  and  $T_h$  are, as previously explained, set as minimal requirements for the regulating organ (5 ms), and  $T_r = 0.93$  ms (4.10) with the chosen parameter values. The numerical value  $67.4 \text{ mm} \cdot \text{s}^{-1}$  is coherent with the required speed for the case study (Sec. 3.1) and provides a comfortable margin, with a speed more than 6 times larger. In addition, it is obvious that the durations related to the regulating organ are here more limiting than  $T_r$ .

### Comments on the energetic performance

The true relative energy factor informs on the performance of the escapement for the task that it is assigned. With a true mechanical relative energy factor  ${}^t_s\eta_{r,m}^* = 22.0$  (and a true mechanical disposable energy factor  ${}^t_s\eta_{d,m}^* = 20.9$ ), the efficiency of the regulating organ should be higher than 25% to fulfil the requirements of a global disposable true energy factor  ${}^t_s\eta_d^* = 5$  stated in the requirements (Sec. 3.1).

### 4.3.2 Sensitivity analysis

A sensitivity analysis can have different roles, such as helping understanding the importance of one or the other parameter of a system in its outcome, or predicting the perturbation due to the modification of a parameter in an existing system. Let us start with a general sensitivity analysis to get a better grip on the functioning of the escapement. Because of the numerous non-linearities of the functions for the speed and energy factors, the sensitivity analysis is not performed analytically, but numerically.

A preliminary analysis is conducted to understand the role of each parameter. The relative

### 4.3. In-depth study of the overall performance

evolution of the theoretical advance speed when each parameter varies of  $\pm 20\%$  around its reference value is shown in Fig. 4.7. Only the curves for relevant parameters are shown and labelled. Without surprise, the pitch of the teeth  $p_t$  is clearly the defining parameter in terms of advance speed because it directly multiplies the maximal actuation frequency. This being set apart, the mass of the blocker  $m_b$  and the spring constant of the recoil spring  $k_r$  have a similar yet opposite influence on the speed. It is expected since they both define the free oscillation frequency of the spring and mass system. The initial and final positions of the blocker  $x_{b,m}$  and  $x_{b,0}$  play a lesser role. Finally, the moment of inertia of the  $\mathcal{L}$ ,  $I_{\mathcal{L}}$ , and the distance between the pivot and the blocker,  $l_{\mathcal{L},b}$ , have a negligible influence. This is mostly because  $I_{\mathcal{L}}/l_{\mathcal{L},b}^2 \ll m_b$ . For all those parameters except for  $p_t$ , rather significant changes in their values yield little variation in  $v_a^{th}$ .

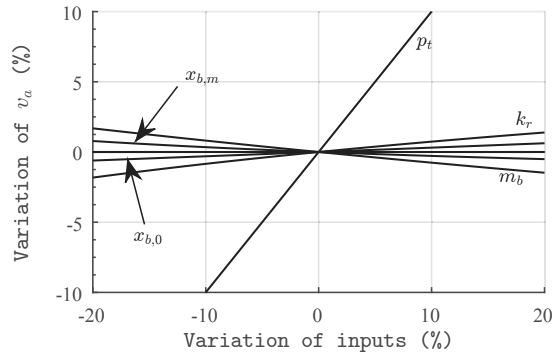


Figure 4.7: Relative variation of  $v_a^{th}$  when a single parameter varies of  $\pm 20\%$  around its reference value.

Let us now analyse the energetic model. The first observation is that the energy necessary to unlock the blocker  $E_{k,ul}$  (4.42) is smaller than the displacement energy  $E_d$  (4.43) in the selected conditions (and so for a thrust force up to 140 N). Therefore,  $E_d$  is the limiting parameter when trying to reduce the step trigger kinetic energy. Fig. 4.8 shows these two quantities for  $F_s \in [0, 200]$  N.  $E_d$  is a linear function composed of a constant value that corresponds to the work of the recoil force and a force-dependent value due to the friction between the rail and blocker. The relative energy factor of a step (Fig. 4.9) obviously increases with the thrust force, because the work of the recoil force becomes less and less significant. This highlights that a larger thrust force is favourable so long as  $E_d$  is the limiting energy. In the same way, if the thrust force is provided by a spring, it should vary as little as possible along the stroke since the same input energy will be applied at every step. In other words, the spring constant  $k_s$  should be as low as possible, but this yields ridiculously long and not feasible springs. With the increasing thrust force, the kinetic unlocking energy  $E_{k,ul}$  takes over, which reduces the energy factor with an asymptote to 0 for very large values of the thrust force.

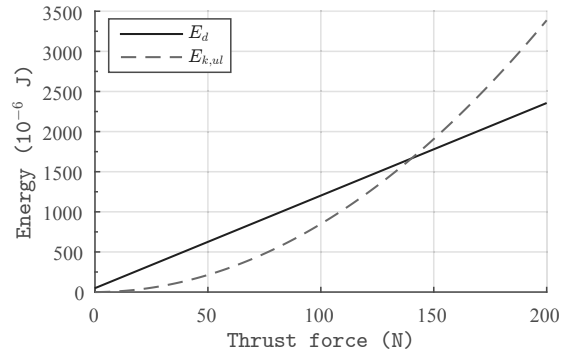


Figure 4.8: Comparison of  $E_{k,ul}$  and  $E_d$  for thrust force up to 200 N.

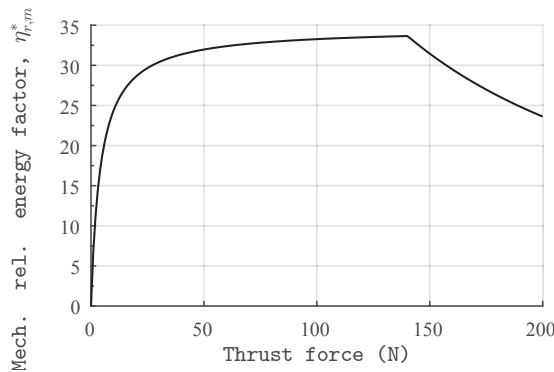


Figure 4.9: Relative energy factor of a step with a thrust force up to 200 N.

Fig. 4.10 shows the variation of the true relative energy factor when each parameter varies of  $\pm 20\%$  around its reference value. Only the most influential parameters are labelled. Among them,  $\alpha$  is obviously and logically the most important, since the inclined plane is the central part of this working principle. Setting  $\alpha$  close to its critical value obviously increases the energy factor but represents a bigger risk. Not surprisingly either,  $\mu_d$  has a strong influence on the performance. The height of the teeth  $h_t$  plays an important role because it directly affects the work of both the recoil force and the friction force. As already foreseen,  $k_s$  is important. Because of its influence on the thrust force, the free length of the main spring  $l_{s,f}$  quite strongly modifies the energy factor. Varying  $l_{s,p}$  oddly has less influence although it changes the thrust force in a similar way, but this is explained because the variation of the parameters is a percentage of their reference value, and not an absolute variation. All of the above save for  $l_{s,p}$  should be minimised since they reduce the energy factor as they increase. The pitch of the teeth  $p_t$  shows the opposite influence simply because less steps are required if it increases. The steps created in the evolution of the energy factor when  $p_t$  varies are due to the fact that the number of steps along the stroke is an integer. Finally, let us mention  $l_{\mathcal{L},m}$

### 4.3. In-depth study of the overall performance

whose influence is rather strong because of its role in the definition of the efficiency  $\eta_{sc}$  of the series of collisions.

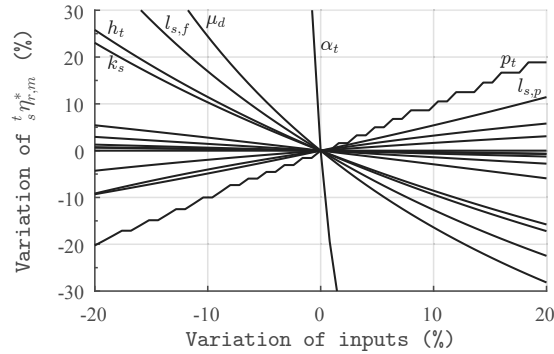


Figure 4.10: Relative variation of  ${}^t_s \eta_{r,m}^*$  when a single parameter varies of  $\pm 20\%$  around its reference value.

This analysis shows that the energetic model is much more sensitive to its parameters than the dynamic model. Consequently, from an industrial point of view, the energetic performance is more critical because of the potential functioning issues that a parameter variation might cause. Let us assume this industrial point of view. The life cycle of a movement starts by the production of its elements. They are then assembled and the movement is placed in a device. This device is sold and used, until the end of its life cycle. During this time, it is not possible to ensure that all parameters keep their reference values. Firstly, mechanical parts are produced within a certain tolerance. Secondly, environmental conditions change (temperature, humidity, etc.). Finally, as the movement is being used, wear also modifies the parameters. Wear can be classified with environmental changes. Let us use the available models to analyse the impact of machining tolerances on the performance.

#### Influence of machining tolerance

The field of tolerance analysis — also called tolerance stackup — proposes a methodology for analysing and forecasting the impact of tolerance and all kinds of possible variations of mechanical parts. Basically, two models are accepted: the ‘worst case’ and the ‘statistical’ tolerance analysis. Both are based on the addition of all relevant dimensions, taking into account their tolerance levels, to obtain the size of an unknown dimension. For more detailed information, the work of Fischer is an interesting reading [Fis11]. Here, a similar methodology is applied, yet for a slightly different objective. Indeed, the tolerances are taken into account to calculate performance rather than other geometric dimensions.

The methodology applied in this experiment is stochastic. We consider that the obtained

## Chapter 4. Modelling of the Mechanical Performance of a Movement

geometric dimensions are distributed around their reference value with a standard deviation equal to half of the tolerance, similarly to what is done in the ‘Six Sigma’ method [PK14]. The tolerance level depends on the machining technique employed. Some of the free parameters do not directly correspond to a geometric dimension of a part, but are the result of an assembly, which yields larger tolerance levels. As would be the case in most industrial applications, parts whose dimensions are out of the tolerance levels are rejected, yielding a truncated normal distribution. The analytical prediction of the distribution of the performance could be calculated, but the non-linearities of the models as well as the truncated distribution are problematic. From an engineering point of view, numerical analysis is efficient enough (on a desktop computer, simulating the results of a hundred thousand parts takes less than three seconds) and its flexibility is a valuable advantage. The obtained results are of course different for every run of the experiment. Nevertheless, if enough samples (here: 100,000) are evaluated, the results are considered representative. Table 4.2 summarises the tolerance level on each parameter.

Parameter	Reference	Tolerance
$k_s$ (N·m <sup>-1</sup> )	400	±5%
$l_{s,f}$ (mm)	240	±5%
$l_{s,p}$ (mm)	85	±0.1
$p_t$ (mm)	0.8	±0.01
$\alpha$ (°)	87	±0.5
$h_t$ (mm)	0.2	±0.01
$m_b$ (g)	0.5	±0.1%
$l_{\mathcal{L},b}$ (mm)	7.2	±0.1
$l_{\mathcal{L},m}$ (mm)	12.2	±0.1
$I_{\mathcal{L}}$ (g·mm <sup>2</sup> )	25.5	±5%
$k_r$ (N·m <sup>-1</sup> )	1000	±5%
$x_{b,0}$ (mm)	0.1	±0.1
$x_{b,m}$ (mm)	0.4	±0.1
$m_a$ (g)	1	±5%

Table 4.2: List of the free parameters and their tolerance level

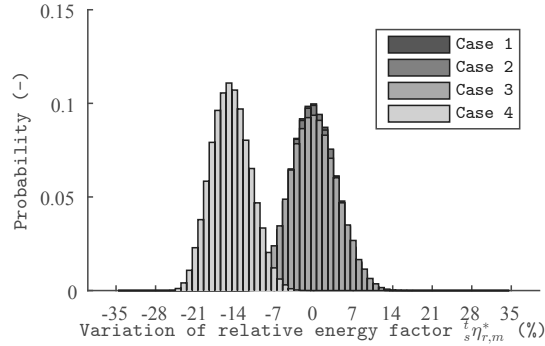
Fig. 4.11a displays a histogram of the probability of obtaining a deviation of  ${}^t_s\eta_{r,m}^*$  compared to the reference value. In a similar way, the variation of the speed  $v_a^{th}$  is shown in Fig. 4.11b. The results are given in four steps:

1. All parameters have their reference value, except for those regarding the main spring who are subject to the truncated distribution.
2. In addition to those of the main spring, the parameters of the release mechanism are altered.
3. The recoil spring parameters are added to the list of altered parameters.

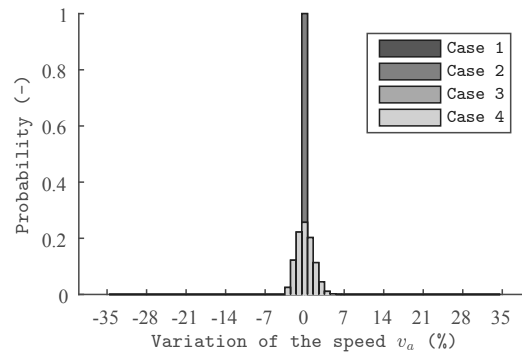


### 4.3. In-depth study of the overall performance

4. Finally, all geometric parameters are subject to machining imperfections.



(a)



(b)

Figure 4.11: Probability of obtaining a certain performance for  ${}^t_s\eta_{r,m}^*$  and  $v_a^{th}$  with the given tolerance on the parameters. The alteration due to cases 1, 2, and 4 is negligible. This explains why case 3 is hidden behind case 4.

#### **Case 1: Influence of the main spring**

By nature, springs have rather large tolerance levels, namely  $\pm 5\%$  for the spring constant  $k_s$  and the free length  $l_{s,f}$ . However, the pre-constrained length  $l_{s,p}$  is defined by machined parts, where medium tolerances are applied, namely  $\pm 0.1$  mm. As seen in Fig. 4.11a, the main spring has very little influence on the true mechanical energy factor, as more than 75% of the obtained movements have a deviation of the performance lower than 2%. Yet, it might have an important impact on the actual minimal thrust force along the stroke. Indeed, almost 35% of the movements do not provide the required 40 N at the end of the stroke. Either stricter tolerance levels should be required, or the spring should be designed to provide a slightly larger thrust force, typically by reducing its preload length  $l_{s,p}$  at the expense of the energy factor  ${}^t_s\eta_{r,m}^*$ .

### ***Case 2: Influence of the release mechanism***

The  $\mathcal{L}$  is milled. Hence, let us consider medium general tolerances, which correspond to  $\pm 0.1$  mm for  $l_{\mathcal{L},m}$  and  $l_{\mathcal{L},b}$ . The moment of inertia, although it partly depends on the two previous, is assigned a  $\pm 5\%$  tolerance. The mass of the mover of the regulating organ  $m_a$  is also assigned a tolerance of  $\pm 5\%$ . Their influence is very limited on both outcomes, but yet observable on the energy factor principally because of  $l_{\mathcal{L},m}$ , as seen earlier.

### ***Case 3: Influence of the recoil***

Because  $x_{b,0} = 0.1$  mm, the tolerance on this dimension cannot be larger than 0.1 mm otherwise the movement might not work properly if the pre-stress of the blocker against the rail disappears because of poorly machined parts. This parameter results from an assembly, therefore the related dimensions are subject to fine tolerances at a higher cost.  $x_{b,m}$  has the same tolerance interval but using medium general tolerances. The laser-machined leaf spring that provides the recoil force has accurate geometric dimensions but its stiffness is allowed a  $\pm 5\%$  variation. Fig. 4.11a clearly shows that these parameters have a stronger effect on  ${}^t_s\eta_{r,m}^*$  than the previous ones. It might not have been expected with the general sensitivity analysis, but the difference this time is that the relative variations due to the tolerances are much larger for these parameters than for the parameters analysed until now because of the very small reference dimensions. Nevertheless, more than 95% of the obtained movements have a performance variation lower than 10%. Their effect on the speed is also extremely clear, but this was expected because of the composition of the dynamic model.

### ***Case 4: Influence of the rail and blockers***

The last studied mechanical parts are a real manufacturing challenge. With most dimensions comprised between 0.05 and 0.2 mm, they can hardly be manufactured with traditional technologies. Let us here consider that these parts are produced using thin-wire electrical discharge machining. This method produces extremely accurate mechanical parts that can be machined with a tolerance lower than 0.01 mm. Unfortunately, it is also very costly and can directly impact the cost of a device in which one or more parts are produced this way. Since the motion is created by rails that have more than one teeth, it is not really relevant to make the teeth parameters vary in a stochastic way. Indeed, along the stroke, the geometry of two steps cannot be similar. It does not really make sense to make it vary along the stroke, so its value is maintained at its reference. Nevertheless, variations of  $h_t$  can impede the correct functioning of the device, or create weak points where parts might break. Similarly, the locking angle of the teeth can create functional issues. Performance-wise, let us consider the worst-case scenario, where  $\alpha = 87 + 0.5 = 87.5^\circ$ . The tolerance of  $\pm 0.5^\circ$  is difficult to achieve in particular because it also depends on the assembly between the rail and the blocker. This is why the histogram of  ${}^t_s\eta_{r,m}^*$  has a similar spread as for case 3, but is simply shifted towards lower performance. The spread is actually slightly smaller because the larger  $\alpha$ , the more

### 4.3. In-depth study of the overall performance

influential it is. This has however no effect on the speed.

The same data can be displayed using a scatter plot (Fig. 4.12) that shows both the energetic and dynamic performance at the same time. It gives a clear view of the spread of the performance due to the tolerance. Yet, it shows clearly that the designed movement produces a relative energy factor larger than 16 and a maximal speed larger than 65 mm·s<sup>-1</sup>.

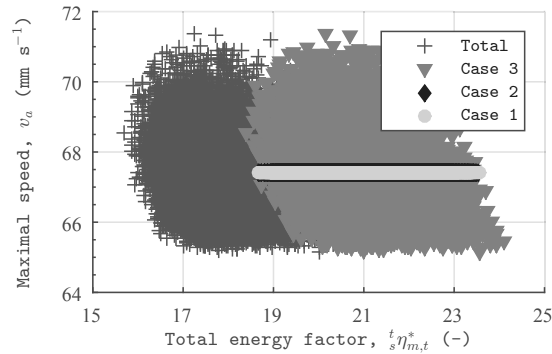


Figure 4.12: Scatter plot of the energetic and dynamic performance in the four cases described above.

The study conducted here on the effect of machining tolerance is an example of how analytical models can be efficiently used in an industrial context. Indeed, the extremely short evaluation times permit to try massive numbers of parameters combinations. However, the study is focused on performance and not on geometric or physical limitations of the movement. For example, the mechanical resistance of the teeth is not evaluated, nor the thrust force specifications, or lateral alignment of parts.

#### Influence of environmental conditions

Regarding environmental conditions, let us focus on the variation of the static and dynamic friction factors  $\mu_s$  and  $\mu_d$ . As seen earlier, for the reference parameters selected, the unlocking energy  $E_{k,ul}$  (which depends on  $\mu_s$ ) is significantly lower than the displacement energy  $E_d$  (which depends on  $\mu_d$ ). This is always the case when the locking angle  $\alpha$  is larger than the critical angle  $\alpha_c$  defined in Sec. 3.3.2. Because the control of both the friction factors and the exact locking angle is difficult in mass production, it is not wise to design a device where  $\alpha$  is not stable for the dynamic friction factor and yet stable for the static friction factor. Therefore, let us simply note that the energy factor unsurprisingly decreases as the dynamic friction factor  $\mu_d$  increases.

### 4.4 Conclusion

In this chapter, we proposed a methodology for modelling the performance of an escapement-based movement. We applied it to a study case of linear escapement. The modelling of the dynamic performance is done by listing all mobile parts in the movement and modelling each of their motions separately. Each mobile part is assigned one or more specific durations that describe critical phases of their motion. These motions are then ordered in a sequence that ensures the correct functioning of the movement. The specific durations also permit to turn this dynamic model into a straightforward design tool, as they can be related to the requirements and provide four simple conditions. The choice of a set of values for the parameters can be confronted to the requirements very easily.

A model for the energetic performance of the movement is also developed. Here again, the sequence of motion is used to break down and identify all the losses in the process of generating a step. A complete analytical model is finally provided, with a contribution in the modelling of the efficiency of a series of collisions.

Finally, these two models are used to analyse the sensitivity of the performance to the parameters. An example shows how it helps identifying the importance of the machining tolerance. However, the performance study is focused solely on the energetic and dynamic behaviour of the escapement, and not on the respect of maximal constraints in the material or other requirements that ensure the integrity of the mechanism. Separate studies should be conducted for an industrial development.

---

Publications related to this chapter:

- Romain Besuchet, Yoan Civet, and Yves Perriard. Influence of manufacturing tolerances on the performance of an electronically-controlled linear escapement. In *The 10th International Symposium on Linear Drives for Industry Applications (LDIA2015)*, 2015.
- Romain Besuchet, Yoan Civet, and Yves Perriard. Study of the efficiency of an electronically-controlled linear escapement. In *Advanced Intelligent Mechatronics, IEEE/ASME International Conference on (AIM 2015)*, 2015.
- Romain Besuchet, Yoan Civet, and Yves Perriard. A novel electronically-controlled linear escapement mechanism. In *Electrical Machines and Systems (ICEMS), 2014 17th International Conference on*, page: 2204 – 2210, 2014.

## **5 Electronically-Controlled Movements**

In this chapter, special kinds of movements, based on electronic control, are discussed. This type of control has promising performance in terms of flexibility and speed. The specifics of these movements are first explained and analysed to highlight the particular challenges relative to them. A dynamic model using elements of analytical and numerical modelling is introduced. Finally, an optimisation strategy for such escapements based on genetic algorithms is proposed. This chapter is based on a practical example that helps understanding the proposed methodology for the design of the regulating organ of an electronically-controlled escapement.

### 5.1 Use of actuators in escapement-based movements

Movements based on a purely mechanical regulating organ suffer severe limitations in terms of speed control. The simplest example is that of clockwork movements that are designed, manufactured and fine tuned to work at a precise frequency. The accuracy of certified chronometers, high-precision watches that passed certification tests [COS15], can maintain a daily error of less than 8 s, which corresponds to an error of 93 ppm. However, should the user want to change this working frequency, he would need to alter one (or more) mechanical parts. In a positioning application where the displacement speed should vary, using a mechanical oscillator such as is done in clockwork requires a complex mechanical system. Electronics are nowadays, and since the democratisation of quartz oscillators, the preferred solution for precise timings thanks to their much higher accuracy and quasi-insensitivity to environmental conditions. Indeed, standard grade quartz watches have a drift under half a second per day, an error lower than 6 ppm [Wik15]. This higher accuracy and the flexibility in terms of control are valuable assets for electronic control against purely mechanical solutions. Because electronics require electrical energy to work, using a quartz oscillator to regulate the motion of an escapement necessitates an electrical to mechanical energy converter, commonly called electric actuator or motor.

Fig. 5.1 shows a general structure for an electronically-controlled regulating organ. An electrical energy supply powers the actuator through driving electronics, but also a microcontroller. The microcontroller, clocked by a quartz oscillator, is used to process the information coming from the user interface (speed of advance, number of steps, moment of the first step, etc.) and manage the automatic control of the actuator. The input electrical energy is conveyed to the actuator, where it is transformed into mechanical energy so as to interface the electrical and mechanical environments. The nature of the energy supply is not defined, in the sense that it could be a battery as well as the output of an energy harvester on the main mechanical energy supply. The external requirements of an electronic regulating organ are exactly the same as for any regulating organ (Table 3.4), with the clarification of R.E.5, which becomes 'Store electrical energy'.

There are innumerable options for the choice of the microcontroller. However, it does not change the structure, the complexity, and the energy consumption of the regulating organ much. On the other hand, the actuator has a huge impact on these three topics. An exhaustive list of solutions will not be given here, but very essential design choices exist, such as the nature of the motion (linear or circular) or the physical effect on which the transducer relies (piezoelectric, electromagnetic, thermal, etc.).

## 5.1. Use of actuators in escapement-based movements

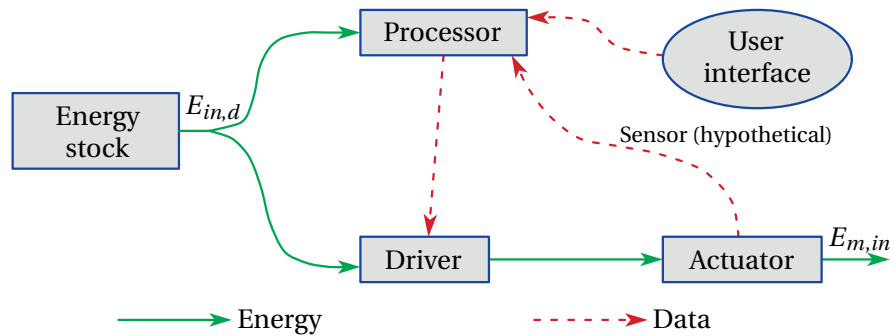


Figure 5.1: Block diagram of the regulating organ considered in this chapter.

### Key characteristics

The accurate identification of the task of the regulating organ in the movement is central to its correct design and optimisation. Of course, its most important role is, when desired, to trigger a step. In other words, it has to provide enough mechanical work to release the escapement. This energy has to be dispensed smartly so as to ensure the releasing. For example, if a certain locking force has to be provided, the mechanical output of the regulating organ should of course overcome it.

From the point of view of the movement, it is important that the target displacement and advance performance are obtained. Given the working assumptions (open-loop) for the discussed movements, it is sufficient to count the number of steps to ensure the correct displacement. Speed control however requires a certain dynamic performance that has to be part of the requirements for the regulating organ.

On the other side of the energy conversion process, the input energy is critical. Indeed, one of the main features of escapement-based movements is their peculiar energy management. As such, whether the regulating organ energy supply is a battery or is harvested from the main energy supply, it is advantageous to use as little energy as possible.

Depending on the application, other features might be equally or even more important. Typically, the manufacturing costs, the volume, the reliability or the use of normalised parts are constraints.

## 5.2 Case study: regulating organ for a linear escapement

Explaining through an example makes the understanding easier. Let us use an escapement of similar structure to the case previously studied (chapter 4). Of course, the selection of the best solution as well as the elaboration of the requirements are the results of several iterations of design conducted in parallel with the design of the rest of the movement. To obtain a coherent and efficient regulating organ, its whole structure has to be considered as a whole. Let us yet focus on the design of the actuator, and accept that the energy stock is a battery (traditional or rechargeable) that supplies a microprocessor or digital signal processor as well as the actuator through driving electronics as simple as possible. With the same objective of simplicity, the actuator is controlled in open loop.

The regulating organ studied in this chapter is designed for a linear escapement with two independent blockers that have to be released alternatively by an impact. To release the mechanism, a mobile part has to collide with a release mechanism with a minimal kinetic energy of 150  $\mu\text{J}$ . The actuator can accelerate its mover on a 1 mm distance between the centre of its stroke and the release mechanism on either of its sides. A maximum actuation frequency of 50 steps per second is required. The cost is not an issue in this application, but the complete mechanism has to be highly manoeuvrable, and thus as small as possible. Nowadays, electric actuators can be based on a very large variety of physical principles or materials [Jan04, HST10]: electromagnetism [RMB<sup>+</sup>14], electrostatics [BCA<sup>+</sup>15], piezoelectricity [Zha11, SCP15], shape-memory alloys [HH14], electro-active polymers [RNYS14], etc. The requirements for the actuator and its driving electronics are given in Table 5.1. The consideration of the actuator together with the driving electronics helps obtaining a compact solution.

ID	Function	Parameter	Value
A.E.1	Receive electrical energy		
A.E.1.1	– Energy supplied by a battery (type undefined)		
A.E.2	Provide mechanical energy		
A.E.2.1	– Type of motion		Linear
A.E.2.2	– Minimal collision kinetic energy	$E_{kin}$ ( $\mu\text{J}$ )	150
A.E.2.3	– Distance between centre of the stroke and release position	$x_u$ (mm)	1
A.E.2.4	– Actuation frequency	(Hz)	[0, 25]
A.E.2.5	– Time to reach the release position	$T_{d,max}$ (ms)	5
A.E.2.6	– Efficiency		Maximised
A.E.2.7	– Symmetric behaviour along the displacement axis of the mover		
A.E.3	Mass, volume, shape		

Table 5.1: External requirements of the actuator.



## 5.2. Case study: regulating organ for a linear escapement

The studied actuator is a prismatic linear electromagnetic actuator, whose structure is shown in Fig. 5.2 and shares similarities with tubular oscillating actuators [ZC09]. The stator is composed of an E-shaped and a back *iron yoke*. A *coil* is wound around the central branch of the E. The *mover* is an amagnetic frame on which two *permanent magnets* (PMs) polarised in opposite directions are mounted. A *leaf spring* guide ensures the linear motion of the mover, but creates a recoil force as soon as the mover leaves the centre of the stroke. To prevent the buckling of the leaf springs, it is important that the air gap between the mover and the back iron yoke is smaller than the air gap between the E and the mover. This way, the PMs of the mover are attracted towards the back iron yoke, which generates a tensile stress in the leaf springs. The symmetrical structure of the actuator ensures a symmetrical behaviour of the output. The direction of motion is defined by the direction of the current in the coil. The energy is supplied by a battery and the driving electronics consists in an integrated H-bridge that allows supplying the actuator with positive or negative current. A capacitor is mounted in parallel with the H-bridge. This structure was selected because it is mechanically simple and has an advantageous shape. In addition, it can work with very basic electronics and at low voltage. Also, a high energy density can be reached with the PMs.

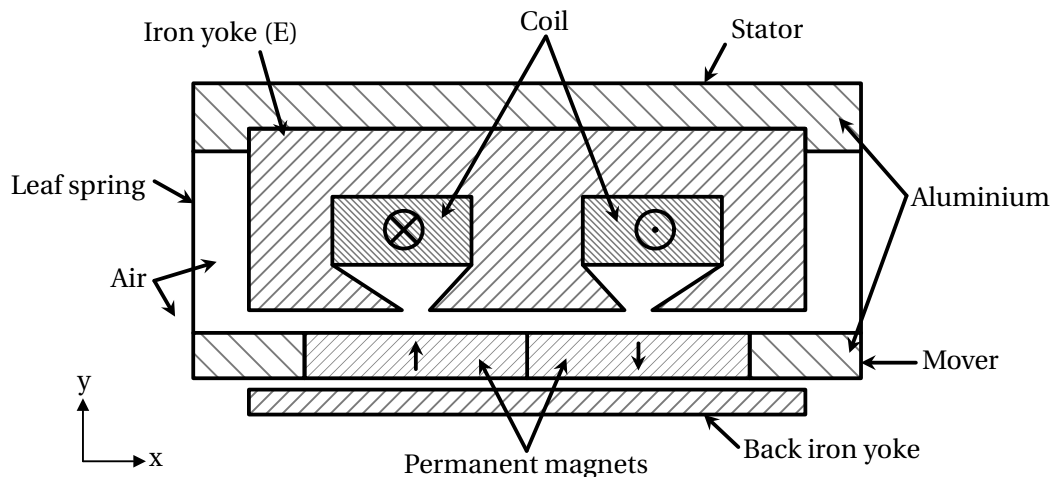


Figure 5.2: Cross-section of the structure of the actuator.

### Definition of the objectives and constraints

Based on the general case in Sec. 5.1, the main objectives and constraints can be clarified. The main constraint is the minimal mover kinetic energy. Another constraint regards the maximal actuation frequency, which is important for the dynamics of the movement. Similarly, the two optimisation objectives are the minimisation of the input energy and of the volume of

the complete regulating organ. Also, the energy supply and electronics will be considered as constraints.

### 5.3 Model of the efficiency and mechanical performance

It is established that all the elements of the regulating organ participate in the overall performance. The energy supply and the actuator obviously have an important influence on the energetic performance. They also define the requirements of the driving electronics, whose selection has an impact on the choice of the microcontroller. To obtain a coherent regulating organ, it is thus necessary that all four components are adapted to each other. This also means that it is beneficial to optimise the whole regulating organ as a group, rather than simply optimising each part separately. To perform this optimisation, it is required to generate a global model of the regulating organ for each objective and constraint.

The suggested strategy is to model the behaviour of the regulating organ during a single step, with the assumption that each step starts at the standstill position and finishes when the mover returns to its initial position. The required outcome of the model is the kinetic energy  $E_{kin}$  acquired by the mover. Additional data regarding the dynamics or the evolution of the electric power  $P_{el}$  (and energy  $E_{el}$ ) are also interesting. The modelled step consists in the following sequence:

1. The mover is in the middle of its stroke, at a stable position. Its speed is null and the coil is not supplied.
2. A voltage step is applied to the coil, creating an electromagnetic force on the mover.
3. The mover reaches the position where it releases the blocker of the escapement. Its speed at this position defines the amount of kinetic energy that it accumulated during the step. The considered input electrical energy  $E_{in,d}$  consumed during a step is the electrical energy between the start of the voltage step and the moment when the mover reaches the release position.
4. The voltage applied to the actuator is returned to 0 V and the mover returns to its central position under the effect of the recoil spring only.

The problematic is thus here to evaluate the kinetic energy acquired by a moving part in a fixed frame, subject to a gravitational field that yields negligible forces. As a reminder, the kinetic energy – or *energy of motion* – of a mass  $m_a$  animated by a speed  $v_b$  is calculated as:

$$E_{kin} = \frac{1}{2} m_a \cdot v_b^2. \quad (5.1)$$

Given the low speeds and short displacements, viscous friction is not accounted for. Ener-

### 5.3. Model of the efficiency and mechanical performance

getically speaking, the situation is summarised in Fig. 5.3. The supplied electrical energy is distributed between several effects. Losses first occur in the electrical components of the driving circuit. The electrical energy is then transformed to magnetic energy, where some of it is also wasted because, among others, of saturation effects. Mechanical energy is the final kind of energy in this conversion process. Without dissipative forces, such as friction forces, the law of conservation of energy states that the total mechanical energy  $E_m$  of a system is the addition of its kinetic energy  $E_{kin}$  and potential energy  $E_{pot}$ . A body has potential energy when it is placed in a force field such as gravity. Similarly, a deformed spring stores potential energy. Since the gravity is neglected, the sources of potential energy in the actuator are the mechanical potential energy due to the leaf spring guide and the magnetic potential energy due to the interaction between the permanent magnets of the mover and the ferromagnetic structure. The mechanical potential is here monotonous so long as the leaf springs are deformed within the elastic limit of the material. However, the magnetomotive force (MMF), responsible for cogging forces in electromagnetic actuators, might not be, creating several stable positions.

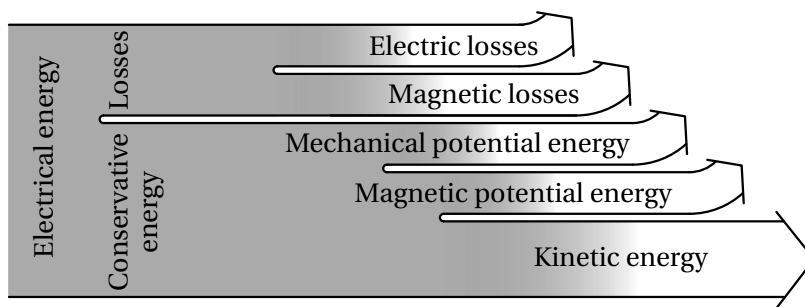


Figure 5.3: Energy conversion from the electric power supply to the kinetic energy of the mover.

From these basic observations, it is clear that the aforementioned effects should be taken into account in the model. The principal information that the model should provide is the position of the mover and its derivative, based on the geometry of the actuator, its components and their material, as well as the electric circuit that drives it. Because of the electromechanical nature of the energy conversion, the model is principally ruled by:

1. Maxwell's equations, through Kirchhoff's circuit laws;
2. Newton's second law of motion.

Because of the nature of the actuator, Maxwell's equations will also be used for their magnetic information. The definition of the model is thus separated in an electrical, a mechanical and a magnetic part. Their interactions will be highlighted during the process.

### 5.3.1 Electric model

Kirchhoff's circuit laws are a result of Maxwell's laws that can be used for electric circuits. Therefore, let us define the equivalent electric circuit of the regulating organ, based on the schematic view shown in Fig. 5.4. The equivalent electric circuit is developed step by step by modelling each part of the regulating organ.

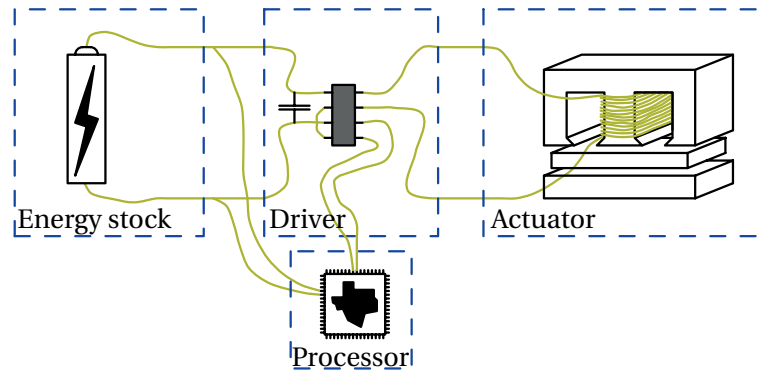


Figure 5.4: Scheme of the equivalent electric model of the regulating organ.

#### Energy supply

In our case, the actuator is battery-powered. A very simple model commonly accepted for batteries is that of a voltage supply  $U_i$  with a series resistance  $R_i$ . These two parameters are sufficient to describe the electrical behaviour of the energy supply, namely that the efficiency of the battery varies with the load. The input energy is computed as follows:

$$E_{in}(t) = \int_{t=0}^t U_i \cdot i_b(t) dt, \quad (5.2)$$

where  $i_b(t)$  is the current delivered by the battery. Let us call the output voltage  $u_b$ ; this value will be useful later on.

Batteries performance vary widely, because of their technology, shape or size. Let us compare the performance of three very common types of batteries found in consumer electronics: AAA, CR123A and CR2032. These batteries can be used alone or by pairs in order to adapt the performance. AAA batteries are for example commonly used in pairs to provide sufficient voltage for consumer electronics applications.

### 5.3. Model of the efficiency and mechanical performance

Property		Battery type		
Parameter	Description	AAA	CR2032	CR123A
$U_i$	Voltage supply (V)	1.5	3	3
$R_i$	Internal resistance ( $\Omega$ )	0.3	20	0.5
	Rated current (mA)	250	3	1000
	Peak current (mA)	600	20	5000
	Capacity (mA·h)	[540, 1200]	[150, 250]	[700, 1500]
	Height (mm)	44	3.2	34
	Diameter (mm)	10	20	17
	Weight (g)	12	3	16

Table 5.2: Properties of commonly used batteries in consumer electronics. All the values given are typical values found on data sheet. Each manufacturer gives different specifications.

#### Microcontroller

The microcontroller serves as interface between the user and the escapement. An uncountable number of microcontrollers can be used in an application where the user can interact with three buttons and receives information via LEDs. The same is true when observing the control tasks of the microcontroller. Indeed, it is expected that the control of the actuator is simple, with at most very few calculations to perform and two pulse-width modulation (PWM) signals to emit. Cost, brand, energy consumption, volume, availability are all valid criteria that the designer might use to make a choice.

From the point of view of modelling, the exact type of microcontroller can be overlooked and very common values can be taken into account for either energy, size or cost. The energy consumption of the microcontroller is furthermore often negligible compared with that of the actuator, even should a slightly more complex voltage stabiliser be used. Nevertheless, these remarks and the previous section yield the equivalent electric circuit given in Fig. 5.5.

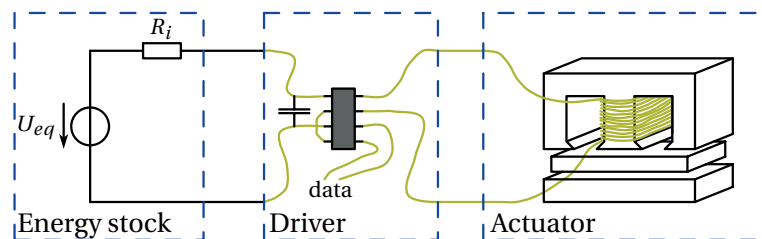


Figure 5.5: Scheme of the equivalent circuit with the selected energy supply and microcontroller.

**Driving electronics**

H-bridges are very common structures for drivers. They allow to apply a bidirectional voltage on a load, controlled with PWM, between  $\pm U_i$ . In practice, it is not possible to reach such voltage because of the voltage drop induced by the conduction resistance of the transistors. Also, the average value of the voltage is controlled by the H-bridge, but not its instantaneous value. The high frequency effects due to the transistors switching are neglected here which is equivalent to making the hypothesis that the output voltage is constant. Because of the symmetry of the actuator and that of the H-bridge, the model for one direction of motion describes both directions, thus the H-bridge is not fully represented. Instead, the transistors in conduction are replaced by the sum of their conduction resistances  $R_H$  and the transistors in cut-off state are omitted. To simulate the selectable level of voltage on the bridge, let us introduce the factor  $D$ , comprised between 0 and 1. The battery internal voltage is replaced by a virtual internal voltage  $U_{eq}$  defined as:

$$U_{eq} = D \cdot U_i \tag{5.3}$$

The capacitor is used to enhance the battery life, maximise the current in the actuator during the impulse, and lower its ripple. Indeed, the losses in  $R_i$  are proportional to the square of the current through it, and the duration. It is therefore advantageous to work with lower currents. The capacitor is thus loaded while the actuator is not powered. As soon as the transistors of the bridge conduct, the capacitor can help the battery to provide energy and thus reduce the joule heating of the battery. Also, it helps reducing the supply voltage drop on the actuator when it is powered. The effect is yet more important for high frequency switching, typically with PWM. Since the model reduces the PWM to an adjustment of the supply voltage  $U_i$ , the capacitor is neglected. Fig. 5.6 shows the equivalent electric circuit at that point.

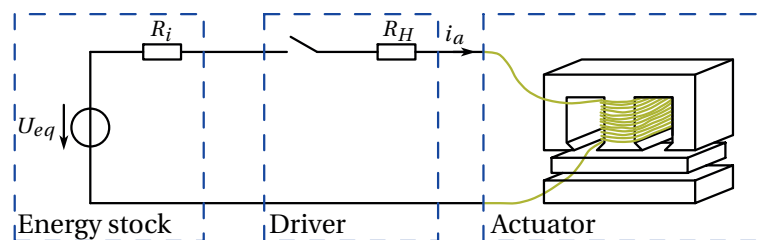


Figure 5.6: Scheme of the equivalent circuit with the selected energy supply, microcontroller and driver.

**Actuator**

The actuator is arguably the most important part of the regulating organ in terms of energy, but also dynamic performance. The model of an actuator generally provides information on the mechanical performance with respect to the electrical input. With the development above, the electrical energy supply has been defined. On this basis, it is possible to describe, either analytically or numerically, the energy conversion process. Electromagnetic actuators can be modelled by their electric resistance and a fictive voltage sources. These sources are a representation of induced voltages in the coils due to the magnetic flux variations that they observe, or in other words, to the magnetic energy variation in the system. It therefore represents the interaction between the magnetic and electric environments. The induced voltage  $u$  is the time derivative of the magnetic flux  $\psi$ .

The described actuator can actually be modelled by a single resistance  $R_a$  in series with a single voltage source  $u_a$ . The electric equivalent model of the regulating organ is therefore given in Fig. 5.7, with the induced voltage  $u_a$ . What is particularly important to understand is that the value of the magnetic flux  $\psi_a$  through the coil varies not only with the current supplied to the coil, but also with the position of the mover. The shape of the equivalent circuit indicates for the use of Kirchhoff's voltage law with  $i_a$  the current in the actuator, which yields:

$$U_{eq}(t) = R_i \cdot i_a(t) + (R_H + R_a) \cdot i_a(t) + \underbrace{\frac{d\psi_a}{dt}(t, x)}_{u_a(t, x)} \tag{5.4}$$

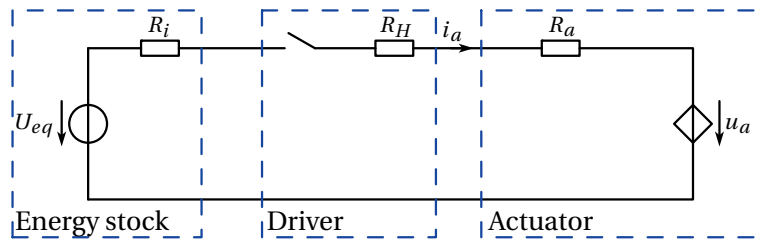


Figure 5.7: Scheme of the complete equivalent electric circuit for the studied regulating organ.

Equation 5.4 is the final electric model of the regulating organ; it yields the magnetic energy transferred to the actuator in function of electrical parameters. However some of the elements in the circuit are not defined. In particular,  $\psi_a$  has not been defined because it depends on the magnetic structure of the actuator. The magnetic modelling, which is necessary

because of the choice of actuator, is done later on. In addition, mechanics appear through the influence of the position of the mover and its derivative.

### 5.3.2 Mechanical model

Newton's second law of motion links the motion of a body of mass  $m_a$  to the net forces applied on this body. In the case discussed here, let us define the electromagnetic force  $F_{em}$  and the net external force  $F_{ext}$  applied on the mover of the actuator. Newton's second law of motion becomes:

$$m_a \cdot \frac{d^2 x}{dt^2}(t) = F_{em}(x, i_a) - F_{ext}(x), \quad (5.5)$$

With the assumption that gravity-related forces are negligible,  $F_{ext}$  consists only in the recoil force of the leaf spring guide of the mover. Let us consider it as a perfect spring, namely that it applies a force proportional to the displacement  $x$  of the mover with respect to the centre of the stroke (5.6).

$$F_{ext} = k_{ls} \cdot x, \quad (5.6)$$

where  $k_{ls}$  is the spring constant. The new expression of (5.5) is:

$$m_a \cdot \frac{d^2 x}{dt^2}(t) = F_{em}(x, i_a) - k_{ls} \cdot x, \quad (5.7)$$

As was the case with the electric model, not all the elements are defined. The electromagnetic force  $F_{em}$ , as its name indicates, needs to be calculated using a magnetic model. Therefore, this magnetic model is the actual interface between the electrical and mechanical environments, in the case studied here.



#### 5.3.3 Global model – Addition of the magnetic model

The objective of the magnetic model is to evaluate the relation between the electrical and mechanical environments. Electromechanical conversion theories show that the force can be derived from the variation of magnetic energy, and thus the magnetic induction and magnetic field in the magnetic circuit. It can be shown that for moving magnet actuators the electromagnetic force  $F_{em}$  at a position  $x$  of the mover along the stroke can be expressed as:

$$F_{em}(x) = \frac{1}{2} \frac{d\Lambda_m}{dx} \Theta_m^2 + \frac{d\Lambda_{mc}}{dx} \Theta_m \Theta_c, \quad (5.8)$$

where  $\Theta_m$  and  $\Theta_c$  are the equivalent MMFs of all the PMs and all the coils in the set-up respectively,  $\Lambda_m$  is the equivalent self-permeance of all the PMs and  $\Lambda_{mc}$  is the equivalent mutual permeance of all the PMs and coils. The evaluation of those quantities can be done either analytically or numerically. Let us review those two options.

#### Analytical modelling

A very common technique consists in describing a so-called ‘equivalent magnetic circuit’, following the same rules as electric circuits and based on equivalent hypotheses. The MMF and flux are respectively assimilated to the electric voltage and current. Therefore, Kirchhoff’s circuit laws are applicable. Resistances are replaced by magnetic reluctances or their inverse: permeances. This approach results in a system of linear equations that allows to evaluate the magnetic field and magnetic induction. However, for this approach to be accurate enough, the system has to be represented in magnetic induction paths, similar to electric wires. The hypotheses on the magnetic flux are thus restrictive and require a very good knowledge of the magnetic field in the studied structure. With this method the actuator can be modelled as shown in Fig. 5.8 where the parameters denoted by  $\Theta$  are MMFs and those denoted by  $\Lambda$  are permeances. All of them except  $\Theta_c$  vary with the position. In this representation, the iron is considered ideal with an infinite magnetic permeability, leakage flux is neglected as well as fringes.

It was shown in the study of a similarly shaped E-core actuator [BGP13] that the validity of this model is restricted to when the mover is in the centre of the stroke (case represented here). For other positions, the influence of the fringes cannot be neglected. Therefore, this simplistic approach cannot be used for the actuator at hands, although it might work wonderfully well for actuators where the magnetic flux is more channelled.

Analytical modelling, applied in the correct conditions, is convenient because it can often be solved by hand and has a very low computing time when solved by a computer. It is thus great for a fast optimisation. However, it has limitations in terms of validity and becomes

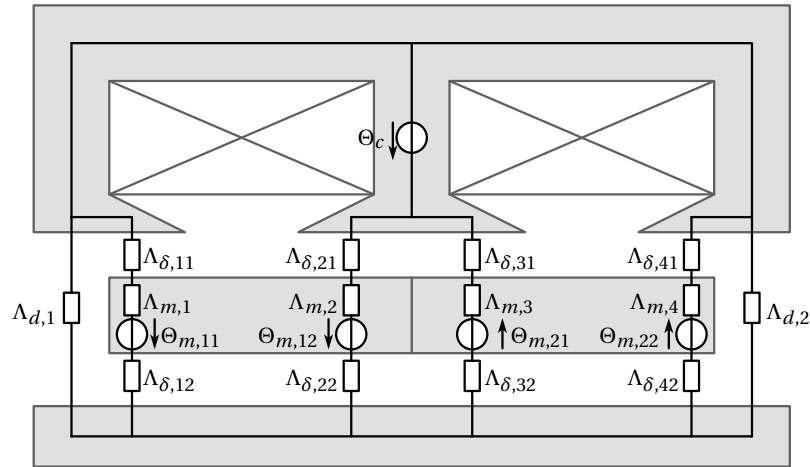


Figure 5.8: Simplified magnetic equivalent circuit of the actuator.

quickly obsolete with non-linearities (*e.g.* saturation).

### Numerical modelling

A very different approach to solving the same equations as previously is numerical modelling. The finite element method (FEM) is based on the decomposition of a domain in smaller and simpler domains. Resolving the equations of the problem on the smaller domains, that can be made of different materials, yields an overall solution to the problem. Among other advantages, let us mention the great flexibility of the method as well as its capabilities with non-linear problems. It nevertheless sometimes requires long computing time. Also, the validity of the obtained results is to be considered as carefully as the results of any model, with the difference that the hypotheses of the model are sometimes less obvious than with an analytical model.

In electromagnetism, FEM-based models are very popular because of the multiphysics nature of the problems. Indeed, the FEM easily permits to simulate the start-up of an electric motor or its heating in a stationary state. Because of its geometry, the actuator is modelled using a 2D planar simulation. The principle is that if a structure of constant section is long enough, almost all the slices have exactly the same behaviour. This is applicable for many theories, including electromagnetism. The extremities of the structure of course suffer from edge effects which alter the electromagnetic behaviour. However, it is negligible if the actuator's depth is long enough. Computing a 2D solution is much easier and faster than solving a full three-dimensional problem.

### 5.3. Model of the efficiency and mechanical performance

Because the FEM allows to take non-linearities into account, it would be ridiculous not to make the most of it. Therefore, the materials used for the actuator are modelled as follows:

- the iron that composes the E-shaped yokes has a B-H curve that shows the first saturation effects for magnetic induction values over 1.2 T, according to the manufacturer's data;
- the magnets have a linear B-H curve and a maximal energy density of  $400 \text{ kJ}\cdot\text{m}^{-3}$ ;
- copper is magnetically considered as air, but has a resistivity;
- non-ferromagnetic materials are not represented, and considered magnetically as air.

Fig. 5.9 shows the field distribution (obtained by simulation with the commercial software *Flux*, by *CEDRAT* [Ced15]) in the actuator when the coil is first not supplied, and then supplied with an electric current. In Fig. 5.9a, the magnetic field is really symmetrical, which indicates that no, or almost no, magnetic force is created along the horizontal axis. However, most importantly, fringes are observed, as lines of flux appear elsewhere than in the air gap and not perpendicularly to the surface of the iron yokes and PMs. This further shows that the analytical model using the equivalent magnetic circuit has a very limited validity. When a current is supplied to the coil of the actuator (Fig. 5.9b), the magnetic force generation is indicated by the unbalance of the magnetic field. It can mostly be observed in the central leg of the iron yoke, but the fringes between the outer legs and the mover also display it.

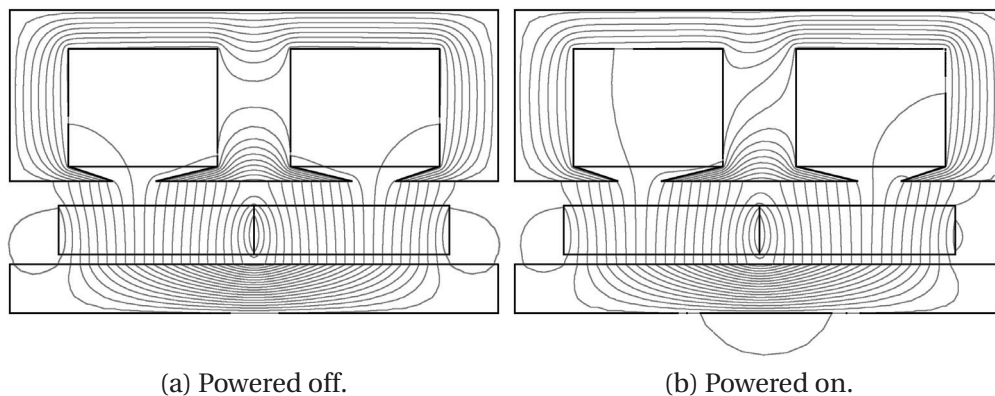


Figure 5.9: Field distribution in the actuator when the coil is not powered (a) and supplied with an electric current (b). Only magnetically-active parts are represented. The leaf springs and the aluminium frames are not shown.

The modelling capabilities of the FEM are yet not restricted to static simulations. Transient (or time-dependent) simulations permit to simulate more complex processes, such as the acceleration of the mover of a linear actuator according to the evolution in time of its electrical energy supply, by splitting the timeline in very short increments of time with the same idea

as the geometry is divided in small domains. The simulation performed at each time step uses the outcome of the previous simulation as initial conditions. Just as a static simulation can yield incoherent results if the hypotheses are not carefully controlled, a time-dependent simulation has to be very carefully designed, particularly regarding the duration of a time step.

The transient model presented here is the response of the actuator to a voltage step applied on the coils. Therefore, the equivalent electric circuit (5.4) discussed above is linked to the magnetic FEM model, which *Flux* is capable of doing. In addition, the software can solve the mechanical equation (5.7) simultaneously. The global model discussed here is thus completely defined using *Flux*. Its input parameters are:

- the geometry of the actuator,
- the materials of the components and their properties (magnetic, electric, mechanical),
- the associated electric circuit and the evolution of its supply along time,
- the external forces on the mobile parts.

After computation, it is possible to retrieve magnetic, electric and mechanical quantities. In particular, the position and speed of the mover as well as the electrical energy are among observable quantities. The objectives set for the model are thus fulfilled. Thanks to the FEM, the same model can also provide a lot of additional information without much effort.

### 5.3.4 Conclusion

The model developed above is capable of evaluating the mechanical as well as electrical performance of the selected actuator. It includes the whole energy chain from the electrical energy of the stock to the mechanical energy that the regulating organ can provide. It has been fully parameterised to allow for the optimisation of its performance.

## 5.4 Multi-objective optimisation

The optimisation of a set of variables looks for the combination of those inputs that yields the best performance. Genetic algorithms (GA) are a subclass of stochastic optimisation algorithms inspired by Darwin's theories on evolution. They are based on *individuals* having a genome where each *gene* corresponds to an input. In other words, in a problem with five variables, the genome of each individual has five genes, each having a value within the accepted boundaries for the corresponding variable. The performance (*fitness*) of the individuals of an initial population with random genomes is evaluated. The individuals are ranked from best to worst with regards to their performance. As for living species, the

weakest individuals are left behind, while the fittest survive and reproduce, thus mixing their genome and giving way to a new *generation*. The genome can also evolve due to random spontaneous mutation of a gene. The new generation is also assessed and ranked, and the process goes on and on. Numerous criteria exist to signify the end of the evolution process. Let us nevertheless mention the number of generations or a satisfying enough fitness.

The stochastic nature of the optimisation process means that not all combinations of genes are evaluated, which of course reduces computation time, but it also means that the best fitness discovered by the algorithm might not be global. This is why GA have to be handled with care.

It is possible to use GA to optimise more than one fitness function at a time. To do this, the ranking of the individuals is done by a special algorithm. It can be done by normalising the values of all the fitness functions and then summing them together for each individual. This solution is equivalent to performing a mono-objective optimisation, and necessitates an *a priori* knowledge of the expected values for each fitness. Another approach is the Pareto efficiency [Auv15]. An individual is Pareto efficient if enhancing one of the objectives can only be at the cost of deteriorating another. Therefore, the set of all Pareto efficient solutions gives an overview of the possible optimal solutions in the sense of the objective functions. The designer can then choose in this set the preferred solution with the addition of other decision criteria. More details regarding optimisation are found in [Mit96, GCL08].

The algorithm used here is a multi-objective (MO) genetic algorithm where individuals are ranked using the Pareto efficiency.

### 5.4.1 Optimisation strategy for highly constrained problems

Optimisation processes can be lengthy and yield uncertain results. In particular, if the domain of acceptable sets of parameters is strongly reduced because of one or more strict constraints, the optimisation might simply fail. To tackle this issue, we propose an optimisation process in two steps:

1. A **preliminary optimisation** (PO) is performed, with the strict constraint(s) as objective function(s).
2. The **multi-objective optimisation** (MOO) is then done using at least one individual that respects all the constraints in the initial population. The objective functions of this optimisation are the actual objectives.

The preliminary optimisation is a necessity in some very strongly constrained problems. Indeed, if we simply started the multi-objective optimisation with a purely random population,

it might take the program many generations to discover one individual that respects the constraints. It might even be possible that no individuals can respect them, and the program would be blindly searching for something that does not exist, because it is just testing the validity of individuals without knowledge of how close they are to being acceptable. The PO is therefore extremely important because it quite rapidly indicates the feasibility of a solution. When one or more acceptable individuals have been found, the MOO can start, with those individuals as part of the initial population. This provides a valid starting point for the optimisation. This strategy, in addition to ensuring that the optimisation yields results, saves computation time.

### 5.4.2 Implementation

The GA is implemented in Python, an open-source programming language, using the library DEAP (Distributed Evolutionary Algorithms in Python) [FDG<sup>+</sup>12]. The code is based on a simple architecture made of the three parts listed below.

- The main Python script (*core*) sets up and runs the GA.
- The *Flux servers* perform the simulations of the individuals using the time-dependent model described above.
- A communication system based on text files permits the interaction between the GA and *Flux*.

The main script is written so as to permit the use of more than one *Flux* server, in order to minimise the actual computation time. The computation task is spread evenly among the servers. Each *Flux* server runs strictly the same code, performs the simulations with the correct parameters and returns relevant quantities to the main script. Thanks particularly to DEAP, the code is concise and very easily applicable to many other optimisations based on different FEM software.

#### Objective functions and constraints

The list of objectives and functional constraints are summarised in Table 5.3. The values correspond to other requirements for the same movement, but the results provide a very interesting basis for the discussion.

The first functional constraint is that the kinetic energy  $E_{kin}$  of the mover has to be large enough, here 150  $\mu\text{J}$ . The actuator is supposed to be completely at rest before the beginning of the step: negligible external acceleration, mover stationary in the centre of the stroke, no electric current in the coil. At time  $t = 0$ , the switch is closed and the actuator is powered.

## 5.4. Multi-objective optimisation

Parameter	Description	Value
Objectives		
$V_a$	Volume of the actuator	(mm <sup>3</sup> ) Minimise
$E_{el}$	Input electrical energy	(μJ) Minimise
Functional constraints		
$E_{kin}$	Mover kinetic energy	(μJ) 150
$x_u$	Release position	(mm) 1
$T_{d,max}$	Maximal time to release position	(ms) 5
—	The mover comes back towards the centre of the stroke	— Yes
—	The geometry is feasible	— Yes

Table 5.3: Objectives and functional constraints for the optimisation.

Because the time the mover needs to reach the release position  $x_u$  is important to the dynamic performance of the actuator, the simulation only computes the first milliseconds following the power on, up to  $T_{d,max}$ , the maximal tolerated actuation duration. To accurately model the evolution of the position of the mover, it is preferable to perform a simulation with time steps as short as possible, at the cost of a longer simulation time. The trade-off chosen here is to have a time step equal to  $T_{d,max}/50$ .  $E_{kin}$  at the release position is then calculated by finding the corresponding time step and its instantaneous speed  $v_m$  (which *Flux* gives).

Another functional constraint regards the stability and reluctant behaviour of the actuator. When the mover reaches the position  $x = x_u$ , it hits the release mechanisms and stops. In order to use as little electrical energy as possible, the most efficient solution to bring the mover back to its starting position is to use the recoil force of the leaf spring guide and the reluctant magnetic force (cogging force). This force is due to the interaction between the PMs and the iron yokes. In certain situations, the cogging force might push the mover in the wrong direction, namely towards the outside of the actuator and cause a malfunctioning of the system. This is of course not tolerable. A simulation can be performed to verify that the mover is attracted towards the middle of the stroke. Because the expected result is qualitative, very few time steps (less than ten) are necessary, which makes it a fast simulation.

The last and obvious condition is that the genome of the evaluated individual corresponds to a valid geometry. If this condition is not satisfied, the simulation can be wrong, or the FEM program might even crash. It is tested by verifying simple geometric conditions.

The volume of the actuator  $V_a$  is also rather straightforward to evaluate using the geometric parameters. Only the volume of the actuator is computed in the simulation. It does not take

into account the volume of the rest of the elements of the regulating organ.

**Parameters and degrees of freedom**

The complete list of input parameters, fixed or free, is given in Table 5.4. It includes geometric parameters, shown in Fig. 5.10, physical properties and design options. The selected values for the supply voltage and the internal resistance of the battery are given above, in Table 5.2. Fixed parameters are either fixed because of requirements or technological limitations. Free parameters are however the degrees of freedom of the optimisation. As set here, the free parameters can largely alter the shape of the section of the actuator.

Parameter	Description	Value
$x_u$	Release position (mm)	1
$e_h$	Height of the E (mm)	10
$e_w$	Width of the E (mm)	[3, 5]
$e_d$	Depth of the system (mm)	5
$e_b$	Thickness of the back of the E (mm)	[0.8, 3]
$e_m$	Thickness of the middle leg (mm)	[0.8, 3]
$e_t$	Thickness of the outer legs (mm)	[0.8, 4]
$n_h$	Height of the slot apertures (mm)	[0.2, 4]
$n_w$	Width of the slot apertures (mm)	[0.2, 2]
$n_{mh}$	Position of the slot apertures (mm)	[0.5, 4]
$p_h$	Height of the PMs (mm)	8
$p_w$	Width of the PMs (mm)	1
$m_a$	Mass of the mover (g)	1
$b_h$	Height of the backiron (mm)	10
$b_w$	Thickness of the backiron (mm)	1
$\delta_e$	Airgap between the iron yoke and the PMs (mm)	0.6
$\delta_b$	Airgap between the back iron yoke and the PMs (mm)	[0.2, 0.4]
$B_0$	Remanence of the PMs (T)	1.43
$\mu_r$	Relative permittivity of the PMs (—)	1.22
$K_{Co}$	Fill factor of the coil (—)	0.45
$w_d$	Wire diameter (mm)	0.12
$r_l$	Linear resistance of the wire ( $\Omega \cdot m^{-1}$ )	1.5
$k_{ls}$	Spring constant of the leaf spring guide ( $N \cdot m^{-1}$ )	250
$R_H$	Resistance of the H-bridge ( $\Omega$ )	0.5
$R_S$	Parasitic series resistance ( $\Omega$ )	0.5

Supplying battery types: AAA, CR2032, CR123A.

Table 5.4: Parameters of the model and their values.



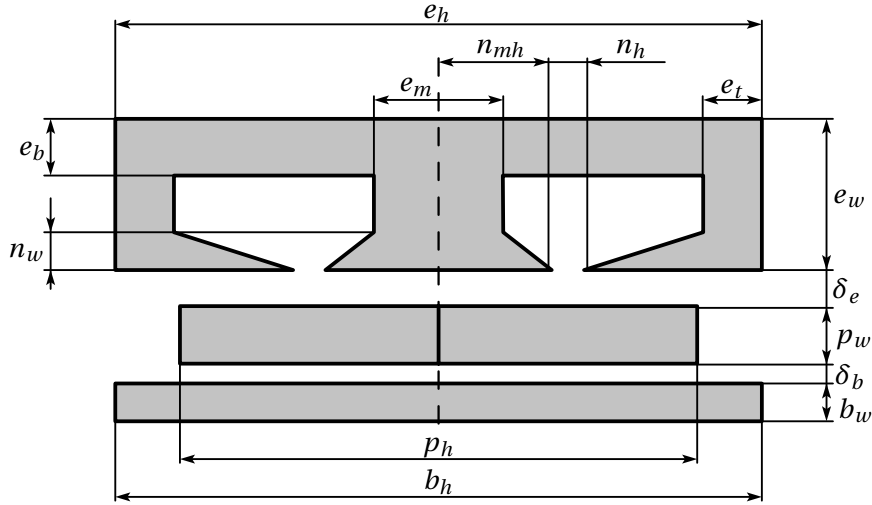


Figure 5.10: Geometric parameters of the actuator.

Because the optimisation is intended to yield the parameters of an actual prototype, the possible values that the free parameters can take are discretised, to take into account fabrication limitations. Therefore, unless otherwise stated, each degree of freedom has a resolution of 0.1 mm. This greatly enhances the worth of the optimisation in industrial terms because it provides comprehensive values for the parameters.

For an application with average or little production, a solution with off-the-shelf PMs is cost efficient. This explains their fixed dimensions. The selected wire for the coil is easy to wind without being too fragile.

Some input parameters are used to determine secondary parameters. For instance, the number of turns  $N$  of the coil is determined according to (5.9) using the fill factor  $K_{Co}$  and some geometric dimensions:

$$N = \frac{S_c}{S_w} \cdot K_{Co}, \quad (5.9)$$

where  $S_c$  is the section of the coil and  $S_w$  that of the wire.

The value of the series resistance of the coil  $R_a$  for the selected wire depends on the length  $w_l$  of wire, itself dependent on the geometry and number of turns, and its linear resistance  $r_l$ , as expressed in (5.10).

$$R_a = w_l \cdot r_l \quad (5.10)$$

### Procedure

The PO has a single objective: the maximisation of the kinetic energy  $E_{kin}$ , but keeps the other constraints. As soon as an acceptable individual is discovered the PO is interrupted. This individual is used in the initial population of the MOO, whose objectives are the minimisation of both the volume  $V_a$  and the electrical energy consumption  $E_{el}$ . The other individuals of the initial population are generated randomly to ensure a variety of genomes. Research might be pursued on the influence of the percentage of the initial population that is taken from the PO, but it is not the purpose of this manuscript. Each optimisation is performed with a population of 64 individuals with a total of 32 children per new generation. These children are either the fruit of mutation or cross-over.

Dealing with out of specifications individuals can be done in several ways, by discarding them, or with the use of penalty factors. Here, the approach is a mix of those: an individual that does not respect one or more constraints is assigned the worst fitness function possible, namely 0 (or  $-\infty$ ) for a maximisation and  $+\infty$  for a minimisation problem. It has the advantage of keeping some diversity, while still making no assumption regarding the value of the fitness, as would be the case for a penalty-based system.

### Simulation

In order to spend as little time as possible computing invalid individuals, the simulation is performed in 3 steps:

1. The geometry of the actuator is evaluated in the core script. Should it prove invalid (*e.g.* two distinct areas of material collide, creating a magnetic short circuit), the parameters are not even sent to the servers, and the fitness of this individual is set as invalid.
2. The parameters of a geometrically valid individual are sent to a server. The latter performs a very short simulation to verify that the actuator is stable in the sense described above. Any individual that fails this step is also assigned invalid fitness.
3. Finally, if the two previous tests are passed, the kinetic energy simulation is performed. If the mover does not reach the release position  $x_u$  in the allowed time  $T_{d,max}$ , the individual is again assigned the invalid fitness value. For the PO, the kinetic energy is then the calculated for the fitness evaluation. The last validity test for the MOO is performed on the kinetic energy that has to be higher than a threshold value. The fitness of the valid individuals is calculated last.

On the recent computer used for the simulations, the computing time of the first step amounts to less than a microsecond. The stability simulation takes 15 seconds and the energy simulation requires 100 seconds. Running four computation servers concurrently,

evolving for a 100 generations necessitates around 15 hours.

### 5.4.3 Discussion

The PO is first discussed, as it quickly yields results that allow a simplification of the MOO. It gives hints regarding the achievable performance of the actuator. Results obtained with the MOO are then scrutinised.

#### Preliminary optimisation

Five power supply configurations (1x AAA, 2x AAA, 1x CR2032, 2x CR2032, 1x CR123A) are tested with the PO. Of course, the optimisation performed here could be done with any other supply configuration, including rechargeable batteries. Since the target is only to find one individual that can provide sufficient kinetic energy, the optimisations are of course interrupted as soon as an individual is found. Therefore, the information that can be recovered from this optimisation is whether the selected power supply can do the task or not. Using two AAA or a single CR123A gives almost immediately satisfying results, with fitness values easily over 150  $\mu\text{J}$ . In a sense, it is not really an optimisation, but rather a test of several random individuals to see if one of them works. These two configurations are electrically extremely close, with similar voltages and internal resistances. The PO with a single AAA is much more interesting and proves its importance. Indeed, a few hours of optimisation (50 generations) were necessary to find a possible candidate whose fitness is higher than 150  $\mu\text{J}$ . In this case, without the PO, the MOO might have wasted hours of computation on individuals whose specifications could not even come close to satisfying the kinetic energy constraint. Quite similarly, it took the PO some tens of generations to provide a suitable individual in the case of a pair of CR2032. The PO also allowed to rule out the solution using a single CR2032. After more than 100 generations, the best individual only had a fitness of 138  $\mu\text{J}$ , which is still 10% lower than the required minimum.

The remaining four candidate solutions apparently offer sufficient performance. Nevertheless, they all have different specifications that might influence the final choice. Indeed, a pair of AAA offers a similar voltage as a single CR123A, but at a lower cost for the user. Yet, its energy consumption should *a priori* be higher because of the larger internal resistance. Therefore, the solution with a pair of AAA will not be optimised because of its redundancy with the single CR123A. A single AAA is very interesting because of its low cost and volume, but its internal voltage of 1.5 V might be an issue for the driving electronics. Finally, a pair of CR2032 has by far the lowest battery volume but the large internal resistance probably hinders the energetic performance.

The MOO is then performed using those three power supplies: single CR123A, single AAA and pair of CR2032.

### Multi-objective optimisation

The Pareto front of the solutions obtained after 750 generations of evolution for each of the three supply configurations is shown in Fig. 5.11. The first observation is that the respective Pareto fronts for each supply configuration are clearly distinct, with a single AAA providing better performance than a single CR123A and the pair of CR2032 finishing last. These results are not particularly surprising because a single AAA has the smallest input voltage and a comparable internal resistance with a CR123A, yielding less internal Joule heating. In the same way, the pair of CR2032 has by far the largest voltage and internal resistance.

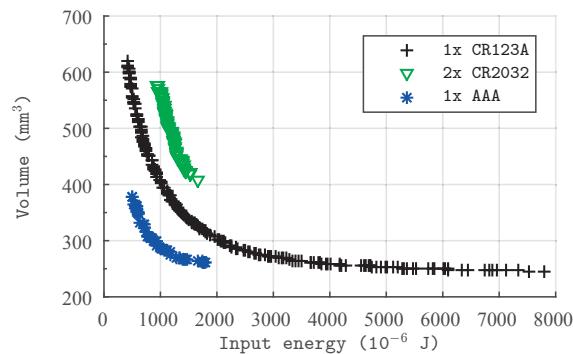


Figure 5.11: Pareto front for the three supply configurations.

The two performances are interesting, but the outcome of the optimisation should also be evaluated in terms of respect of the constraints, namely the provided kinetic energy and dynamic performance. Fig. 5.12 shows the kinetic energy  $E_{kin}$  that each individual of the Pareto fronts provides. The success of the optimisation process is proven by the fact that many individuals generate a kinetic energy close to the required  $150 \mu\text{J}$ . It clearly shows that most of the actuators for a CR123A are oversized because they generate a kinetic energy up to more than twice what is required. It is thus understood that the CR123A provides a larger power surge than the others, offering a larger force from the interaction between the coil and the magnets. This explains why it has a much larger Pareto front that covers a larger spectrum of values for both performances. It appears clearly on the plot that obtaining extreme performance in one or the other performance is more troublesome because the individuals at both ends of the front generate less kinetic energy.

By controlling the driving voltage in a CR123A supply (by applying a constant lower voltage using PWM), it is possible to further optimise the actuator and obtain performances similar —

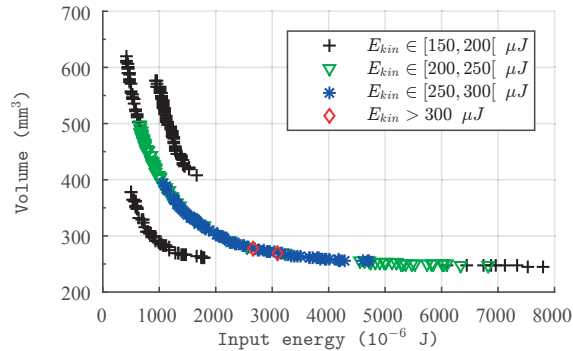


Figure 5.12: Kinetic energy provided by the individuals of the Pareto fronts.

if not better — to those with a AAA battery, with the comfort of having a larger voltage for the electronics. However, this requires another round of optimisation where the driving voltage  $U_{eq}$  is a free parameter. This has not been done, but performances of the individuals of the CR123A front have been recalculated with  $U_{eq} = 1.5$  and  $U_{eq} = 2$  V. This can be achieved by using PWM on the driving H-bridge. With  $U_{eq} = 1.5$  V, none of the individuals were capable of providing  $150 \mu\text{J}$  of kinetic energy, but the results with  $U_{eq} = 2$  V are really close to those obtained with a AAA (Fig. 5.13), yet slightly less good, with a larger energy consumption or a similar actuator volume. Still, they generate slightly more kinetic energy because the individuals are not fully optimised.

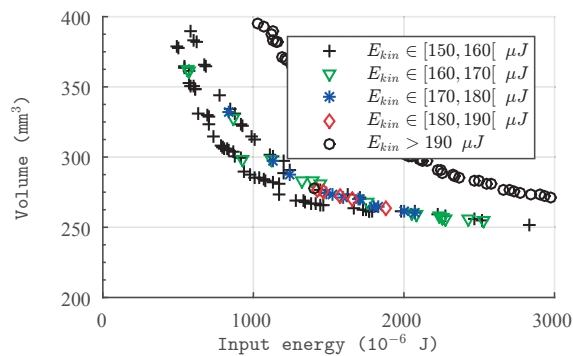


Figure 5.13: Close-up on the individuals of the AAA Pareto front with the addition of the modified voltage CR123A.

From the point of view of dynamics, the rising duration of the mover  $T_d$  is of particular interest because it directly participates in the definition of the maximal actuation frequency. The Pareto fronts are here given with  $T_d$  in Fig. 5.14. Among all the individuals,  $T_d$  is included between 1.8 and 2.6 ms, significantly shorter than the maximal accepted duration  $T_{d,max}$ .

## Chapter 5. Electronically-Controlled Movements

The high power surge capabilities of the CR123A are again observed, as the individuals of the corresponding front are typically faster than the others. The CR123A with a reduced voltage are also globally faster than the individuals for a AAA.

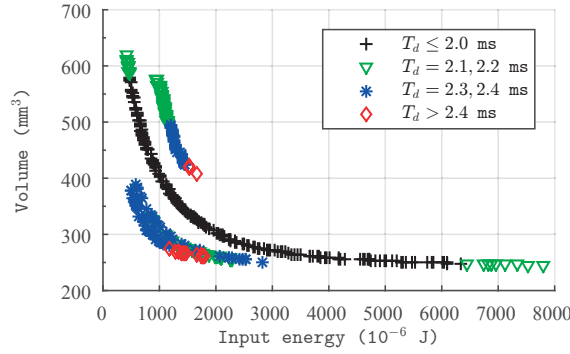


Figure 5.14: Rising time of the individuals of the Pareto fronts.

A correlation is observed between  $T_d$  and  $E_{kin}$ . Obviously, a faster actuator globally yields more kinetic energy, since both depend on the speed of the mover, although not exactly in the same way. Fig. 5.15 is a scatter plot of the kinetic energy versus the rising time. The tendency of faster individuals to generate more kinetic energy is clear. In addition, it clearly shows that in terms of constraints, the actuators obtained for the modified voltage CR123A yield similar results to the pair of CR2032. In this sense, they fare better, since their performance is better.

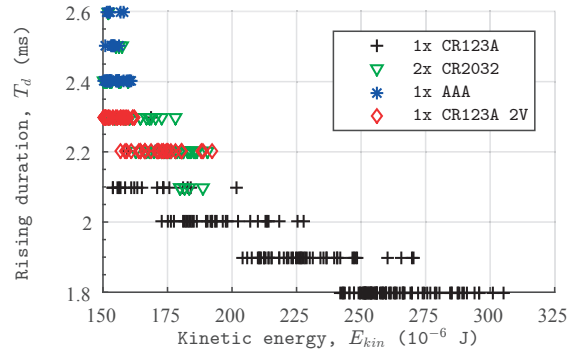


Figure 5.15: Kinetic energy and rising duration obtained for the individuals of the Pareto fronts.

Finally, let us investigate the actual shape of the optimised actuators. A comparison of all the individuals of the fronts shows that not a single individual is part of two fronts. However, the analysis of each parameter separately brings up some information. Firstly, the airgap between the back iron yoke and the PMs  $\delta_b$  is always minimal because its influence on the volume is more important than the effect on the force. For a future optimisation, it is advised

to set this parameter. The shape of the iron yoke varies widely among the solutions. The whole span of possible values of its width  $e_w$  is covered, with of course the larger individuals having larger values of  $e_w$ . It is observed that for the pair of CR2032, the minimal value of  $e_w$  is never present, whereas the largest is never obtained for the AAA. The thickness of the back of the iron yoke  $e_b$  varies very little and is almost always as small as possible, between 0.8 and 0.9 mm, but going up to 1.3 mm in a case, as would dictate the minimisation of the volume. However, this also means that the volume of iron is sufficient to limit the losses, typically saturation. Energetically speaking, the ideal thickness of the external legs of the yoke  $e_t$  for the CR123A is between 0.9 and 1.2 mm, but to obtain the smallest possible actuator, its value increases up to 3.3 mm. The ideal value is around 1.3 mm for the pair of CR2032, and 2.1 mm for the AAA. Because the thickness of the middle leg  $e_m$  has no influence on the volume but only on the input energy, it is not particularly stable and is comprised for all supplies between 0.8 and 1.9 mm.

Last, let us focus on the shape of the slot apertures. Their width  $n_w$ , which affects the volume strongly, is always close to its lowest allowed value, between 0.2 and 0.4 mm. Regarding their height, the value of  $n_h$  changes very little for both the pair of CR2032 and the AAA, around 1.4 and 1.5 mm respectively. For the CR123A, it is around 1.1 mm for the more energy-efficient individuals but increases up to 2.2 mm for the others. The position offset of the slot apertures to the middle of the actuator  $n_{mh}$  does almost not change for each supply configuration. However, much more interestingly, if we analyse the distance between the notch and the boundary of the actuator  $n_t$ , calculated as  $n_t = e_h - 2 \cdot n_{mh} - 2 \cdot n_h$ , we observe that its value is almost the same for all individuals of the fronts for the three supply configurations, with the exception of the very small individuals for the CR123A where it diminishes. It therefore appears that  $n_t$  has an optimum around 2 mm. It is probably due to its role in both the definition in the stability of the actuator as well as the generated kinetic energy. The shape of three representative individuals from each Pareto front is shown in Fig. 5.16.

This clearly shows how much the individuals of the CR123A front vary, particularly compared to those of other fronts. Here again, it is due to the better capabilities of the CR123A for providing larger power surges that allow for a greater flexibility in the design. Nevertheless, the shape of most of the individuals is comparable to that of the CR123A individual in the middle.

A short insight in the actual efficiency — or ratio between the output energy and the input energy — of the obtained individuals highlights a poor efficiency, as the best individual generates 150  $\mu\text{J}$  using 400  $\mu\text{J}$  of input energy, corresponding to an efficiency of 37.5%. It is low partly because the evaluation cycle for the output energy starts with the mover at standstill, a situation in which the mechanical power is close to null.

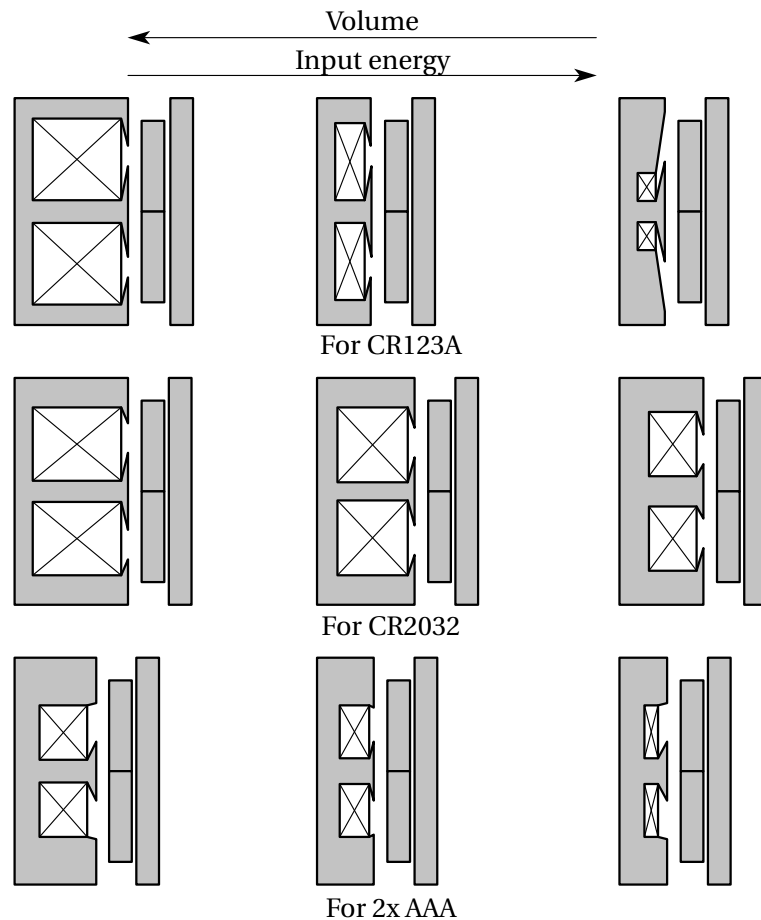


Figure 5.16: Shape of three optimised individuals selected from the Pareto front of each supply configuration.

The final choice of actuator is of course left to the designer. Typically, a cost study including an analysis of the influence of machining tolerance would be a good complement to the optimisation.

#### 5.4.4 Optimisation for the studied movement

A round of optimisation has been performed using the requirements for the linear movement studied in chapter 4, or in other words with a minimal kinetic energy  $E_{kin} = 950 \mu\text{J}$ . This high energy is troublesome, and therefore the PO had to be run with several different supply configurations before obtaining satisfactory results. The MOO was therefore performed using a pair of CR123A batteries, which is a quite bulky configuration. The obtained Pareto front is shown in Fig. 5.17.



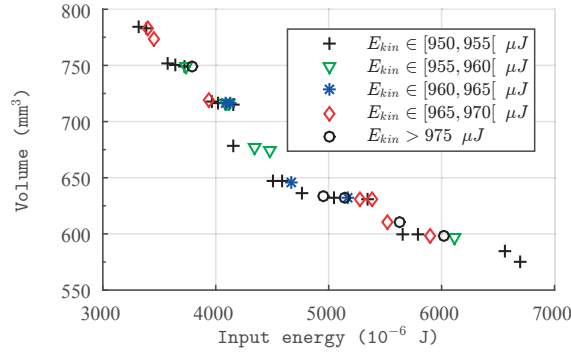


Figure 5.17: Kinetic energy of the individuals of the Pareto front for the studied linear movement.

The performance of the obtained configurations varies across a large span with the most energetically-efficient consuming half the energy of the smallest actuators. In terms of size, the variation is smaller. The choice of the actual actuator is down to the designer, but let us assume that the most efficient actuator is selected. It is now possible to calculate the relative true energy factor of the devised linear movement by dividing the minimal required output energy during a step by the input energy:

$${}^t_s\eta_r^* = \frac{(40 + 1) \cdot 0.4 \cdot 10^{-3}}{3.3 \cdot 10^{-3}} = 5.0. \quad (5.11)$$

In the same way, the disposable true energy factor  ${}^t_s\eta_d^*$  is evaluated at 4.8. This value almost fulfils the requirement of  ${}^t_s\eta_d^* = 5.0$ . Since there is a margin of 20% on the required mover kinetic energy, the actuator's performance might actually be better than modelled and therefore the objective attained. Tests should be conducted on a prototype to validate the results. Yet, compared to a traditionally powered movement, typically composed of a DC motor, some gears and a ball screw mechanism, this value provides a battery life at least five times higher, since the theoretical limit for an ideal system such as this is 1. The main objective of the development is therefore reached.

Also, the maximal advance speed can be computed. The retained actuator configuration has a mover rising duration  $T_d = 1.5$  ms. The minimal thrust force along the stroke and the load and friction values yield a rail moving duration  $T_m < 1$  ms. Therefore, the minimal main cycle duration  $T_a$  is limited by the dynamics of the blocker, embodied by the blocker return duration  $T_r = 6$  ms. The maximal advance speed is therefore  $v_a = 67.4 \text{ mm} \cdot \text{s}^{-1}$ , which is much larger than the required  $10 \text{ mm} \cdot \text{s}^{-1}$ .

### 5.5 Conclusion

The multi-objective optimisation process gives an example on how to deal with the many constraints and degrees of freedom of the design of the actuator. The optimisation relies on a numerical model of the actuator and its driving electronics using the FEM. The suggested strategy, based on genetic algorithms, uses a preliminary optimisation that shows the potential of a given solution to respect a constraint or a set of constraints. This optimisation, which can be really short, allows to rule out unfit solutions and therefore narrow down the number of free parameters. Afterwards, the multi-objective optimisation is done in order to help the designer enhance certain aspects of the performance of the regulating organ, using one or more of the suitable solutions of the preliminary optimisation. This optimisation methodology can be applied to any problem where respecting a constraint is already challenging.

This optimisation of the regulating organ is as important as the mechanical design in the process of devising an energetically-efficient electronically-controlled linear actuator. The combination of the preliminary and multi-objective optimisations works well and produces good results. A large variety of quite different geometries can be obtained with conclusive performance.

The application of the optimisation methodology to the studied movement yielded several candidate sets of parameters for the actuator. Even the least efficient of them results in a disposable true energy factor larger than 1, which is the theoretical limit for a traditional drive system.

---

Publications related to this chapter:

- Romain Besuchet, and Yves Perriard. Optimisation of the mover kinetic energy of a miniature linear actuator. In *Electrical Machines and Systems (ICEMS), 2014 17th International Conference on*, page: 2197 – 2203, 2014.
- Romain Besuchet, Alexandre Gabella, and Yves Perriard. Design of a miniature short-stroke constant-force linear actuator. In *The 9th International Symposium on Linear Drives for Industry Applications (LDIA2013)*, 2013.

## **6 Prototypes & Experiments**

The target of this chapter is to present the prototypes that have been developed in the scope of this research. It is separated in two parts. First, a miniature linear actuator comparable to the one discussed in chapter 5 is introduced. Its performance is confronted to its associated numerical model. Secondly, an embodiment of the movement devised in chapters 3 and 4 is presented. It is characterised and its dynamic and energetic performance is confronted to the models.

### 6.1 Regulating organ – a miniature linear actuator

With view towards the realisation of an electronically-controlled escapement, a specialised miniature linear actuator has been designed. However, the prototype presented here was devised for a slightly different escapement principle that will not be described here. The interested user will find more information in [BGP13]. The specifications of the actuator were still close enough to what was required to use it with the more recent escapement structure.

#### 6.1.1 Structure and parameters

This linear actuator (Fig. 6.1) is composed of a stator consisting in two E-shaped ‘soft’ iron yokes, and a mover made of two PMs polarised in opposite directions and press-fitted in an aluminium frame guided by a parallel leaf spring stage. On each of the iron yokes, a coil is wound around the central leg. They are connected such that they generate a magnetic field of the same polarity in their respective middle leg. The parameters of this structure (Fig. 6.2) are summarised in Table 6.1. The mover is constrained pseudo-linearly by a parallel leaf spring stage.

#### 6.1.2 Characterisation

An FEM-based model implemented in the software *Flux*, capable of simulating the steady state and dynamic behaviour of the actuator, has been used as a guide for the design. The prototype is then used to estimate the quality of the model.

#### 6.1.3 Steady state performance

The experimental process for the validation of the numerical model is straightforward. The actuator, mounted on a fixed frame, is supplied with electric current. The displacement of the mover is measured using a laser displacement sensor\*. The produced force is evaluated using a commercial scale with a resolution of 0.01 g. The force is evaluated every 0.01 mm along a stroke of  $\pm 1$  mm around the middle of the stroke. The set-up is shown in Fig. 6.3.

On the other hand, the FEM-based model is evaluated setting the same current in the coils. In addition to the electromagnetic force that is evaluated using the FEM, the recoil force induced by the leaf spring stage has to be computed. Yet, it is extremely simple as the latter is modelled as a spring of spring constant  $k_{ls} = 250 \text{ N}\cdot\text{m}^{-1}$ .

Fig. 6.4 shows the comparison of the electromagnetic force produced by the actuator when

---

\*Keyence LK-GD500 and LK-G82, <http://www.keyence.eu/products/measure/laser-1d/lk-g3000/>

## 6.1. Regulating organ – a miniature linear actuator

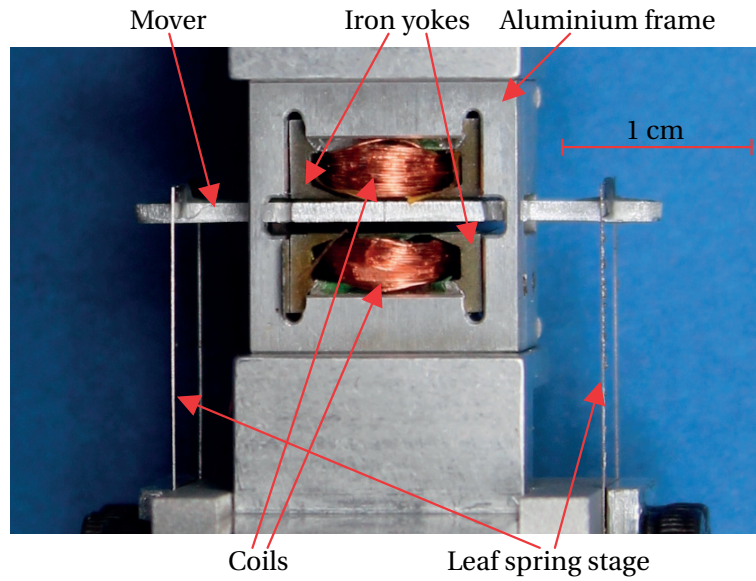


Figure 6.1: Picture of the actuator prototype.

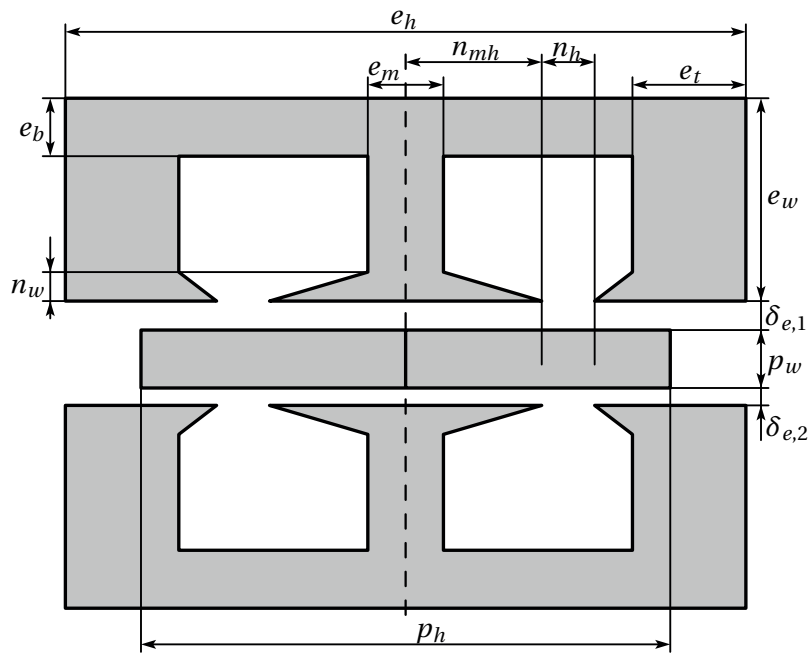


Figure 6.2: Cross-section of the prototyped actuator. Only magnetically active parts are shown.

Parameter	Description	Value
$x_u$	Release position (mm)	0.95
$e_h$	Height of the E (mm)	10
$e_w$	Width of the E (mm)	5
$e_d$	Depth of the system (mm)	10
$e_b$	Thickness of the back of the E (mm)	1.65
$e_m$	Thickness of the middle leg (mm)	1.3
$e_t$	Thickness of the outer legs (mm)	1.1
$n_h$	Height of the slot apertures (mm)	0.6
$n_w$	Width of the slot apertures (mm)	0.65
$n_{mh}$	Position of the slot apertures (mm)	1.7
$p_h$	Height of the PMs (mm)	8
$p_w$	Width of the PMs (mm)	1
$\delta_{e,1}$	Airgap between an iron yoke and the PMs (mm)	0.65
$\delta_{e,2}$	Airgap between the other iron yoke and the PMs (mm)	0.3
$B_0$	Remanence of the PMs (T)	1.43
$\mu_r$	Relative permittivity of the PMs (—)	1.22
$N$	Number of turns of each coil (—)	180
$R_a$	Resistance of the two coils ( $\Omega$ )	20
$w_d$	Wire diameter (mm)	0.12
$k_{ls}$	Spring constant of the leaf spring stage ( $\text{N}\cdot\text{m}^{-1}$ )	400
$m_a$	Mass of the mover (g)	0.94

Table 6.1: Parameters of the model and their values.

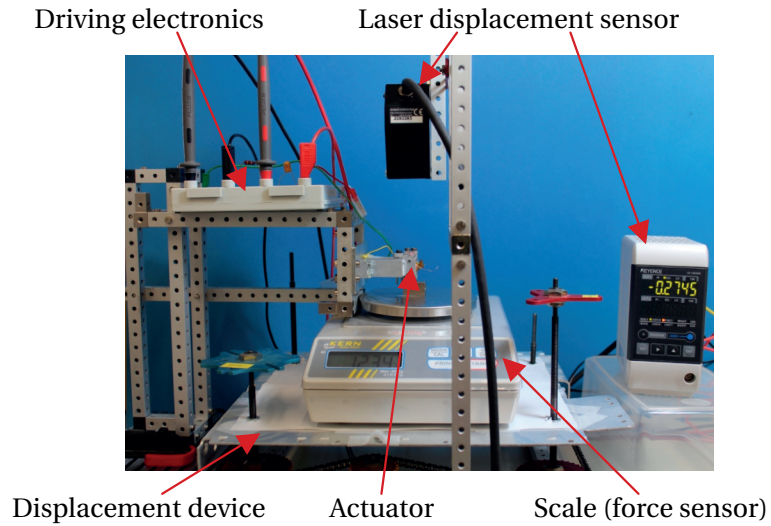


Figure 6.3: Picture of the experimental set-up for the steady state performance of the actuator.

## 6.1. Regulating organ – a miniature linear actuator

the mover is in the middle of the stroke. The results obtained are of excellent quality, with an error between the simulation and the experimental results lower than 3%.

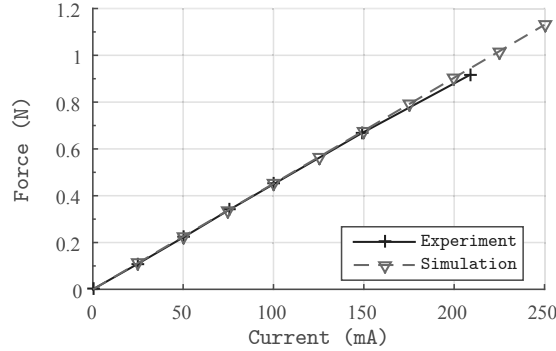


Figure 6.4: Comparison between the modelled and measured electromagnetic force produced in the middle of the stroke.

The electromagnetic force generated when the mover is not in the centre of the stroke cannot be measured directly because of the parasitic force induced by the leaf spring stage. In the same way, the spring constant  $k_{l_s}$  of the leaf spring stage cannot be measured because of the construction of the actuator. Let us show here a workaround to estimate its value. Based on the good accuracy of the FEM model for the centre of the stroke, let us assume that it is also accurate in other positions. The force applied by the mover is measured as previously, but while the actuator is not powered and at several positions along the stroke. These results are compared to simulation results for the electromagnetic force under identical conditions. By adding to it the parasitic force of the stage, it is obtained that  $k_{l_s} = 400 \text{ N}\cdot\text{m}^{-1}$  yields good consistency with the experimental results (Fig. 6.5). The divergence for extreme values of the position can be explained by the fact that the approximation of the parasitic force as being purely proportional to the displacement is a linearisation valid for small displacements.

Using the newly estimated value for the recoil spring, it is possible to compare the experimental and estimated net force along the stroke when the actuator is supplied. Fig. 6.6 shows the case when a current of 100 mA is supplied. The observation is similar, namely that the estimation is very good for most positions, but slightly deteriorates for extreme positions, where the maximal error is around 20%.

### 6.1.4 Dynamic performance

Based on the same model, it is possible to evaluate the temporal evolution of the position of the mover under given driving conditions. As seen in chapter 5, it is necessary to know the driving electronics circuit to assess the behaviour correctly. Using the same circuit, with

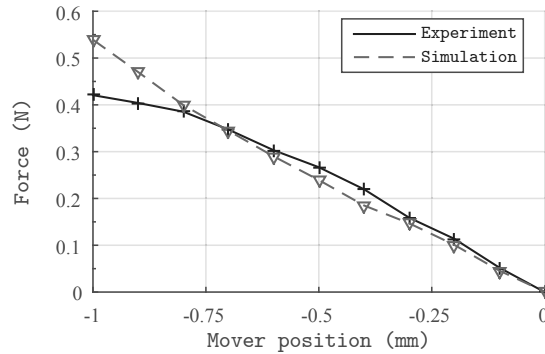


Figure 6.5: Comparison between the experimental and modelled net force applied on the mover when the actuator is not powered.

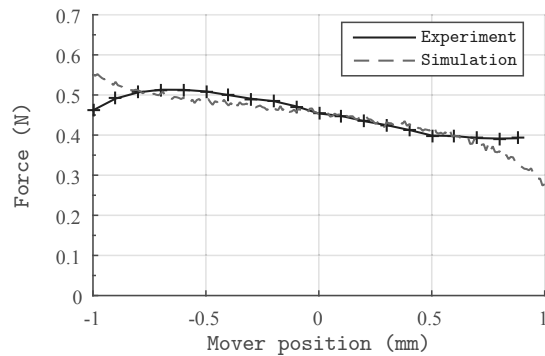


Figure 6.6: Comparison between the modelled and measured electromagnetic force produced along the stroke for a given input current.

the difference that the voltage source is ideal ( $R_i = 0$ ), the FEM-based model can provide this information. As was done previously, the input signal is a voltage step. The speed of the mover is measured at the time when it reaches the unlocking position  $x_u$ .

The experiment with the prototype is set up in the same way. A PWM signal is used to adapt the higher voltage of a stabilised power supply to the actuator. With a high-speed camera<sup>†</sup>, the position of the mover is measured and its speed is evaluated. The accuracy of this method is limited but still permits a comparison between the modelled and actual motion of the mover.

Fig. 6.7a shows the evolution of the position of the mover for a step when the driving voltage is 3 V. In this case, the simulation underestimates the time for the mover to reach its extreme

<sup>†</sup>Phantom v210, <http://www.visionresearch.com/Products/High-Speed-Cameras/v210/>



## 6.1. Regulating organ – a miniature linear actuator

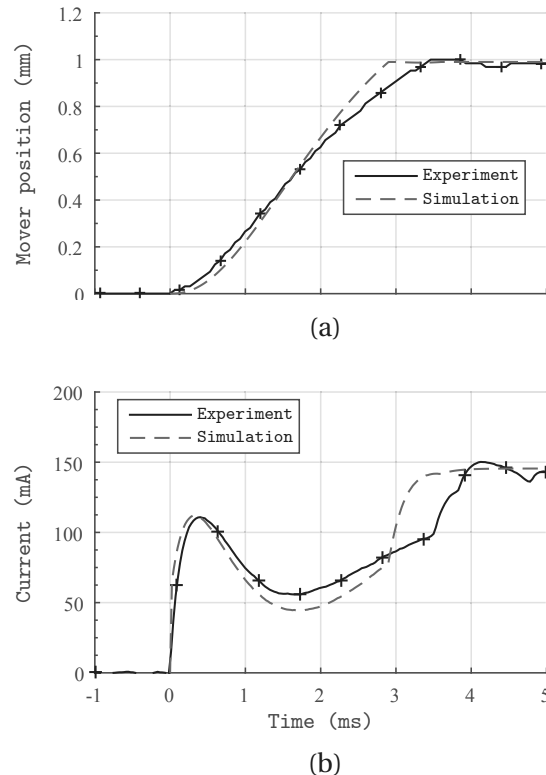


Figure 6.7: Temporal evolution of the position (a) and the current in the coils (b) of the actuator under a driving voltage of 3 V. The displacement is mechanically limited to 1 mm.

position of 15%. This is however the worst of the 10 cases observed. The evolution of the current in the coils of the actuator is represented in Fig. 6.7b. Until the mover reaches its extreme position, the model and the experiment show a similar evolution. After the extreme position is reached, they diverge because the rebound of the mover against the mechanical stop is not modelled. The model fares better with higher voltages (tested up to 5 V). The effect of the voltage induced in the coils by the motion of the mover is clearly observed between 0.5 and 4 ms. Indeed, the current exponentially increases very early in the step, but then its magnitude drops. The evaluation of the current is directly related to the evaluation of the input energy consumed by the actuator for displacing the mover. The simulation corresponds quite closely to the measurements until the mover reaches its limit position. From there on, the two obviously differ. The evaluation of the simulated and measured input energy before the mover reaches the unlocking position yields an error very similar to that of the time to reach it.

Finally, let us try to evaluate the speed of the mover. Because of the rather low sampling rate

of the position, the resolution of the speed measurement is huge ( $200 \text{ mm}\cdot\text{s}^{-1}$ ). The quality of the speed measurement is therefore mediocre. Nevertheless, given filtering, it is possible to observe the similarity between the expected and measured speed, as shown in Fig. 6.8. The filtering permits the overall evaluation of the shape of the speed, but deteriorates the numerical value too much for a correct evaluation.

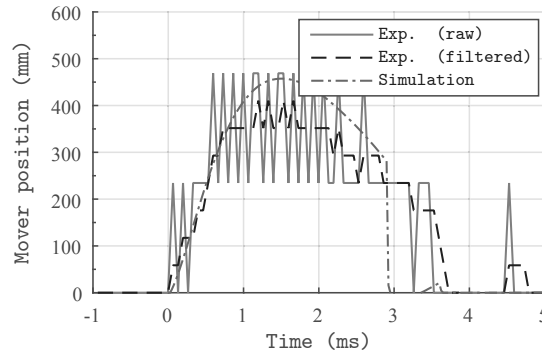


Figure 6.8: Evolution of the speed of the mover under a driving voltage of 3 V.

The quality of the measurement is therefore not sufficient to correctly evaluate the speed, especially when the speed at one precise position is desired. Nevertheless, the comparison between the measured and simulated position tends to show that the model yields results within acceptable boundaries and thus consider it as qualitatively representative and quantitatively overestimating.

Let us observe the evolution of the kinetic energy acquired by the mover after travelling the distance  $x_u$  with respect to the driving voltage (Fig. 6.9). As would be expected, for low voltages the mover never even reaches  $x_u$  because the electromagnetic force cannot overcome the recoil force of the leaf spring stage. Also, the kinetic increases with the square of the voltage because the electromagnetic force, which determines the acceleration of the mover, is directly proportional to the voltage. Of course, it is not a perfect parabola because of the induced voltage effect and the force offset due to the stage.

### 6.1.5 Conclusion

This prototype shows the validity and limitations of the model developed in chapter 5. The model is excellent for the static performance of the actuator. The dynamic performance modelling is less accurate, but it is inherent to dynamic modelling due to the accumulation of error. The experiments conducted showed that the kinetic energy is overestimated, so for an optimisation, a safety margin of 20% is suggested. Also with a view towards optimisation, the model of the input electrical energy has been validated with an error smaller than 3%.

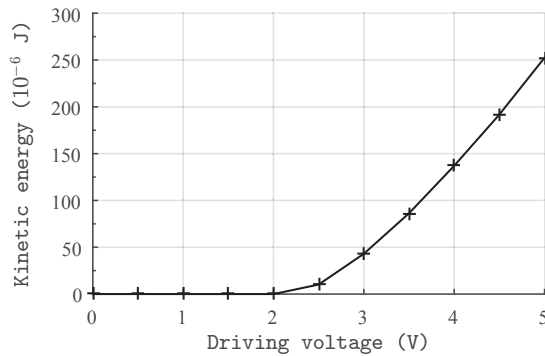


Figure 6.9: Modelled evolution of the kinetic energy with respect to the driving voltage.

## 6.2 An electronically-controlled linear movement

The prototype of the complete movement is made of an escapement such as described in chapter 3, with a regulating organ composed of the actuator and driving electronics discussed in the previous section. This prototype has been developed mostly as a test bench and a proof of concept, it is therefore not optimised, although it was designed for good performance. It serves to validate the dynamic and energetic models developed earlier. Therefore, its specifications in terms of resolution, thrust force and energetic performance are different to what was presented before. All the main functions for the escapement and energy stock are achieved with industrially viable solutions with a view towards the realisation of an injector, but not with a high degree of integration so as to facilitate characterisation and modification. Less interesting functions such as the guiding of the rail and the spring are done using prototyping solutions that ensure a correct functioning but could not be used as such in a product either for cost or size reasons. Fig. 6.10 shows the prototype. On the left, the main spring and its linear bearing can be seen. A simple nut permits to adjust the preload of the spring, thus defining the thrust force. The free end of the spring is connected to the rail, which is mounted on an aluminium plate guided by a linear bearing. In another embodiment, this linear bearing is replaced by two POM plain bearings. The assembly in the middle is the transmission & escapement as well as the regulating organ.

A close-up on the escapement and the regulating organ (Fig. 6.11) clarifies the location of the different elements. The rail, the blockers and their teeth, made of stainless steel are in the middle in the bottom. The leaf spring stages of the blockers can also be distinguished. The two  $\mathcal{L}$  are disposed on either side of the mover of the actuator.

The values of the parameters defined in earlier sections of the thesis are summarised in Table 6.2.

## Chapter 6. Prototypes & Experiments

Parameter	Description		Reference value
Requirements			
$s_o$	Stroke	(mm)	40
$r_o$	Resolution	(mm)	0.4
$F_l$	Force of the load	(N)	10
	Friction force on the rail	(N)	1
Modelled information			
$v_a^{th}$	Theoretical advance speed	(mm·s <sup>-1</sup> )	100
$s\eta_{r,m}^*$	Relative mechanical energy factor	(—)	30.1
$t\eta_{r,m}^*$	True relative mechanical energy factor	(—)	21.2
Parameters			
$k_s$	Main spring constant	(N·m <sup>-1</sup> )	240
$l_{s,f}$	Free length of the main spring	(mm)	175
$l_{s,p}$	Preload length of the main spring	(mm)	85
$p_t$	Pitch of the teeth	(mm)	0.8
$\alpha$	Angle of the locking face	(°)	89
$h_t$	Height of the teeth	(mm)	0.2
$m_b$	Mass of a blocker	(g)	0.5
$\mu_s$	Static friction factor	(—)	0.4
$\mu_d$	Dynamic friction factor	(—)	0.05
$l_{\mathcal{L},b}$	Distance between the pivot of the $\mathcal{L}$ and the blocker	(mm)	7.2
$l_{\mathcal{L},m}$	Distance between the pivot of the $\mathcal{L}$ and the mover	(mm)	12.2
$I_{\mathcal{L}}$	Moment of inertia of the $\mathcal{L}$	(g·mm <sup>2</sup> )	6.6
$\epsilon$	Coefficient of restitution	(—)	0.9
$k_r$	Recoil spring constant	(N·m <sup>-1</sup> )	1000
$x_{b,0}$	Standstill deformation of the recoil spring	(mm)	0.1
$x_{b,m}$	Maximal deformation of the recoil spring	(mm)	0.55
$m_a$	Mass of the mover	(g)	1
$T_d$	Mover rising duration	(ms)	} 3
$T_h$	Mover hold duration	(ms)	

Table 6.2: List of parameters of the dynamic and energy models of the escapement

## 6.2. An electronically-controlled linear movement

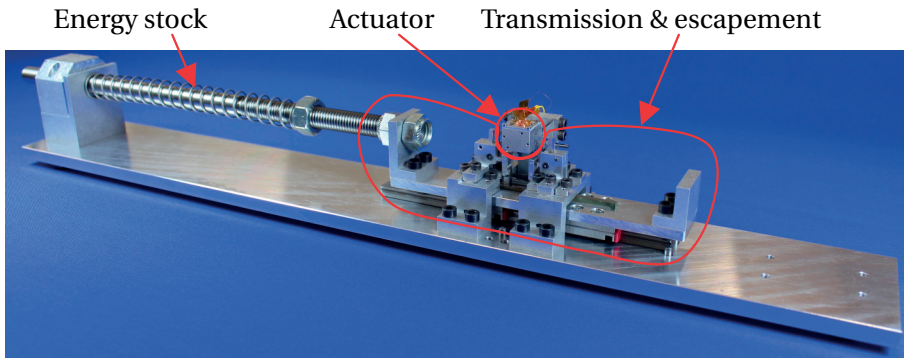


Figure 6.10: Picture of the movement prototype.

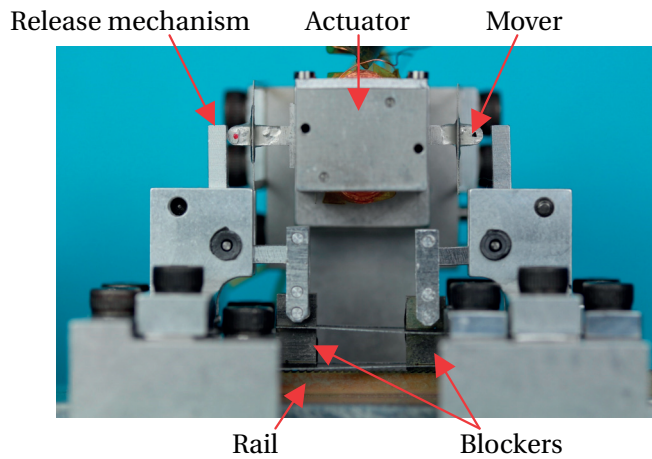


Figure 6.11: Close up on the escapement and regulating organ of the movement prototype.

### 6.2.1 Dynamic performance

The dynamic performance of the prototype is tested in two parts. Firstly, the blocker return duration  $T_r$  modelled in chapter 4 is measured. Secondly, and more interestingly, the displacement of the output.

#### Return duration

In Sec. 4.1.2, the return duration  $T_r^f$  is modelled as:

$$T_r^f = \sqrt{\frac{m_{b,e}}{k_r}} \cdot \arccos\left(\frac{x_{b,0}}{x_{b,m}}\right), \quad (6.1)$$

where  $m_{b,e}$  is the mass of the moving parts,  $k_r$  the recoil spring constant,  $x_{b,0}$  the deformation of the spring at rest, and  $x_{b,m}$  the deformation of the spring right before release.

With the values of the prototype, it yields a theoretical return time of 1.1 ms. By measuring the position of the blocker with a fast laser displacement sensor, the return time has been estimated to be 1 ms. Given the strong influence of  $x_{b,0}$ , which is difficult to measure exactly due to the mounting process, this result is satisfactory. This therefore yields, in the sense of the definition of the theoretical maximal speed given in Sec. 4.3,  $v_a^{th} = p_t/2 \cdot (T_d + T_h + T_r) = 100 \text{ mm} \cdot \text{s}^{-1}$ , considering  $T_d + T_h = 3 \text{ ms}$ . The safety factor compared to the expected maximal advance speed is of 3. With the prototyped actuator, this performance is achievable but with a driving voltage slightly larger than 3 V.

### Output displacement

The purpose of the escapement-based movement is indeed the displacement of the output. The position of the output is again measured using a laser displacement sensor while the advance is controlled by the regulating organ described above. Over the stroke of 40 mm, the thrust force  $F_s$  linearly decreases from 20 N at the beginning of the stroke to 11 N at the end. The following experiments will always be conducted in three different load conditions:

1. Without load (*no load*);
2. With an empty syringe (*syringe*);
3. With a syringe filled with water (*water*).

The use of syringes relates to the industrial application mentioned in introduction. Experimenting using real loads rather than artificially generated loads permits a more accurate representation of what will happen when the device is in use.

Two steps are measured for each load condition because the movement cannot be perfectly symmetrical. Indeed, a step released from the left blocker (step 1) is not exactly identical to a step released from the right blocker (step 2). Symmetrical steps could be obtained if the distance between the two blockers  $d_b = (k + 0.5) \cdot p_t$ ,  $k \in \mathbb{N}_+$ , which is not feasible in practice. In fact, the error on  $d_b$  yields an asymmetry twice the size of that error. Fig. 6.12 shows the temporal evolution of the position of the output for two steps taken in three different load conditions. It clearly shows that one step is 0.05 mm longer than the other. In other words, it is a rather large deviation of 12.5%. In addition, the importance of the load is clear. Without load, the distance of a step is covered in less than 5 ms, a duration that increases to 25 and 40 ms for the case with a syringe and water respectively. The case without load displays two other interesting phenomena due to the leaf spring stage. A disruption in the displacement of the output is observed when the rail interlocks with the second blocker. The steady position

## 6.2. An electronically-controlled linear movement

is observed to be slightly further than the position of the collision because of the elasticity of the leaf spring stage. It results in each step being slightly shorter than the previous. This elasticity as well as the nature of the energy stock (a spring) a responsible for the oscillations before the stabilisation of the position.

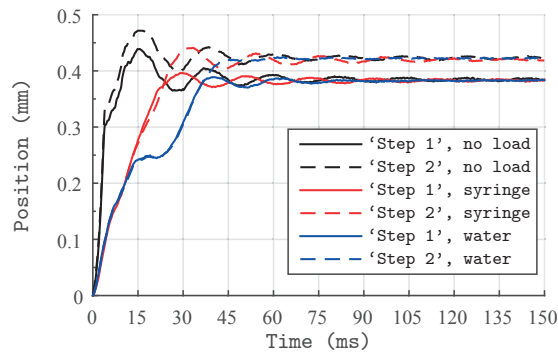


Figure 6.12: Evolution of the position of the output for three different load conditions.

The comparison between the syringe and water cases is more interesting in terms of nature of the load. The beginning of a step is completely similar for both cases, which tends to show that at first the compliance of the syringe is the most important effect. Then, at about 2.5 mm, the importance of the water is observed because the curves diverge. Once the step is accomplished, the position still oscillates before stabilisation because of the elastic deformation of the parts, yet to a smaller extent.

Fig. 6.13 shows the position of the output for two different series of eight step with a syringe as a load. One series (full line) is successful and the other one (dotted line) skips a step, which eventually creates a positioning error of two steps. The successful and failed series are performed with a different thrust force. In the first series, it is observed that the syringe is not constrained at the beginning because the first step starts really fast before slowing down. Quite similarly, in the second series, the first two steps are required to constrain the syringe. This is simply due to mounting where the plunger of the syringe is only pushed on by the rail and not bonded to it. In a commercialised device, this would of course happen, but it is equivalent to what practitioners do before injecting when they ensure that there is no air in the syringe before starting the injection. Whereas the steps come one after another harmoniously in the first series, the third step of the second series is too slow, which causes the subsequent step to be initiated too early. The rail is therefore blocked by the blocker that was supposed to have released the previous step, which causes yet another step to be skipped. The sequence then resumes normally.

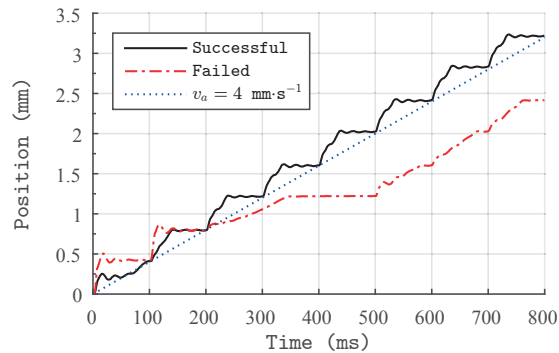


Figure 6.13: Evolution of the position of the output for two different series of eight steps and the theoretical advance speed.

Finally, Fig. 6.14 shows the advance on the whole stroke for each load case at a speed of  $4 \text{ mm}\cdot\text{s}^{-1}$ . Without load, it works normally. In the syringe and water cases, some steps are skipped but there are no rules as to when the steps are skipped. With the reduction of the thrust force along the stroke, it is expected that steps are skipped more often towards the end of the stroke, but since the loads are real and not constant, some steps are skipped in different locations along the stroke. Tests conducted with a speed of  $2 \text{ mm}\cdot\text{s}^{-1}$  showed that in these conditions the system never skips a step. This proves the importance of the thrust force in the definition of the dynamic performance of the movement.

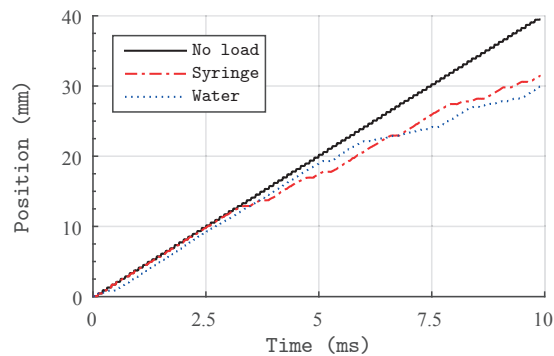


Figure 6.14: Evolution of the position of the output on the whole stroke for each load case, at a commanded average speed of  $4 \text{ mm}\cdot\text{s}^{-1}$ .



### 6.2.2 Energetic performance

To conclude this chapter, let us analyse the model of the energetic performance.

#### Mechanical energy factor

A first experiment targets the validation of the model of the mechanical energy developed in chapter 4. To do so, the kinetic energy  $E_{k, trig}$  necessary to initiate a step under a given thrust force  $F_s$  is measured. The designed set-up is extremely basic (Fig. 6.15): a pendulum (polymer rod of known mass and centre of mass) collides with the  $\mathcal{L}$  of the release mechanism. The conversion of the potential energy of the rod to kinetic energy is supposed ideal (no friction on the pivot). Therefore, measuring the angle formed by the initial position of the pendulum and the position when it hits the  $\mathcal{L}$  permits to determine the amount of kinetic energy provided to the system.

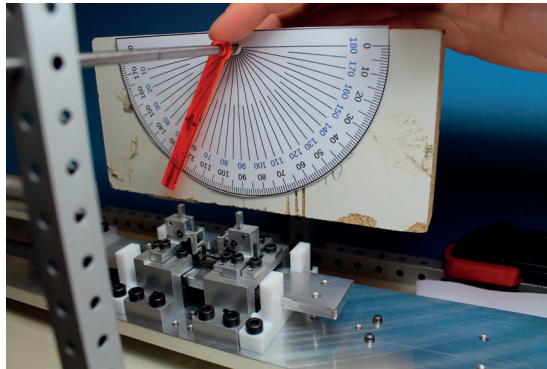


Figure 6.15: Picture of the experimental set-up for the validation of the model of the mechanical energy.

Of course, since the conditions are not exactly the same as when the movement is in normal use, some adaptations are required. The major difference regards the unlocking condition. Previously (4.44), it was established that to initiate a step, the kinetic energy should be higher than the largest of the displacement  $E_d$  or unlocking energy  $E_{k, ul}$ , based on the assumption that the time  $t_\infty$  necessary for all the collisions of a series of collisions to have taken place is negligible. However, it is no longer the case in this experiment, where a single collision happens because the force on the rod is small. Therefore, the efficiency of a single collision is substituted to the efficiency of a series of collisions in (4.43) to yield:

$$E_d = \frac{W_{f,r} + W_{E,lock}}{\eta_{fc}}. \quad (6.2)$$

Although small, the difference is important as the efficiency of the first collision is significantly

lower than that of a series of collisions. Similarly, since the mass of the provider in a collision influences the efficiency, the mass of the rod is used instead of the mass of the mover of the actuator.

The experiment has been conducted for thrust force values between 5 and 20 N. The comparison with the modelled value (Fig. 6.16) shows a rather large error yet not to an alarming extent, mainly because the trend is similar to the model. Indeed, most of the parameters of the system are known accurately, but some, such as the coefficient of restitution  $\epsilon$  are difficult to evaluate accurately. To make matters worse, its value strongly influences the estimated required energy. In a similar way, the friction factor is hard to determine and has a strong influence on the result.

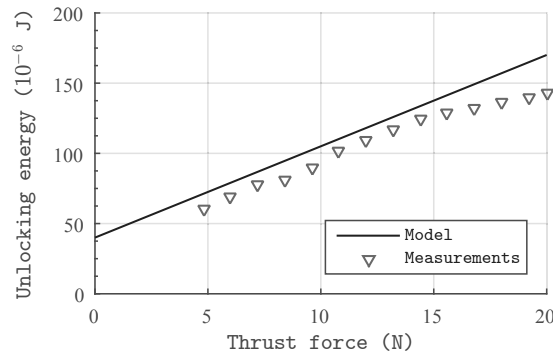


Figure 6.16: Comparison between the modelled and measured unlocking energy.

Energetically-speaking, it is interesting to note that the measured performance is better than expected. Here again, it is understood that this is due to the uncertainty on some of the parameters values. Going back to the initial definitions and parameters values, the measurements yield a mechanical relative energy factor on the stroke equal to:

$${}_s\eta_{r,m}^* = \frac{{}_sE_{m,ad}}{{}_sE_{k,trig}} = \frac{{}_sE_{m,ad}}{n_{steps} \cdot \max(E_{k,trig})} = 35.7, \quad (6.3)$$

a value slightly larger than the modelled 30.1. The mechanical true relative energy factor is calculated at 25.2, opposed to the modelled 21.2. The error in both cases is close to 20%. It is large, but tolerable with regards to the measurement conditions.

### Energy factor

Finally, let us measure the actual relative energy factor  ${}_s\eta_r^*$ . It was discussed in chapter 5, that the efficiency of the regulating organ is low and it negatively affects the relative energy factor. The experiment conducted consists in applying a 1 ms voltage pulse on the actuator.

## 6.2. An electronically-controlled linear movement

The electrical energy is provided by a stabilised voltage source, whose voltage and delivered current are measured. The integration along time of the multiplication of these two values yields the input electrical energy. This test is conducted for different thrust force values. Fig. 6.17 shows the electrical energy required to generate a step and compares it with the unlocking energy discussed in the previous section. It clearly highlights how important the optimisation of the regulating organ is.

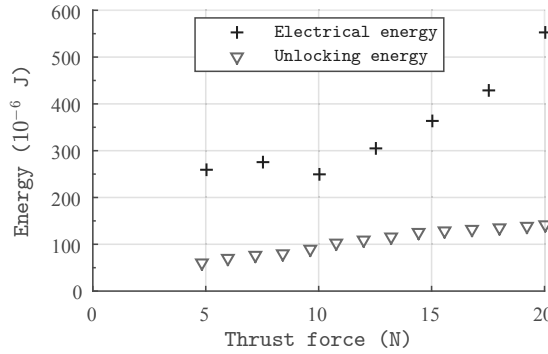


Figure 6.17: Electrical energy required to initiate a step.

For low values of the thrust force, the electrical energy is constant for a simple reason: it is the minimal energy required for the mover to reach the unlocking position in the given impulse duration. Therefore, there is a large waste of energy in particular because the mover hits the release mechanism with a kinetic energy much larger than necessary.

The parabolic shape of the curve is the result of the actuator having a constant force factor and the unlocking being almost proportional to the thrust force. Assuming a constant electromagnetic force along the stroke of the actuator, which is good enough for a qualitative study, the necessary force to obtain the unlocking energy is the latter divided by the unlocking distance. With the constant voltage-to-force ratio, the driving voltage is almost directly proportional to the thrust force. Finally, since the electrical energy is the integration along time of the square of the voltage divided by the resistance, the electrical energy is proportional to the square of the thrust force.

Since the thrust force along the stroke is  $F_s \leq 20$  N, the relative energy factor measured is:

$${}_s\eta_r^* = \frac{{}_sE_{m,ad}}{{}_sE_e} = \frac{{}_sE_{m,ad}}{n_{steps} \cdot \max(E_e)} = 11.3, \quad (6.4)$$

where  ${}_sE_e$  is the total electrical energy consumed to perform the 100 steps of the stroke. The relative true energy factor  ${}_s\eta_r^*$  has a value of 7.2. The relative energy factor is more than three times lower than the mechanical energy factor, indicating that, in the devised prototype, the

actuator is the weak link in the target of reducing electrical energy consumption. However, the optimisation strategy proposed in chapter 5 shows that better performance can be obtained.

### 6.2.3 Discussion

The experiments conducted on the prototype prove that the proposed concept for a linear escapement-based movement can fulfil the imposed technical requirements. It was also shown that the model of the consumed electrical energy developed in chapter 4 is of good quality. It nevertheless suffers from its strong dependency on certain design parameters that are difficult either to assess or to manufacture, but this is inherent to the retained solution. The results obtained in this section validate all the models except for that of the case when the actuator is supplied by a battery. Further testing should be made towards the validation of this part of the model, for example by counting the number of steps that can be successfully initiated on a given battery. Yet, as the actuator currently is, it cannot provide sufficient energy when it is powered by a battery and such test is not really relevant.

Many other aspects of the structure could be tested. For example, it would be interesting to study how rapidly wear alters the behaviour of the mechanism. Because of the forces at stake it is probably the biggest issues of the selected escapement principle. It is mitigated by the fact that the rail could actually be an expendable part made of softer material to protect the integrity of the blockers. The behaviour of the movement when subject to external accelerations or in different environmental conditions could also be studied.

### 6.3 Conclusion

The prototypes used in this section served their purposes as demonstrators for the retained working principles for the linear movement. The models relative to the actuator have been proved to be of good quality. To a smaller extent, the models regarding the movement and in particular the escapement are interesting indicators of the performance of the mechanism, but the uncertainty on manufactured parts and key parameters (friction factors, spring constants, etc.) did not permit the assessment of the actual accuracy of the models. Nevertheless, they are qualitatively satisfactory.

From the point of view of the application, the retained working principle showed good results. The relative true energy factor of 7.2 promises a battery life more than 10 times longer than for a traditional motor-driven injection. Indeed, a global efficiency of 50% between the battery electrical energy and the actual provided mechanical energy (yielding a gain of 14.4 with the escapement-based device) would represent a good performance. Dynamically speaking, it has been measured that the prototype can consistently and reliably provide an advance speed of  $2 \text{ mm}\cdot\text{s}^{-1}$ , which is acceptable for the desired application. If desired, this speed can be enhanced without modifying the movement itself but by using a linear bearing that generates less friction on the rail.

The movement is already small, yet it would be interesting to further work on it for several reasons. For now, only the core functions of the movement have been really miniaturised: the teeth of the rails, the leaf spring stages guiding the blockers and the actuator. To efficiently design an overall miniaturised movement, it is necessary to also work on the miniaturisation of the release mechanism (the  $\mathcal{L}$ s), the rail itself, and all the support and guiding parts that have not been mentioned. Another industrially interesting topic would be the optimisation of the cost through the enhancement of the fabrication and mounting processes.



## 7 Conclusion

This thesis addressed the issue of the design of a mechatronic (or purely mechanical) device. The major challenge of the design resides in its management of available energy with a view towards energetic independence. Inspired by clockwork mechanisms, this research is centred on so-called escapement-based movements. A definition of an escapement-based movement as considered in the thesis is given.

Rather than limiting the research to a single mechanism fulfilling given requirements, this work broadened its scope and proposed the functional analysis of a generic movement. The energy and data flows between the constitutive elements of the movement were in particular analysed to define their requirements. A canvas for the preparation of the requirements for any escapement-based movement within the scope of the given definition has been elaborated. Along with this analysis, evaluation tools were proposed to permit the evaluation of the feasibility and fitness of a solution at any time during the design process. The focus was set on the dynamic and energetic performance of the devised mechanism through a modelling methodology that strongly links the requirements with the design parameters.

A case study has been presented to give an example of application of the proposed methodology. The requirements of said example have been defined and a functional principle retained, where the mechanical structure is as important as the electrical controller. This mechatronic system was modelled as much as possible analytically, to benefit from the very fast evaluation of such models, but a numerical model, based on the finite element method (FEM), proved necessary to adequately describe the behaviour of the electrical part of the system. The accuracy of the developed models has been tested with prototypes that showed their quality and limitations.

The analysis of the mechanical performance of the devised movement has been performed in two steps. Firstly, the sensitivity of the performance to large variations of the design

parameters has been evaluated, providing design guidelines for the choice of the reference value of each parameter. Secondly, for a more industrial approach, the influence of the deviation of the parameters due to machining tolerance has been analysed. This is important for mass production, as stricter tolerance yields higher machining costs. Both of these analyses are made easier by the analytic nature of the mechanical model. Indeed, more than a hundred thousand evaluations of the model have been necessary.

An optimisation methodology using genetic algorithms (GA) has also been proposed for highly constrained problems. This methodology, based on a preliminary optimisation where the constraints are set as objectives, has been successfully applied to optimise the electrical part of the movement, using an FEM-based model.

The results obtained with the functional prototype showed an interesting potential for such movements in the field of controlled injection. The quality of the results also shows that the design methodology helps the design process efficiently.

### 7.1 Original contributions

The major part of the thesis revolves around three themes: analysis, modelling and optimisation. Naturally, the main contributions relate to these multidisciplinary fields. Here, they are applied to mechatronics, and therefore strongly tainted with mechanical and electrical engineering. Mechatronics being multidisciplinary, an approach of the complete system, from the user to the result, is encouraged. Failure of doing so often yields poor or flawed results.

- *Escapement-based movements as positioning devices:*

Very little literature regarding escapement-based movements is available. Of course, the niche situation in which they find themselves can explain it. Therefore, the functional analysis of escapement-based movements as positioning devices is a novelty. To support the idea, two take-home elements are given:

1. *The general structure of an escapement-based movement*, given with precise definitions, formalises the movement. This structure is given as a frame for the development, and it helps with the identification of the environment in which the movement is to be used, which is of primal importance.
2. *The canvas for the elaboration of the requirements* provides guidelines to ensure that the main functions are represented in the functional requirements. They are also written in such a way that the performance that matters to the user is clearly given. This way, the designer is constantly confronted to the objectives when consulting the requirements.



- *Performance modelling of escapement-based movements:*  
A strategy for the development of models of escapement-based movements is given. For dynamic models, it is advised to dissect the run of a step as a sequence of events. Each event is assigned specific durations that are individually modelled. Then, the temporal relation between these durations is used to model the run of a step. The initial conditions of each step can be taken into account to model a series of steps. For the energetic model, the strategy is similar but instead of dissecting the step in a sequence of events, the energy necessary to displace or prevent the displacement of each moving part is calculated. Here again, consecutive steps can be added to evaluate a series of steps. The modelling strategy is also designed so that the performance requirements are a direct output of the models.
- *Optimisation strategy for highly constrained problems:*  
Highly constrained problems are particular in the sense that not only objectives have to be optimised, but the optimal individuals are subject to severe constraints. Therefore, the space of acceptable individuals is largely reduced. In this case, a traditional optimisation algorithm might waste hours of computation simply to find an individual that respects the constraints. The first step of the developed strategy is to run a preliminary optimisation where the constraints are defined as objectives. The obtained fit individuals are then used as starting points for the actual optimisation. In the thesis, it is implemented with a genetic algorithm, but this strategy can be applied to most optimisation strategies, be they stochastic or deterministic.
- *Novel electronically-controlled escapement-based movement:*  
Finally, the escapement-based movement proposed as a study case gives an interesting example of a movement optimised for a specific application, with results showing enhancement compared to the performance of existing devices. The novelty in this prototype does not only consist in the functional principle, but also in some of the technical solutions. The leaf spring stage designed for the blockers shrewdly combines several functions in only two mechanical parts that ensure a reliable working and are rather cheap to produce.

Other lesser contributions include a generalisation of the *collision-based energy transmission model* proposed in [Con07]. The model described in this thesis considers collisions between two constantly-accelerated particles instead of a free particle and a constantly-accelerated particle. The *use of the dynamic model as a design tool* based on constraints on the specific durations is also proposed. This alternative usage of the dynamic model permits a rapid evaluation of the performance of a set of parameters but also a rapid understanding of the

limitations of this set in terms of performance, by clearly showing what constraint is the limiting factor. The optimisation of the electrical part of the escapement is also peculiar because one of its objectives is the kinetic energy acquired by the mover of the actuator in given conditions. It is really a performance oriented choice that is not commonly found in the literature.

### 7.2 Outlook

This thesis opens perspective on several different levels. The research conducted could be completed, but also on a larger scale, innovative uses of escapement-based movement could be devised. Let us single out the following points.

- *Methodology enhancement:*

The research on the methodology could be pushed further. The work presented here paved the way to the formalisation of the design of escapement-based movements used as positioning devices, but there is still work to do. As it is now, the regulating organ and the escapement are designed concurrently but separately. It would probably add up to the quality of the design process to design them together, in the sense that the model of the transmission & escapement would be based on the design parameters of the regulating organ rather than on the performance of the latter. The issues with such an approach would however be a largely increase of the complexity of a task that is already not simple. The added degrees of freedom might prove too much to obtain good results in a tolerable amount of time. Yet, it would still be interesting to investigate in this direction.

- *Optimisation:*

Following this development, a global optimisation of the movement could be contemplated, with the complexity still being a potential fatal flaw. Indeed, the increase of degrees of freedom requires more computational power, which might very easily become an issue in case some parts of the model have to be resolved using the FEM or similar methods. Still on the topic of optimisation, there are interesting perspectives on an optimisation strategy for the transmission & escapement that not only takes into account dynamic and energetic performance, but also the structural resistance of the mechanism. This would require to incorporate the evaluation of the maximal stresses and strains in the structure as constraints in the optimisation process.

- *On the functional prototype:*

Because this work has been triggered by an industrial project, it is relevant to mention

the enhancements and further steps required before the prototype can be sold as a product.

- The rail is planned to be an expendable part, serving for only one injection. This corresponds to a commercial plan but is also functionally important. Indeed, as it is, the rail is extremely costly to produce, and so are the blockers to a smaller extent because of their smaller size. An expendable rail could be made of a softer material that would reduce the wear of the expensive blockers. With a wise material and machining technique selection, the rail could become much cheaper, in particular because its lifespan should be a single injection.
  - Some work is necessary for the integration of the movement. As it is now, the core of the movement is made of parts of small dimensions, but they are assembled with a prototyping mindset, namely in a way that it is easy to mount, dismantle, modify, and so that ‘secondary’ functions such as assembly functions can be ruled out in case of malfunction. It is of course not optimal for obtaining a miniature movement.
  - Finally, the industrialisation of the movement is an obvious task. It consists in all tasks that regard production, extensive testing, validation of fabrication processes, lifespan evaluation, etc.
- *Develop other escapement-based movements:*  
With one of the objectives of this thesis being to create enthusiasm surrounding escapement-based movements, it is only natural to encourage the design of such movements for alternative applications or innovative solutions for existing applications.



# A Alternative functional principles and solutions

This appendix provides alternative ideas or principle that have been imagined but discarded for the case study. In the first section, different working principles are given. The second one is focused on alternative solutions for the functions of the retained working principle. This appendix is presented as a collection of reflections on various key topics for the movement for the case study.

## A.1 Alternative working principles

Mechanical energy is either provided as a force over a linear displacement or a torque on a rotary motion. Therefore, in the movement, each mechanical function can be imagined as linear or circular. The desired mechanical work produced by the injector has to be a force along a linear stroke. Let us see how this influences the design.

### Transmission

The transmission is directly influenced by the nature of the output. It is its task to transform any kind of motion into the desired force on the desired displacement. Because of this, a linear system has a large advantage in terms of complexity, because the transmission can be a simple and straightforward link between the energy stock and the output. Yet, this necessitates that the energy stock provides the energy directly in agreement with the output requirements. In opposition, including some rotary parts is more complex but it allows to modify the conditioning of the energy between the stock and the output, typically through a gear box; it provides more flexibility. The transmission is therefore totally dependent on the energy stock and the output. By design, it will of course also strongly influence the escapement and thus also the regulating organ.

## Appendix A. Alternative functional principles and solutions

---

The elements constituting the transmission are typically basic mechanical devices, such as rods, pivots, gear boxes, levers, bearings, etc.

### Energy stock

Mechanical energy storage can be achieved by two global concepts: statically or dynamically, or in other words as potential or kinetic energy. Springs are probably the most common devices for potential energy storage. By deforming a part within its elastic limits, energy can be stored almost without losses. The same principle can be applied to gases, such as the well-known compressed air. This solution is however more complicated and less stable in particular because of leaks and the complexity of thermodynamics.

Kinetic energy storage systems usually comprise a flywheel. The speed at which this wheel spins depends on the kinetic energy that it is storing. Friction on the bearings is one of the causes for this solution's losses. It is not really indicated for start-stop applications. Shorter-term kinetic energy storage can be done in a translating mass, such as a hammer head. However, it is definitely not a viable solution for situations where the energy might be consumed little by little.

	Solution	Pros	Cons
Potential	Spring	+ Reliable + Stable	- Force profile
	Compressed air	+ Flexible design + Force profile	- Leaks - Complex
Kinetic	Flywheel	+ Compact	- Complex - Friction - Manoeuvrability

Table A.1: Common mechanical energy storage solutions.

### Creation of the stepper motion

As said in the main matter of the thesis, a stepper system has spatially invariant stable positions. Time-based stepping is not considered as a stepper system. These stable positions are created by local minima of potential energy. However, the conditions in which the stability has to be maintained, or in other words the depth of the potential wells, depend on the application. Here again, mechanical energy plays a central role, but any type of energy can create this potential. In practice, the shaping of a potential field can most easily be done at a scale such as we desire using mechanics or magnetism.

Mechanically, the stepper motion is created by material interference. The magnetic solution

requires at least a permanent magnet or coil electrically supplied, and a ferromagnetic structure. The shape of the structure and the position of the magnets can create a controlled magnetic field in which a secondary ferromagnetic structure has stable positions. Displacing the secondary structure out of a stable position requires mechanical or magnetic energy supply. Stepper motors are an extremely good example of such a system, where magnetic energy is supplied to one of the ferromagnetic structures via electromagnets to get the rotor moving on to the next stable position.

### **Escapement**

Many options for the escapement can be contemplated. Among others, the degree of stability, or number of stable positions of the locking element(s) that interfaces the regulating organ and the transmission. In our case study, we can talk of bistability because either one of the two blockers can provide a stable position of the movement. Most clockwork escapements are also bistable. However, escapements such as the chronometer escapement are monostable. It would be the equivalent of having a single mover in our movement. This requires the blocker to come back to its initial (blocking) position faster than the rail advances in order to only let one step escape. The escapement designed by Marshall and Rolfe is also monostable because of their choice of regulating organ that constrains their collar in one given position when not powered. Another degree of stability in purely mechanical escapements however seems unlikely to provide more advantages than downsides. Yet, stepper motors are often more than bistable because it offers a better angular resolution. The Lavet type stepper, widely used in clockwork, is a notable exception of bistable stepper motor.

### **Regulating organ**

Similar options are offered for the regulating organ, but a major difference exists: the regulating organ works as a time-base and counter for the movement. The way these data are treated is a defining point. Nowadays, counting time and arithmetic operations are almost always done electronically. Historically, most of these functions could be performed mechanically, although usually with less accuracy in the case of measuring time and with less flexibility for arithmetic operations. Therefore, an electronic control has many advantages in terms of performance, but requires electrical energy to work, which might be a prohibitive drawback in certain cases. Purely mechanical movements will thus not be discussed any further.

## **Appendix A. Alternative functional principles and solutions**

---

### **A.1.1 Movements ideas**

The discussion in previous sections, even being far from exhaustive, highlights the large number of possibilities for each and every function. The most important point to make of it is that a choice in any of the subsystems of the movement can have an influence on the other subsystems, which is a reminder that the design process of the movement relies on a large number of iterations. Still, a few alternative functioning principles are presented here.

#### **Dependent blockers for a linear escapement**

In the solution studied in the thesis, the two blockers are kinematically independent. It has many advantages in particular to recharge the main spring, but also in terms of mounting issues and manufacturing tolerance. During earlier stages of the industrial project, a slightly different functional structure was tested, where the blockers were moving simultaneously, quite similarly to the pallets and the anchor in a Swiss lever escapement in clockwork. It has a great safety advantage in that if the teeth of one of the blocker are disengaged for any reason, the second blocker can only be in a blocking position. It also has an energetic advantage, because the recoil springs are no longer necessary, so the rather important losses that they generate are avoided. However, this solution is problematic when it comes to the manufacturing and mounting of the movement. It requires extreme precision. Another major flaw of this design is the way to guide the blockers. They could be mounted on a pivoting part, exactly as the anchor is mounted in the Swiss lever escapement, but the shape of the teeth would have to be adapted to the rotational distortion when the teeth engage and disengage. Also, the friction on the pivot would be huge. On the other hand, using linear guides requires additional joints as well as probably large friction in the case where the linear guide is a plain bearing. An alternative to plain bearings would be the use of leaf spring stages, which would reintroduce the recoil force in the system. Therefore, this solution has been evaluated as inferior to the proposed one.

#### **Rack and pinion output and circular escapement**

A rack and pinion system is a circular-to-linear motion transformer. A cogged wheel (pinion) and a toothed rail (rack) interact by way of their teeth. A rotation of the pinion induces a displacement of the rack and inversely. A rack and pinion can be designed so that any position is stable. Therefore, the resolution of such a system can be very high without requiring really precise positioning, by connecting the pinion to a gear box and controlling the position of the last wheel of the gear box. It is also a good way to drastically reduce the stress on the critical parts of the movement.



A particularly interesting concept in the case of electronically-controlled movements is to connect a stepper motor to the pinion through a gear train. The cogging torque inherent to the motor is tasked to blocking the advance of the system. A step is generated by supplying the motor with electric current exactly as it would be done in a positioning application where the stepper motor provides all the mechanical energy. The difference is that the main spring actually provides the mechanical energy, and the electrical energy can just be used to overcome the cogging force rather than attract the rotor to the next step.

Two main options are available for the main spring. It could be a linear spring stressing the rail itself, or a torsion spring applied on the pinion directly or through a gear train.

Functionally speaking, this movement fulfils qualitatively most requirements. The major drawback is its handling of function M.E.4 (Table 3.1): 'Have a mechanical energy stock rechargeable by hand'. Indeed, it is specified that disposable energy should not be necessary to recharge the mechanical energy stock, and that the recharge force should not be too high. Without disposable energy, the cogging torque should be added to the force of the main spring during recharge, which is an issue. It can be overcome by providing a way to disconnect the stepper motor from the gear train, but this is a weakness prone to causing the failure of the system.

One last thing about this mechanism is the potential dynamic issues due to the gear train. The increase of inertia that a high gear ratio generates can slow down the movement.

### **Nut-screw type output and circular escapement**

Another radically different type of movement makes use of a nut-screw mechanism and a circular escapement. The screw is used exactly as the toothed rail was in the previous example, to provide the position of the output. The main difference with the previously discussed movement is that the nut-screw naturally offers a rather high resolution if the screw thread is fine. Apart from this, the functioning is very similar, with the possibility of connecting the nut to a gear train and, for example, a stepper motor. It can also be stressed by a linear or torsion spring, applied respectively on the screw or on the nut.

The nut-screw mechanism can be set up with either the nut or the screw moving forward. The choice depends on many parameters, but *a priori* the screw should be the moving part. This solution suffers from similar issues as the previous one in terms of recharge of the mechanical energy stock and dynamics.

### Inchworm type stepper mechanism

A significantly different method for the creation of the steps has also been contemplated. Instead of having potential energy wells defined by the mechanical or magnetic structure of the escapement or regulating organ, the stable positions of the output could be such that they only exist for a given timespan. An example could be simply by clamping a shaft. Indeed, the shaft does not have inherently stable positions that the toothed rail has, but by applying an external force on it, it can be blocked, achieving the desired function. Yet, the definition of escapement-based movements given in chapter 2 states that the mechanism should have a stepper behaviour, which is not the case as such with this blocking solution. However, there exist solutions to this issue. One of them is shown in Fig. A.1, and its functioning is the following:

1. Clamp A is closed, clamp B is open, and the system is at rest. The main spring constrains the shaft, which is blocked by the clamp A. The step spring forces the clamp B against the furthest mechanical step.
2. Clamp B is closed to prevent the shaft from having a motion relative to this clamp.
3. Clamp A is opened, so the main spring displaces the shaft, clamp B, and the load. The displacement is limited by the other mechanical stop. The step spring is now compressed.
4. Clamp A is closed.
5. Clamp B is opened. Under the influence of the step spring, it is pushed back against the furthest blocker. And the system is back to a stable state, ready for a new step.

This system is slightly more complicated, but it has the advantage of making the shaft much simpler. In terms of dynamics, it probably displaces larger masses than the system proposed in the thesis. From the point of view of energy consumption, there are doubts as to its performance because active elements (the clamps) are required to work for longer durations. Of course, it is completely dependent on the actual solutions retained to accomplish all the functions. Yet, this system is worth noting.

#### A.1.2 Conclusion

The four functioning principles given above simply show how radically different the movement could be. In particular, they show that it might be possible to use circular escapements in linear applications, with advantages being the possibility to easily adapt torque and speed, but certain drawbacks such as dynamics and the rewinding capabilities. There are of course many other possibilities, but these four are interesting and not too eccentric solutions.

## A.1. Alternative working principles

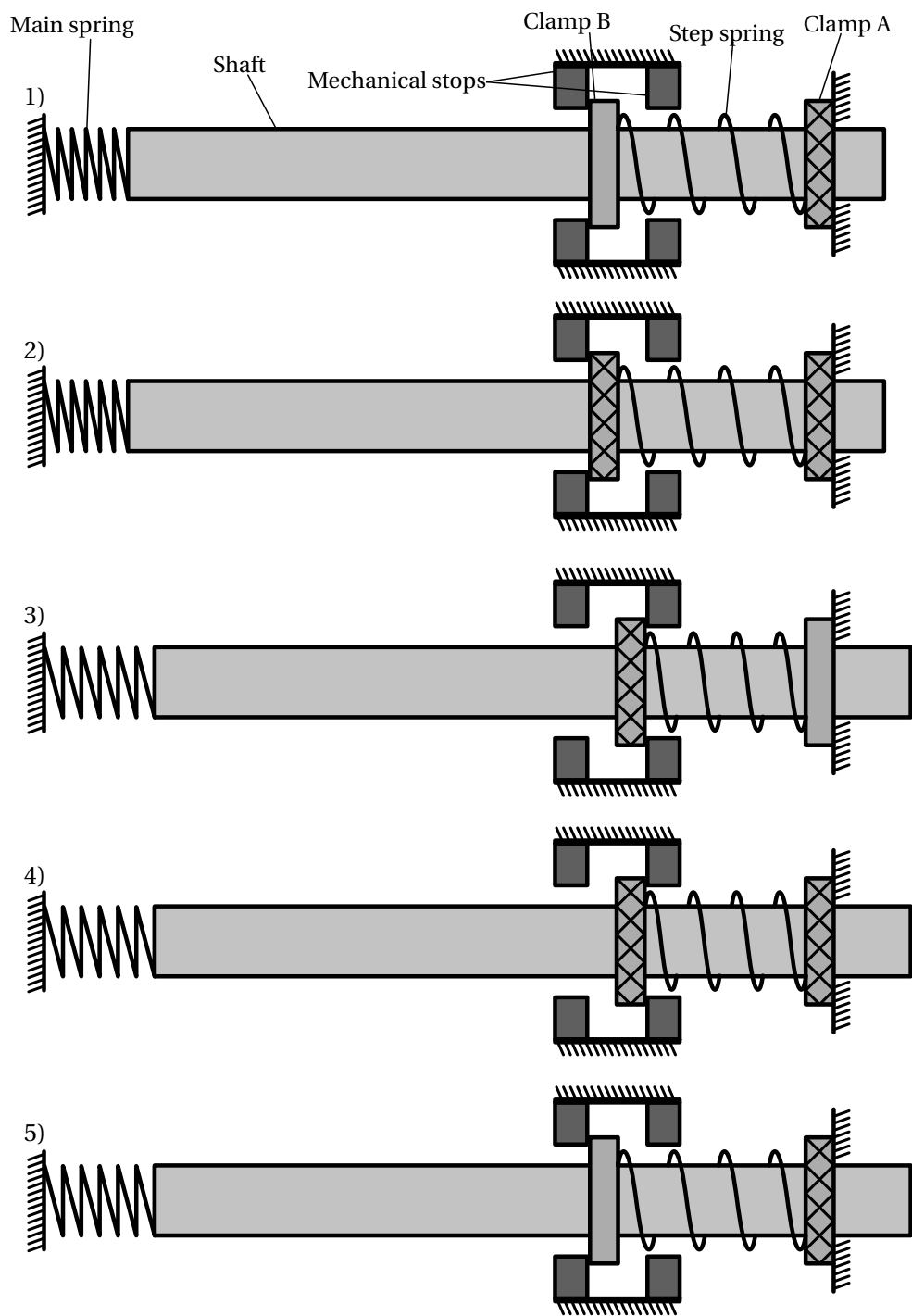


Figure A.1: Sequence for the execution of a step.

### A.2 Alternative solutions

This section discusses a few solutions worth noting for the movement discussed in the thesis. Some comments are also given regarding some of the selected solutions.

#### Energy stock

- The very traditional compression spring selected for the application can actually be replaced by two springs, one coiled clockwise and the other anti-clockwise of a different diameter so one can fit inside the other.
- A tension spring could also be used, but for a slightly larger volume due to the hooks necessary to transmit the force.
- Constant-force springs are also a good option, in particular because those springs have a very low spring constant, which has been demonstrated to be efficient. Yet, for the targeted force, the required spring size is not convenient.
- A compressed air based solution has been studied, with the objective of obtaining a lower spring constant, but the quality of the solution is hindered by its leaks, weight and cost.

#### Transmission & escapement

- The teeth of the blockers and the rail could be done quite differently. One idea would be to replace the teeth by small pins, to reduce manufacturing costs. Historically, a clockwork escapement called the pin-pallet escapement was manufactured in a similar manner to reduce costs. This could also lead to a very interesting optimisation of the shape of the blockers teeth to ensure a correct locking but at the same time reduce the energy necessary to unlock.
- The guides of the blockers and the recoil springs could be made differently but I truly believe that the selected leaf spring stage is a very good solution. In the prototype, the leaf spring stage is realised in such a way that the two stages slot together so as to be more compact (Fig. A.2).
- The guide for the rail can be made with a more or less expensive solution. The plain bearing used in the prototype is cheap, but might create too much friction for some applications. Whatever the solution, it is highly important that the positioning between the rail and the blockers is well controlled.

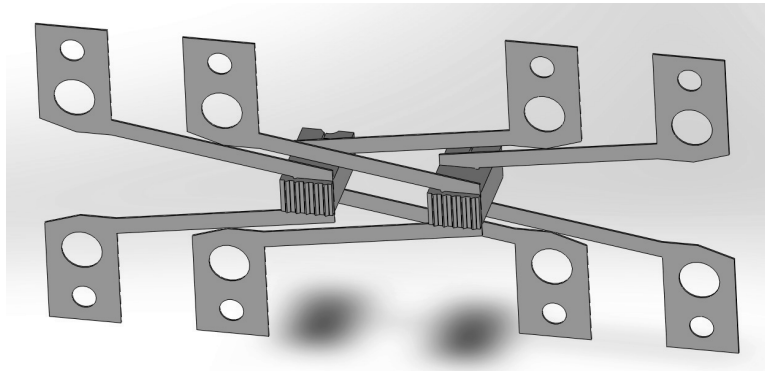


Figure A.2: Leaf spring stages used in the prototype.

### Regulating organ

- The type of actuator offers a very wide range of choices. One of the attractive alternative solutions is the use of a commercial DC motor, particularly when the movement is used to perform a rather large number of steps. The speed of advance can be translated to the angular velocity of the motor.
- A large variety of solutions is also available for the electrical energy storage. In addition to those stated in chapter 5, let us mention rechargeable accumulators, such as lithium-polymer batteries. It is a commercial issue to decide whether a rechargeable battery is a good solution or not.
- From the electronics point of view, there are also countless solutions for the driving circuit as well as the microcontroller and the user interface. Since the electronics are not particularly challenging, it is considered an industrialisation task to design the suiting electronics driver.



## **B Collision-Based Energy Transmission**

Using collisions to produce large amounts of energy and instantaneous power with little force is very common. It is done when hammering a nail in a wall, where the kinetic energy accumulated by the hammer is transmitted in a very short amount of time to the nail. It generates a force sufficient to pierce the wall and drive the nail in. Because this technique is used in the mechanism, we shall model it analytically. In particular, the efficiency of the energy transmission is analysed. Another phenomenon occurring in collisions is that of rebound. Experience shows that, when dropping a ball from a certain height, it will bounce a few times before stopping. It is due to the nature of collision energy transmission and the fact that the ball is driven towards the floor by an external force: gravity. In this appendix, a similar series of collisions is modelled in the general case, so as to predict more precisely the behaviour of the collision-based energy transmission in the escapement.

## B.1 Modelling

The following development is a generalisation of the analysis performed by T. Conus [Con07]. Let us consider a one-dimensional space, in which two free particles are animated by collinear speeds and accelerations. Throughout this demonstration, the particle of mass  $m$  providing the energy – the *provider* – is animated by a speed  $v$  before the collision and  $\tilde{v}$  after. The symbols representing the other particle – the *receiver* – are the same but with an apostrophe, namely  $m'$ ,  $v'$  and  $\tilde{v}'$ . For the collision to actually happen, it is necessary that  $v > v'$ , a condition maintained throughout the whole demonstration.

### B.1.1 Single Collision

Let us start by analysing a single collision. It can be described combining the law of the conservation of the momentum and the definition of the coefficient of restitution  $\epsilon$ :

$$\begin{cases} m\tilde{v} + m'\tilde{v}' = mv + m'v' \\ \tilde{v}' - \tilde{v} = \epsilon(v - v') \end{cases} \quad (\text{B.1})$$

By definition,  $0 \leq \epsilon \leq 1$ . However,  $\epsilon = 1$  is a theoretical maximum that will be ignored because it is physically not feasible and cause mathematical issues. We thus consider  $0 \leq \epsilon < 1$ .

The system (B.1) can be written:

$$\tilde{\vec{v}} = L\vec{v}, \quad \text{where} \quad \vec{v} = \begin{pmatrix} v \\ v' \end{pmatrix} \quad \text{and} \quad \tilde{\vec{v}} = \begin{pmatrix} \tilde{v} \\ \tilde{v}' \end{pmatrix}, \quad (\text{B.2})$$

with the matrix  $L$  as:

$$L = \frac{1}{(m + m')} \begin{pmatrix} m - \epsilon m' & (1 + \epsilon)m' \\ (1 + \epsilon)m & m' - \epsilon m \end{pmatrix}, \quad (\text{B.3})$$

The efficiency of the energy transmission of a single collision can be defined as the increase of kinetic energy of the receiver divided by the initial kinetic energy of the provider:

$$\eta_{fc} = \frac{m'}{m} \cdot \frac{\tilde{v}'^2 - v'^2}{v^2} = k_m \cdot \frac{(1 + \epsilon)(1 + \epsilon + 2u + 2uk_m)}{(1 + k_m)^2(1 + u)^2}, \quad (\text{B.4})$$



with the variables change suggested by Conus:

$$k_m = \frac{m'}{m} \quad \text{and} \quad u = \frac{v'}{v - v'}. \quad (\text{B.5})$$

It is easy to demonstrate that the theoretical largest efficiency for a given value of  $\epsilon$  is obtained when  $k_m = 0.5$ , which is equivalent to  $m = 2m'$ .

### B.1.2 Series of Collisions

Based on the previous results, let us model a series of collisions happening when the two particles  $m$  and  $m'$  are submit to accelerations  $a$  and  $a'$  respectively, with the condition that  $a > |a'|$  (otherwise there is only one collision, or the system might start backwards). The accelerations  $a$  and  $a'$  are due to the forces  $f$  and  $f'$  respectively and are expressed  $a = f/m$  and  $a' = f'/m'$ .

Let us find a general expression for the position and speed of both the provider and the receiver at any time  $t$ . The position  $x(t)$  and  $x'(t)$  of the provider and receiver between two collisions are written:

$$\begin{cases} x(t) = \frac{1}{2}a(t - t_i)^2 + \tilde{v}_i(t - t_i) + x(t_i) \\ x'(t) = \frac{1}{2}a'(t - t_i)^2 + \tilde{v}'_i(t - t_i) + x(t_i) \end{cases} \quad (\text{B.6})$$

Of course, since the particles collide, for  $t = t_{i+1}$ ,  $x(t_{i+1}) = x'(t_{i+1})$ . It is thus possible to calculate  $(t_{i+1} - t_i)$ , which will be useful further on, using (B.6):

$$\frac{1}{2}(a - a')(t_{i+1} - t_i)^2 - (\tilde{v}'_i - \tilde{v}_i)(t_{i+1} - t_i) = 0. \quad (\text{B.7})$$

This equation has a trivial solution for  $(t_{i+1} - t_i) = 0$ , but the physically interesting solution is:

$$(t_{i+1} - t_i) = \frac{2(\tilde{v}'_i - \tilde{v}_i)}{(a - a')}. \quad (\text{B.8})$$

## Appendix B. Collision-Based Energy Transmission

---

The position  $x(t_n)$  of the  $(n + 1)^{\text{th}}$  collision is written as:

$$\begin{aligned} x(t_n) &= x(t_0) + \sum_{i=0}^{n-1} \left[ \frac{1}{2} a' (t_{i+1} - t_i)^2 + \tilde{v}'_i (t_{i+1} - t_i) \right] \\ &= x(t_0) + \sum_{i=0}^{n-1} \left[ 2a' \frac{(\tilde{v}'_i - \tilde{v}_i)^2}{(a - a')^2} + 2\tilde{v}'_i \frac{(\tilde{v}'_i - \tilde{v}_i)}{(a - a')} \right], \end{aligned} \quad (\text{B.9})$$

where  $x(t_0)$  is the position of the first collision.

Similarly, the time  $t_n$  at which the  $(n + 1)^{\text{th}}$  collision happens, with  $t_0$  the time of the first collision, is calculated as:

$$t_n = t_0 + \sum_{i=0}^{n-1} (t_{i+1} - t_i) = t_0 + \sum_{i=0}^{n-1} \frac{2(\tilde{v}'_i - \tilde{v}_i)}{(a - a')}. \quad (\text{B.10})$$

The speed at the time of the  $i^{\text{th}}$  collision can be written as:

$$\begin{cases} v_{i+1} = a(t_{i+1} - t_i) + \tilde{v}_i \\ v'_{i+1} = a'(t_{i+1} - t_i) + \tilde{v}'_i \end{cases}. \quad (\text{B.11})$$

With (B.8), (B.11) becomes:

$$\begin{cases} v_{i+1} = \frac{2a(\tilde{v}'_i - \tilde{v}_i)}{(a - a')} + \tilde{v}_i = \frac{2a\tilde{v}'_i - (a + a')\tilde{v}_i}{(a - a')} \\ v'_{i+1} = \frac{2a'(\tilde{v}'_i - \tilde{v}_i)}{(a - a')} + \tilde{v}'_i = \frac{-2a'\tilde{v}_i + (a + a')\tilde{v}'_i}{(a - a')} \end{cases}. \quad (\text{B.12})$$

Let us introduce the matrix  $A$  such that:

$$\vec{v}_{i+1} = \begin{pmatrix} v_{i+1} \\ v'_{i+1} \end{pmatrix} = \frac{1}{(a - a')} \begin{pmatrix} -a - a' & 2a \\ -2a' & a + a' \end{pmatrix} \begin{pmatrix} \tilde{v}_i \\ \tilde{v}'_i \end{pmatrix} = A \cdot \vec{\tilde{v}}_i. \quad (\text{B.13})$$

We can then write:

$$\vec{v}_{i+1} = A \cdot L \cdot \vec{v}_i = M \cdot \vec{v}_i. \quad (\text{B.14})$$

to evaluate the speed difference between two consecutive steps.

Let us now calculate  $M = A \cdot L$ , with  $\Delta a = (a - a')$  and  $\Sigma m = (m + m')$ :

$$M = \frac{1}{\Delta a \cdot \Sigma m} \begin{pmatrix} a((1+2\epsilon)m + \epsilon m') - a'(m - \epsilon m') & -a((\epsilon-1)m' + 2\epsilon m) - a'(1+\epsilon)m' \\ a(1+\epsilon)m + a'((\epsilon-1)m + 2\epsilon m') & a(m' - \epsilon m) - a'(\epsilon m + (1+2\epsilon)m') \end{pmatrix}. \quad (\text{B.15})$$

Let us analyse what happens after a sequence of successive collisions. The speed after the  $(n+1)^{\text{th}}$  collision is:

$$\vec{v}_n = L \cdot M^n \cdot \vec{v}_0. \quad (\text{B.16})$$

The analytical computation of (B.16) is very complicated. Therefore, let us introduce the variables  $w_i$  and  $w'_i$ , obtained thanks to the eigenvectors of  $M$ . The eigenvalues of  $M$  are 1 and  $\epsilon$ . We suggest the following eigenvectors:

$$\begin{pmatrix} 1 \\ 1 \end{pmatrix} \quad \text{and} \quad \begin{pmatrix} a((\epsilon-1)m' + 2\epsilon m) + a'(1+\epsilon)m' \\ a'((\epsilon-1)m + 2\epsilon m') + a(1+\epsilon)m \end{pmatrix}, \quad (\text{B.17})$$

in order to perform the following substitution:

$$\vec{v}_i = \begin{pmatrix} 1 & a((\epsilon-1)m' + 2\epsilon m) + a'(1+\epsilon)m' \\ 1 & a'((\epsilon-1)m + 2\epsilon m') + a(1+\epsilon)m \end{pmatrix} \begin{pmatrix} w_i \\ w'_i \end{pmatrix} = C \cdot \vec{w}_i, \quad (\text{B.18})$$

where:

$$\begin{cases} w_i = \frac{(a(1+\epsilon)m - a'((1-\epsilon)m - 2\epsilon m'))v_i - (a'(1-\epsilon)m' - a(1-\epsilon)m' - 2\epsilon m)v'_i}{(a-a')(m+m')(1-\epsilon)} \\ w'_i = \frac{v'_i - v_i}{(a-a')(m+m')(1-\epsilon)} \end{cases}. \quad (\text{B.19})$$

Equation B.14 becomes much simpler:

$$\begin{pmatrix} w_{i+1} \\ w'_{i+1} \end{pmatrix} = \begin{pmatrix} 1 & 0 \\ 0 & \epsilon \end{pmatrix} \begin{pmatrix} w_i \\ w'_i \end{pmatrix}. \quad (\text{B.20})$$

We can then write:

$$\begin{pmatrix} w_n \\ w'_n \end{pmatrix} = \begin{pmatrix} 1 & 0 \\ 0 & \epsilon \end{pmatrix}^n \begin{pmatrix} w_0 \\ w'_0 \end{pmatrix}, \quad (\text{B.21})$$

## Appendix B. Collision-Based Energy Transmission

---

which yields:

$$\begin{cases} w_n = w_0 \\ w'_n = \epsilon^n w'_0 \end{cases} . \quad (\text{B.22})$$

$v_n$  and  $v'_n$  are extracted by injecting (B.19) in (B.22):

$$\begin{cases} (a(1+\epsilon)m - a'((1-\epsilon)m - 2\epsilon m'))v_n - (a'(1-\epsilon)m' - a((1-\epsilon)m' - 2\epsilon m))v'_n \\ = (a(1+\epsilon)m - a'((1-\epsilon)m - 2\epsilon m'))v_0 - (a'(1-\epsilon)m' - a((1-\epsilon)m' - 2\epsilon m))v'_0 , \\ v'_n - v_n = \epsilon^n(v'_0 - v_0) \end{cases} , \quad (\text{B.23})$$

which yields:

$$\begin{aligned} v_n &= \left\{ a[\epsilon^{n+1}(2m + m')(v'_0 - v_0) - \epsilon^n m'(v'_0 - v_0) + (\epsilon + 1)mv_0 + ((1-\epsilon)m' - 2\epsilon m)v'_0] \right. \\ &\quad \left. + a'[\epsilon^n(1+\epsilon)m(v'_0 - v_0) + \epsilon m'(2v_0 - v'_0) - (1-\epsilon)mv_0 - m'v'_0] \right\} / ((1-\epsilon)\Delta a \cdot \Sigma m), \\ v'_n &= \left\{ a'[\epsilon^{n+1}(m + 2m')(v'_0 - v_0) - \epsilon^n m(v'_0 - v_0) - (\epsilon + 1)m'v'_0 - ((1-\epsilon)m - 2\epsilon m')v_0] \right. \\ &\quad \left. + a[\epsilon^n(1+\epsilon)m(v'_0 - v_0) + \epsilon m(v_0 - 2v'_0) + (1-\epsilon)m'v'_0 + mv_0] \right\} / ((1-\epsilon)\Delta a \cdot \Sigma m). \end{aligned} \quad (\text{B.24})$$

For the case where  $a' = 0$ , the results demonstrated by Conus are obtained\*.

### B.1.3 Infinite Series of Collisions

Let us now focus on the behaviour of the series of collisions when  $n \rightarrow \infty$ , keeping in mind that  $\epsilon < 1$ . This implies a known result that will prove very useful:

$$\sum_{i=0}^{\infty} \epsilon^i = \frac{1}{1-\epsilon}. \quad (\text{B.25})$$

---

\*Although a typographic mistake in his thesis says  $(v_0 - v'_0)$  where it should read  $(v'_0 - v_0)$ . The mistake is propagated in his further formulae. The plots are however correct. It is proved wrong because the obtained formula for calculating the time necessary for all the collisions to happen gives an absurd negative time if  $v_0 > v'_0$ , whereas it is the only physical possible configuration for the first collision to happen.

The time for an infinity of collisions to happen  $t_\infty$  is calculated from (B.10), (B.2) and (B.23):

$$\begin{aligned}
 t_\infty &= t_0 + \sum_{i=0}^{\infty} \frac{2(\tilde{v}'_i - \tilde{v}_i)}{(a - a')} = t_0 + \sum_{i=0}^{\infty} \frac{2\epsilon(v_i - v'_i)}{(a - a')} \\
 &= t_0 + \sum_{i=0}^{\infty} \frac{2\epsilon(v_0 - v'_0)\epsilon^i}{(a - a')} = t_0 + \frac{2\epsilon(v_0 - v'_0)}{(a - a')} \sum_{i=0}^{\infty} \epsilon^i \\
 &= t_0 + \frac{2\epsilon(v_0 - v'_0)}{(a - a')} \lim_{i \rightarrow \infty} \frac{(1 - \epsilon^i)}{1 - \epsilon} \\
 &= t_0 + \frac{2\epsilon(v_0 - v'_0)}{(1 - \epsilon)(a - a')}. \tag{B.26}
 \end{aligned}$$

The computation of the value of  $x(t_\infty)$  is more tedious. It starts in the same way as for the speed and time, by rewriting (B.9) and using (B.23):

$$\begin{aligned}
 x(t_\infty) &= x(t_0) + \sum_{i=0}^{\infty} \left[ 2a' \frac{(\tilde{v}'_i - \tilde{v}_i)^2}{(a - a')^2} + 2\tilde{v}'_i \frac{(\tilde{v}'_i - \tilde{v}_i)}{(a - a')} \right] \\
 &= x(t_0) + 2 \sum_{i=0}^{\infty} \left[ a'\epsilon^2 \frac{(v_i - v'_i)^2}{(a - a')^2} + \tilde{v}'_i \epsilon \frac{(v_i - v'_i)}{(a - a')} \right] \\
 &= x(t_0) + 2 \sum_{i=0}^{\infty} \left[ a'\epsilon^2 \frac{(v_0 - v'_0)^2}{(a - a')^2} \epsilon^{2i} + \tilde{v}'_i \epsilon \frac{(v_0 - v'_0)}{(a - a')} \epsilon^i \right] \\
 &= x(t_0) + 2a' \frac{\epsilon^2(v_0 - v'_0)^2}{(a - a')^2} \lim_{i \rightarrow \infty} \frac{1 - \epsilon^{2i}}{1 - \epsilon^2} + 2\epsilon \frac{(v_0 - v'_0)}{(a - a')} \sum_{i=0}^{\infty} (\epsilon^i \tilde{v}'_i) \tag{B.27}
 \end{aligned}$$

Let us express  $\tilde{v}'_i$  in terms of  $w$  and  $w'$ , using (B.2), (B.18) and (B.22):

$$\begin{aligned}
 \tilde{v}'_i &= w_i + \epsilon(a(1 + \epsilon)m + a'((1 - \epsilon)m + 2m'))w'_i \\
 &= w_0 + \epsilon^{i+1}(a(1 + \epsilon)m + a'((1 - \epsilon)m + 2m'))w'_0 \tag{B.28}
 \end{aligned}$$

This yields, after (a lot of) simplification:

$$\begin{aligned}
 x(t_\infty) &= x(t_0) + 2a' \frac{\epsilon^2(v_0 - v'_0)^2}{(a - a')^2} \lim_{i \rightarrow \infty} \frac{1 - \epsilon^{2i}}{1 - \epsilon^2} + 2\epsilon \frac{(v_0 - v'_0)}{(a - a')^2} \frac{K_1 v_0 + K_2 v'_0}{(m + m')(1 - \epsilon^2)} \lim_{i \rightarrow \infty} \frac{1 - \epsilon^i}{1 - \epsilon} \\
 &= x(t_0) + 2a' \frac{(v_0 - v'_0)^2}{(a - a')^2} \frac{\epsilon^2}{1 - \epsilon^2} + 2\epsilon \frac{(v_0 - v'_0)}{(a - a')^2} \frac{K_1 v_0 + K_2 v'_0}{(m + m')(1 - \epsilon^2)(1 - \epsilon)}, \tag{B.29}
 \end{aligned}$$

## Appendix B. Collision-Based Energy Transmission

---

where:

$$K_1 = (a - a')(1 + \epsilon)m + 2\epsilon^2(m + m')a' \quad (\text{B.30})$$

$$K_2 = (a - a')(m' - \epsilon m) - \epsilon^2(m + m')(a + a'). \quad (\text{B.31})$$

The easiest thing to calculate is the speed after an infinite series of collisions. Theoretically, the two particles will reach a state at the instant  $t = t_\infty$  where they behave as a single particle of mass  $(m + m')$  moving at a speed  $v_\infty = v'_\infty$ . Of course, right after that instant, the accelerations  $a$  and  $a'$  will modify that speed as usual. Because  $n \rightarrow \infty$ ,  $\epsilon^n = 0$ , and thus we obtain, from (B.24):

$$v_\infty = \frac{a((1 + \epsilon)mv_0 + ((1 - \epsilon)m' - 2\epsilon m)v'_0) - a'(((1 - \epsilon)m - 2\epsilon m')v_0 + (1 + \epsilon)m'v'_0)}{(1 - \epsilon)(a - a')(m + m')}. \quad (\text{B.32})$$

This relation can be verified by applying  $n \rightarrow \infty$  to the value of  $v_n$  or  $v'_n$  of (B.24). It is observed that both indeed yield the same result.

All the previous results yield the results demonstrated by Conus when  $a' = 0$ . For a more complete modelling of the dynamics of the series of collisions, it is interesting to evaluate the behaviour of the two particles after  $t_\infty$ , or said differently, after the two particles get in permanent contact. Let us perform this through the calculation of the speed. At any time  $t > t_\infty$ , the two particles move together at a speed  $v = v'$  that is altered along time by the action of the forces  $f$  and  $f'$ . The equation for the speed is thus, using (B.32) and (B.26):

$$v|_{t > t_\infty} = v_\infty + \frac{am + a'm'}{(m + m')}(t - t_\infty) = \frac{am + a'm'}{(m + m')}t + \frac{mv_0 + m'v'_0}{(m + m')}. \quad (\text{B.33})$$

Interestingly enough, this result can also be obtained by considering that, from the first collision at time  $t_0$ , the two particles move as a single particle of mass  $(m + m')$  animated by a speed  $v_g$  and under the action of a force  $(f + f')$ . Let us find the initial condition of the speed, which is given by the total quantity of movement divided by the total mass:

$$v_g|_{t=t_0} = \frac{mv_0 + m'v'_0}{(m + m')}. \quad (\text{B.34})$$

Afterwards, the action of the forces alters the speed, which yields:

$$v_g|_{t>t_0} = \frac{mv_0 + m'v'_0}{(m + m')} + \frac{am + a'm'}{(m + m')}t. \quad (\text{B.35})$$

Equations (B.33) and (B.35) prove that  $v|_{t>t_\infty} = v_g|_{t>t_\infty}$ . It is however not possible to calculate the speed of each particle before  $t_\infty$ , nor  $t_\infty$  itself, using the second method. What this result shows is that the speed of the particles at any given time  $t > t_\infty$  does not depend on the coefficient of restitution  $\epsilon$ .

#### B.1.4 Efficiency of Energy Transmission

In addition to the efficiency of a single collision, be it the first or another of the series, it is interesting to evaluate the efficiency  $\eta_{sc}$  of the energy transmission over the span of the infinite series of collisions. Its definition is rather similar to that of the efficiency of a single collision in the sense that it evaluates the increase of kinetic energy of the receiver with respect to the initial kinetic energy of the provider. Yet, it differs from it because the provider and the receiver form a single particle at the end of the series of collisions. Thus, the definition of the efficiency of a series of collisions is:

$$\eta_{sc} = \frac{(m + m')v_\infty^2 - m'v_0'^2}{mv_0^2}, \quad (\text{B.36})$$

which respects  $\eta_{sc} \leq 1$  by definition of the principle the conservation of energy, and can be rewritten as:

$$\eta_{sc} = 1 - \frac{\frac{1}{2}mv_0^2 + \frac{1}{2}m'v_0'^2 - \frac{1}{2}(m + m')v_\infty^2}{\frac{1}{2}mv_0^2} = 1 - {}^R_L E_c. \quad (\text{B.37})$$

The second part of that equation represents the energetic losses during the series of collisions with relation to the initial energy of the provider. It was earlier demonstrated that the evolution of the position of the two particles after the end of the series of collisions is the same as the particles would follow in the theoretical case with  $\epsilon = 0$ . Therefore, the losses due to the series of collisions are independent from the values of  $\epsilon$ . Let us thus calculate the losses for  $\epsilon = 0$ . Using the variable  $k_m$  defined earlier, the relative losses become:

$${}^R_L E_c = \frac{k_m}{1 + k_m} \frac{(v_0 - v_0')^2}{v_0^2}. \quad (\text{B.38})$$

## Appendix B. Collision-Based Energy Transmission

---

This is true for any situation where the series of collisions is complete. In such a situation, we can therefore state that the efficiency of a series of collisions is expressed as:

$$\eta_{sc} = 1 - \frac{k_m}{1 + k_m} \frac{(v_0 - v'_0)^2}{v_0^2}. \quad (\text{B.39})$$

To maximise the efficiency, the mass of the provider should be as large as possible and that of the receiver as small as possible. Similarly, the speed difference between the two particles should be as small as possible.

### B.2 Conclusion

The model developed here describes a rather simple configuration, where the external forces are constant. It could be refined, but this goes beyond the scope of this work, especially so since in our case this model is sufficient.



## C Estimated Performance of Marshall and Rolfe's Design

This section is intended to demonstrate briefly the application of the concepts introduced in the thesis to other devices. The example here is a device such as Marshall and Rolfe describe in their patent [MR13]. All information contained in this appendix is an evaluation and the accuracy of any of the values given cannot be verified. Still, the qualitative remarks about the mechanism show that the proposed methodology is applicable to other systems and permits to rather easily highlight and quantify functional imperfections.

### C.1 Mechanical performance

The functioning principle of this system (Fig. C.1) is based on a principle similar to ours. A step is initiated by deforming the piezoelectric actuator (27). Through a lever (28), it displaces the teathed collar (24). Thus, it releases the ratchet plunger (17) that advances of the length of a step because of the thrust force applied by the spring (23).

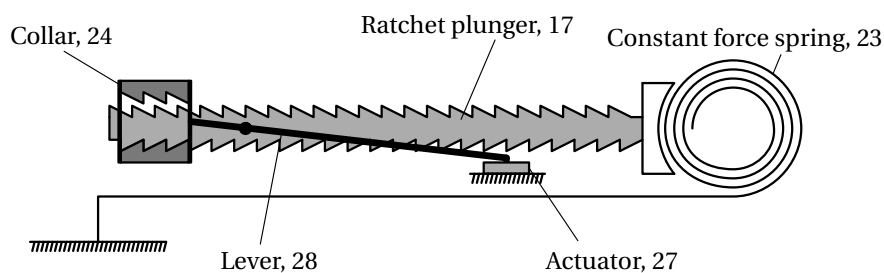


Figure C.1: Functioning principle of Marshall and Rolfe's injection.

As was done in chapter 4, let us evaluate the performance of the movement, excluding the regulating organ. The only material provided for this analysis is the patent, which is of course does not provide any quantitative information. However, it does state that it is mainly

## Appendix C. Estimated Performance of Marshall and Rolfe's Design

---

for insulin cartridges, and there are schematics of the movement (one of which is shown in Fig. C.2, with labels associated to some parts of the mechanism). Let us start with this information.

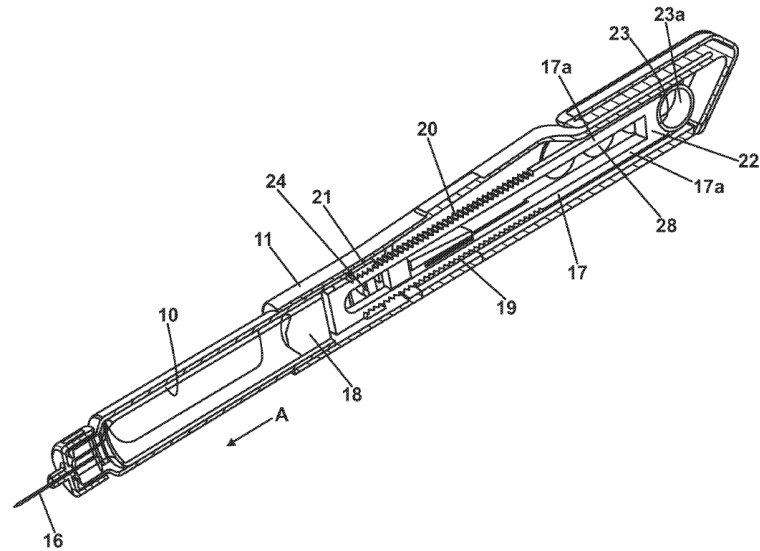


Figure C.2: Cross-section of an embodiment of Marshall and Rolfe's invention [MR13].

Typically, insulin is delivered in up to 1 ml. Such syringes usually have a barrel of about 30 mm long and an internal diameter around 6.5 mm. Thus, let us assume that the maximal usable volume for the movement is a  $10 \times 10 \text{ mm}^2$  by an indefinite length.

The constant force spring (23a) has to fit within this volume. A research in manufacturers' catalogues yields a maximal thrust force  $F_s = 6.41 \text{ N}$  [Spr15]. This value is in the low bracket of injection force values found in other injection pens [ASKY09]. The selected type of spring ensures that the force along the stroke is rather constant, which is a good thing, as was discussed in chapter 4.

The resolution of the system is deduced in a similar way. The so-called ratchet plunger (17) is drawn with 40 teeth, which yields a 75 steps (two per tooth, with five deduced because of the structure of the collar (24)). Therefore, a step has a length of  $l_s = 0.2 \text{ mm}$  and the pitch of the teeth is 0.4 mm. On the drawing, the pitch is twice the height of a tooth which yields  $h_t = 0.2 \text{ mm}$ . The lever used to reduce the required force to initiate a step is drawn with a ratio of about 2.5. The unlocking motion thus consists in the application of a force on a 0.5 mm distance.

Regarding materials, it is hard to guess what the authors plan on using. It might be metal or polymers depending on the choices they make in terms of durability, flexibility, costs, etc.

### C.1.1 Dynamic performance

The dynamic performance of this device is not limited by any part of the mechanics, unlike what is the case in the main case study. This is due to the fact that the whole mechanism is rigidly linked. In other words, the displacement of the collar is entirely dependent on the regulating organ that actually consists in a microcontroller, a battery and a piezoelectric actuator. Because this study is based on assumptions and observation without precise specifications, the dynamic performance is not further investigated.

### C.1.2 Energetic performance

The working principle used in this invention is extremely straight forward. The losses are exclusively located at the interaction between the ratchet surfaces of the plunger and the collar. In addition, the thrust force is considered constant and as a consequence, the mechanical energy factor of a step is the same as the mechanical energy factor on the whole stroke. The friction force is calculated as:

$$F_f = \mu_d \cdot F_s, \quad (C.1)$$

with  $\mu_d$  the dynamic friction factor. Since the work of a force is the integration of its magnitude along a path, we obtain the admitted energy during a step:

$$E_{m,ad} = F_s \cdot l_s, \quad (C.2)$$

and the step trigger energy:

$$E_t = F_f \cdot h_t. \quad (C.3)$$

The relative mechanical energy factor therefore becomes:

$$\eta_{r,m}^* = \frac{E_{m,ad}}{E_t} = \frac{F_s \cdot l_s}{\mu_d \cdot F_s \cdot h_t} = \frac{l_s}{\mu_d \cdot h_t}. \quad (C.4)$$

This is obviously dependent only on the friction factor, the tooth height and the length of a step. It is true if the lever is considered lossless, which means that the friction in the pivots is neglected.

With a friction factor  $\mu_d = 0.1$  similar to that used in our case study, we obtain  $\eta_{r,m}^* = 10$ , which is much lower. It can be explained very simply by the locking angle of the teeth. Because the contact faces are perpendicular to the motion, the friction factor is not attenuated. Of course, this is a secure configuration, but the energy consumption is impaired. Table C.1 summarises

## Appendix C. Estimated Performance of Marshall and Rolfe's Design

the comparable values between the two discussed mechanisms.

Parameter	Description	Value	
		Ours	M & R
Specifications			
$s_o$	Stroke (mm)	50	30
$r_o$	Resolution (mm)	0.4	0.2
$F_s$	Thrust force (N)	40	< 7
Modelled information			
$v_a^{th}$	Theoretical advance speed (mm·s <sup>-1</sup> )	67.4	Unknown
$t_{s,r,m}^*$	True mechanical relative energy factor (—)	22.0	10.0

Table C.1: Comparison of the values between our movement and an embodiment of Marshall and Rolfe's invention.

### C.2 Regulating organ

The question of the regulating organ is a little bit more complicated. First of all because the drawings do not match with any commercially available devices, and by far. Indeed, it was estimated that a displacement of about 0.5 mm is necessary to unlock the teeth and a force around 0.2 N. Yet, the bender piezoelectric actuators suggested in the patent are not a very judicious choice because they struggle at providing both a correct range and an acceptable force for the available volume. The force created by the piezoelectric effect in a bender does two things: it bends the structure to provide a displacement and it provides useful force. The specifications of such actuators are usually given by the force it can provide when not deflected and the maximal applicable deflection (*i.e.* when the deformation force of the bender is equal to the force generated by the piezoelectric effect). It means that a substantial amount of energy is wasted in bending the mechanical structure. Thus in the case at hands, the useful force should be 0.2 N over the 0.5 mm displacement mentioned earlier. Physik Instrumente (PI) is one of the main providers of piezoelectric actuators. Among their bender actuators\*, only one can provide this and it is 45 mm-long, for a width of 11 mm and a thickness of 0.6 mm, which constitutes a poor shape factor and does not match at all the drawings. In addition to an inconvenient shape factor, the driving electronics are slightly complicated due to the high voltage. The price of such actuators (probably around 150 USD/pc.) might also be a drawback.

Another comment about the regulating organ regards the rigid link between its actuator and the escapement. It makes it more complicated to assemble and requires a better accuracy in the manufacturing of the parts, as the manufacturing tolerances pile up. Also, the way it is set

\*<http://www.piceramic.com/product-detail-page/pl112-pl140-103000.html>

up, the mechanism has a resolution of 0.2 mm, but it is actually monostable, in the sense that without electric power, the collar only has one stable position. Therefore, there is a stable step and a transient step. This yields an actual resolution twice as large of 0.4 mm. The energetic and dynamic performance are not analysed because of the uncertainty surrounding the actuator.

The incoherence between the actuator of the regulating organ and the escapement can be caused by mistakes in the estimations, or because the drawings are not an accurate representation of reality. Typically, the teeth would be represented larger than they actually are, but extremely complex manufacturing and industrialisation issues would rise up with teeth smaller than they are currently estimated. Even more so if the actuator of the regulating organ is rigidly connected to the collar.

### C.3 Discussion

This short analysis shows that the device presented in Marshall and Rolfe's pattern has interesting performance but is perfectible. In particular, the constant-force spring is a very good feature, as its spring constant is close to 0, which is an optimal discussed in the thesis. However, the shape of the teeth is not very good because of the perpendicular locking faces. The most critical design flaw is the choice to bind the actuator to the collar rather than having a free mover. This would moreover allow to use the 0.2 mm resolution.

In terms of performance, their movement has a finer resolution than ours, but some design choices make it unusable for higher thrust forces. Still on the topic of large thrust forces, the dimensions of constant-force springs make them less adequate for ours. Both movements, if the same step length is considered, have a relative mechanical energy factor around 20. The mechanical energetic performance of our movement is partly impaired by the collision-based energy transmission, which has an estimated efficiency of 75%. Yet, this loss in energetic performance is balanced by the structural advantages of having a free mover.



# Nomenclature

## Collisions model

<i>Symbol</i>	<i>Unit</i>	<i>Description</i>
$\epsilon$	—	Coefficient of restitution.
$\eta_{fc}$	—	Efficiency of a single collision.
$\eta_{sc}$	—	Efficiency of a series of collisions.
$a$	$\text{m}\cdot\text{s}^{-2}$	Acceleration.
$f$	N	Force.
$k_m$	—	Mass factor.
$m$	kg	Mass.
$t_0$	s	Time of the first collision.
$t_\infty$	s	Time of the last collision.
$u$	—	Speed factor.
$v$	$\text{m}\cdot\text{s}^{-1}$	Speed.
$w$	—	Alternative variable.
$x$	m	Position.

## Regulating organ and actuator

<i>Symbol</i>	<i>Unit</i>	<i>Description</i>
$\delta_b$	mm	Airgap between the back iron yoke and the PMs.

## Nomenclature

---

$\delta_e$	mm	Airgap between the iron yoke and the PMs.
$\Lambda_m$	H	Self-permeance of the magnet.
$\Lambda_{mc}$	H	Mutual permeance of the magnet and coil.
$\mu_r$	—	Relative permeability of the PMs.
$\psi_a$	Wb	Magnetic flux through the coil.
$\Theta_c$	A	Magnetic potential of the coil.
$\Theta_m$	A	Magnetic potential of the magnet.
$B_0$	T	Remanence of the PMs.
$b_h$	mm	Height of the back iron yoke.
$b_w$	mm	Height of the back iron yoke.
$D$	—	Duty cycle of the PWM.
$E_{kin}$	J	Kinetic energy.
$E_{pot}$	J	Potential energy.
$e_b$	mm	Thickness of the back of the iron yoke.
$e_d$	mm	Depth of the iron yoke and the actuator.
$e_h$	mm	Height of the iron yoke.
$e_m$	mm	Thickness of the middle branch of the iron yoke.
$e_t$	mm	Thickness of the outer branches of the iron yoke.
$e_w$	mm	Width of the iron yoke.
$E_{el}$	J	Electrical energy.
$E_{mag}$	J	Magnetic energy.
$E_m$	J	Mechanical energy.
$F_{em}$	N	Electromagnetic force on the mover.
$F_{ext}$	N	External force on the mover.
$i_a$	A	Electric current in the actuator.



$i_b$	A	Battery current.
$K_{Co}$	—	Fill factor of the coil.
$k_{ls}$	$\text{N}\cdot\text{m}^{-1}$	Spring constant of the leaf spring guide of the actuator.
$L_a$	H	Inductance of the actuator.
$m_a$	g	Mass of the mover.
$n_{mh}$	mm	Position of the slot apertures.
$n_h$	mm	Height of the slot aperture of the iron yoke.
$n_t$	mm	Composed position of the slot apertures.
$n_w$	mm	Width of the slot aperture of the iron yoke.
$N$	—	Number of turns of the coil.
$p_h$	mm	Height of the PMs.
$p_w$	mm	Width of the PMs.
$R_a$	$\Omega$	Resistance of the actuator.
$R_H$	$\Omega$	Series resistance of the H-bridge.
$R_i$	$\Omega$	Battery internal resistance.
$r_l$	$\Omega\text{m}^{-1}$	Linear resistivity of the wire.
$R_S$	$\Omega$	Parasitic series resistance.
$S_c$	$\text{mm}^2$	Section of the coil.
$S_w$	$\text{mm}^2$	Section of the wire.
$u_a$	V	Induced voltage of the actuator.
$u_b$	V	Battery output voltage.
$U_i$	V	Battery internal voltage.
$U_l$	V	Voltage applied on the actuator.
$U_{eq}$	V	Battery virtual internal voltage.
$V_a$	$\text{mm}^3$	Volume of the actuator.

## Nomenclature

---

$v_b$	$\text{m}\cdot\text{s}^{-1}$	Speed of a body.
$v_m$	$\text{m}\cdot\text{s}^{-1}$	Speed of the mover.
$w_d$	mm	Wire diameter.
$w_l$	mm	Wire length.
$x_u$	mm	Unlocking position.
$x$	mm	Position of the mover.

## Requirements and quantifiers

<i>Symbol</i>	<i>Unit</i>	<i>Description</i>
$\eta_a^*$	—	Rechargeable energy factor.
$\eta_d^*$	—	Disposable energy factor.
$\eta_r^*$	—	Relative energy factor.
$\eta_{d,m}^*$	—	Mechanical disposable energy factor.
$\eta_{r,m}^*$	—	Mechanical relative energy factor.
${}^t\eta_a^*$	—	Rechargeable true energy factor.
${}^t\eta_d^*$	—	Disposable true energy factor.
${}^t\eta_r^*$	—	Relative true energy factor.
${}^tE_{out}$	J	Output energy required.
$a_e$	$\text{m}\cdot\text{s}^{-2}$	External parasitic acceleration.
$E_{in,a}$	J	Input rechargeable energy.
$E_{in,d}$	J	Input disposable energy.
$E_{in}$	J	Input energy.
$E_{out}$	J	Output energy.
$F_{rec}$	N	Maximal recharge force.
$F_l$	N	Resistive force of the load.
$F_f$	N	Friction force on the rail.

$m_{tot}$	g	Total weight of the movement.
$m_l$	g	Mass of the load.
$r_o$	mm	Resolution of the output.
$s_o$	mm	Stroke of the output.
$T_{rec}$	s	Maximal recharge time.
$T_{rep}$	s	Maximal time for expendables replacement.
$v_o^{max}$	mm·s <sup>-1</sup>	Maximal average speed of the output.
$v_o^{res}$	mm·s <sup>-1</sup>	Average speed resolution.
$V_{tot}$	mm <sup>3</sup>	Total volume of the movement.
$v_o$	mm·s <sup>-1</sup>	Advance speed of the output.

**Transmission & escapement, models and design parameters**

<i>Symbol</i>	<i>Unit</i>	<i>Description</i>
$\alpha_c$	°	Critical angle for stability.
$\alpha$	°	Angle of the locking face of the teeth.
$\beta$	°	Angle of the rear face of the teeth.
$v_a^{th}$	mm·s <sup>-1</sup>	Theoretical advance speed.
$t_*$	s	Local time variable.
$\mu_d$	—	Dynamic friction factor.
$\mu_s$	—	Static friction factor.
$\frac{R}{L}E_c$	—	Relative losses due to a series of collisions.
${}_L E_{rm}$	J	Losses in the release mechanism.
${}_L E_{ro}$	J	Energy consumed in the regulating organ.
${}_L E_{rs}$	J	Energy consumed in the recoil spring.
${}_L E_c$	J	Losses in the collision-based energy transmission.
${}_L E_c$	—	Losses due to a series of collisions.

## Nomenclature

---

${}_L E_l$	J	Friction losses at the interface rail–blocker.
$d_{block}$	mm	Distance between two consecutive blockers.
$d_b$	mm	Distance between the blockers.
$E_d$	J	Mechanical energy required to displace the blocker.
$E_e$	J	Electrical energy required to trigger a step.
$E_{\mathcal{L},def}$	J	Deformation energy of an $\mathcal{L}$ .
$E_{ul,b}$	J	Mechanical energy necessary to unlock the blocker.
$E_{k,trig}$	J	Step trigger kinetic energy.
$E_{k,ul}$	J	Kinetic energy required to unlock the blocker.
$E_{m,ad}$	J	Admitted mechanical energy for a step.
$E_{m,in}$	J	Kinetic energy required to trigger a step.
$F_1$	N	Reaction force in the leaf spring stage.
$F_2$	N	Reaction force in the leaf spring stage.
$F_{lock}$	N	Escapement locking force.
$f_{steps}$	Hz	Number of steps per second.
$F_{ul}$	N	Unlocking force on the blocker.
$F_f$	N	Resistive force on the rail.
$F_h$	N	Holding force.
$F_r$	N	Recoil force on a blocker.
$F_s$	N	Thrust force.
$F_{ul,A}$	N	Unlocking force on the release mechanism.
$F_{ul}$	N	Unlocking force on the blocker.
$h_t$	mm	Height of a tooth.
$I_{\mathcal{L}}$	kg·m <sup>2</sup>	Moment of inertia of an $\mathcal{L}$ .
$k_{\mathcal{L}}$	N·m <sup>-1</sup>	Spring constant of an $\mathcal{L}$ .

$k_r$	$\text{N}\cdot\text{m}^{-1}$	Spring constant of a recoil spring.
$k_s$	$\text{N}\cdot\text{m}^{-1}$	Spring constant of the main spring.
$l_{\mathcal{L}}^*$	—	Length ratio of the $\mathcal{L}$ .
$l_s$	mm	Length of a step.
$l_t$	mm	Length of a tooth.
$l_{\mathcal{L},b}$	mm	Length of a leg of an $\mathcal{L}$ .
$l_{\mathcal{L},m}$	mm	Length of a leg of an $\mathcal{L}$ .
$l_{s,f}$	mm	Free length of the main spring.
$l_{s,p}$	mm	Loaded length of the main spring.
$m_b$	g	Mass of a blocker.
$m_r$	g	Mass of the rail.
$m_{\mathcal{L},e}$	g	Equivalent mass of an $\mathcal{L}$ .
$m_{b,e}$	g	Equivalent mass of a blocker.
$n_{block}$	—	Number of blockers in the escapement.
$n_{steps}$	mm	Number of steps.
$p_t$	mm	Pitch of the repetition of the teeth.
$S$	—	Safety factor on the durations.
$T_a$	s	Main cycle duration.
$T_d$	s	Mover rising duration.
$T_h$	s	Mover holding duration.
$T_m$	s	Rail moving duration.
$T_p$	s	Mover return duration.
$T_r$	s	Blocker return duration.
$v_a$	$\text{mm}\cdot\text{s}^{-1}$	Advance speed of the output.
$W_{F,lock}$	J	Work of the holding force.

## Nomenclature

---

$W_{f,r}$	J	Work of the recoil force.
$W_{F_b,r}$	J	Work of the friction forces on the bearings of the rail.
$w$	mm	Position of the output.
$x_1$	N	Horizontal position of a leaf spring in the stage.
$x_2$	N	Horizontal position of a leaf spring in the stage.
$x_b$	mm	Displacement of a blocker.
$x_{\mathcal{L},A}$	mm	Deformation of an $\mathcal{L}$ .
$x_{b,0}$	mm	Recoil of the blocker at rest.
$x_{b,m}$	mm	Maximal recoil of a blocker.
$z_1$	N	Vertical position of a leaf spring in the stage.
$z_2$	N	Vertical position of a leaf spring in the stage.

# Bibliography

- [AA93] Randy E. Armbruster and Peter Affolter. *Portable Hand-held Power Assister Device*, 1993. US Patent 5,269,762, filed Dec. 14, 1993.
- [All81] Eugene E. Allen. *Instrument for transfusion of blood*, 1881. US 249,285, filed Nov. 8, 1881.
- [Ant15] Anteis. Injection system - user manual. [http://www.anteis.com/Pdf/Anteis\\_Injection\\_System\\_Manual.pdf](http://www.anteis.com/Pdf/Anteis_Injection_System_Manual.pdf), 2015. [Online; accessed 7-September-2015].
- [ASKY09] Tetsuo Asakura, Haruyoshi Seino, Mari Kageyama, and Noriaki Yohkoh. Evaluation of Injection Force of Three Insulin Delivery Pens. *Expert Opinion on Pharmacotherapy*, 10(9):1398–1393, 2009.
- [Auv15] Christophe Bruno Auvigne. *Electrical and Magnetical Modeling of Inductive Coupled Power Transfer Systems*. PhD thesis, École polytechnique fédérale de Lausanne, 2015.
- [Bar98] Jo Ellen Barnett. *Time's Pendulum: From Sundials to Atomic Clocks, the Fascinating History of Timekeeping and How Our Discoveries Changed the World*. Plenum Press, 1998.
- [BCA<sup>+</sup>15] Emanuele Bertarelli, Alice Colnago, Raffaele Ardito, Gabriele Dubini, Alberto Corigliano, and Politecnico Milano. Modelling and Characterization of Circular Microplate Electrostatic Actuators for Micropump Applications. In *16th International Conference on Thermal, Mechanical, Multi-Physics Simulation and Experiments in Microelectronics and Microsystems*, 2015.
- [Ber11] Hans Bernhard. *Design Methodology and Innovative Device Concept for Acoustic Hearing Implants*. PhD thesis, École polytechnique fédérale de Lausanne, 2011.
- [BGP13] Romain Besuchet, Alexandre Gabella, and Yves Perriard. Design of a miniature short-stroke constant-force linear actuator. In *The 9th International Symposium on Linear Drives for Industry Applications (LDIA2013)*, 2013.

## Bibliography

---

- [Blo86] Anders Blomberg. *Injection Device*, 1986. US Patent 4,617,016, filed Oct. 14, 1986.
- [Bru04] Eric Bruton. *The History of Clocks & Watches*. Chartwell Books, reprinted edition, 2004.
- [CD65] Cecil Clutton and George Daniels. *Watches*. Viking Press, revised edition, 1965.
- [Ced15] Cedrat. Design solutions for electrical engineering. <http://www.cedrat.com/index.php>, 2015. [Online; accessed 30-September-2015].
- [Con07] Thierry Conus. *Conception et optimisation multicritère des échappements libres pour montres-bracelets mécaniques*. PhD thesis, École polytechnique fédérale de Lausanne, 2007.
- [COS15] COSC. Contrôle officiel suisse des chronomètres. <http://www.cosc.ch/>, 2015. [Online; accessed 3-August-2015].
- [Dan81] George Daniels. *Watchmaking*. Philip Wilson Publishers Ltd., London, 2011 revised edition, 1981.
- [Deh04] Bruno Dehez. *Elaboration et application d'une approche multidisciplinaire pour la conception d'un actionneur électrique à rotor sphérique*. PhD thesis, Université catholique de Louvain, 2004.
- [FDG<sup>+</sup>12] Félix-Antoine Fortin, François-Michel De Rainville, Marc-André Gardner, Marc Parizeau, and Christian Gagné. DEAP: Evolutionary algorithms made easy. *Journal of Machine Learning Research*, 13:2171–2175, jul 2012.
- [Fis11] Bryan R. Fischer. *Mechanical Tolerance Stackup and Analysis*. CRC Press, Boca Raton, second edition, 2011.
- [Flu10] Markus Fluckiger. *Sensorless Position Control of Piezoelectric Ultrasonic Motors: a Mechatronic Design Approach*. PhD thesis, École polytechnique fédérale de Lausanne, 2010.
- [Gal15] Galderma. Restylane injector. <http://www.q-medpractitioner.com/International/Restylane/Product-Range/Needles-and-Injection-Devices/Restylane--Injector/>, 2015. [Online; accessed 7-September-2015].
- [GCL08] Mitsuo Gen, Runwei Cheng, and Lin Lin. Multiobjective Genetic Algorithms. In Rajkumar Roy, editor, *Network Models and Optimization: Multiobjective Genetic Algorithm Approach*, chapter 1, pages 1–47. Springer, London, 2008.



- [Hea02] Mark V. Headrick. Origin and evolution of the anchor clock escapement. *IEEE Control Systems Magazine*, pages 41–52, 2002.
- [Hen01] Simon Henein. *Conception des guidages flexibles*. PPUR, 2001.
- [HGG74] Charles Huguenin, S. Guye, and M. Gauchat. *Echappements et moteurs pas-à-pas*. Fédération des Ecoles Techniques de Suisse (FET), Neuchâtel, 1974.
- [HH14] Donghyun Hwang and Toshiro Higuchi. A Rotary Actuator Using Shape Memory Alloy (SMA) Wires. *Transactions on Mechatronics*, 19(5):1625–1635, 2014.
- [HST10] Toshiro Higuchi, Koichi Suzumori, and Satoshi Tadokoro (Eds.). *Next-Generation Actuators Leading Breakthroughs*. Springer, London, 2010.
- [Jan04] Hartmut Janocha (Ed.). *Actuators: basics and applications*. Springer, Berlin Heidelberg, 2004.
- [Juv15] Juvaplus. Juvapplus, injection system. <http://www.juvapplus.com/>, 2015. [Online; accessed 7-September-2015].
- [MBC<sup>+</sup>10] Mark W. McBride, David A. Boger, Robert L. Campbell, Gregory P. Dillon, Stephen A. Hambric, Robert F. Kunz, Boris Leschinsky, Thomas M. Mallison, James P. Runt, and Justin M. Walsh. *Heart Assist Device with Expandable Impeller Pump*, 2010. US Patent 7,841,976 B2, issued Nov. 30, 2010.
- [Mil47] Willis I. Milham. *Time & Timekeepers*. The MacMillan Company, 1947.
- [Mit96] Melanie Mitchell. *An introduction to genetic algorithms*. A Bradford Book The MIT Press, Cambridge, Massachusetts, 1996.
- [MR13] Jeremy Marshall and Steven M. G. Rolfe. *Electrically Actuated Injector*, 2013.
- [PBF07] Gerhard Pahl, Wolfgang Beitz, Joerg Feldhusen, and Karl-Heinz Grote. *Engineering Design - A Systematic Approach*. Springer, 3rd editio edition, 2007.
- [PK14] Thomas Pyzdek and Paul Keller. *The Six Sigma Handbook*. McGraw-Hill Professional, fourth edi edition, 2014.
- [Pri15] Primequal. Primequal — pharamceutical pre-filled. [http://www.primequal.com/pha\\_pref.php](http://www.primequal.com/pha_pref.php), 2015. [Online; accessed 7-September-2015].
- [RE95] Norbert F. M. Roozenburg and Johannes Eekels. *Product Design: Fundamentals and Methods*. Wiley, 1995.

## Bibliography

---

- [RMB<sup>+</sup>14] Leopoldo Rossini, Stefan Mingard, Alexis Boletis, Eugenio Forzani, Emmanuel Onillon, and Yves Perriard. Rotor design optimization for a reaction sphere actuator. *IEEE Transactions on Industry Applications*, 50(3):1706–1716, 2014.
- [RNYS14] Gianluca Rizzello, David Naso, Alexander York, and Stefan Seelecke. Modeling, Identification, and Control of a Dielectric Electro-Active Polymer Positioning System. *IEEE Transactions on Control Systems Technology*, 23(2):632–643, 2014.
- [SCP15] D Shi, Y Civet, and Y Perriard. Design and Optimization of Piezoelectric Actuated Plate Eigenmodes for Workpiece Transportation. In *2015 IEEE International Conference on Advanced Intelligent Mechatronics (AIM)*, pages 1265–1270, Busan, Korea, 2015.
- [SEK97] Mark T. Smith, James W. Ellis, and Gerald P. Keogh. *Electronic Syringe*, 1997. US Patent 5,690,618, filed Nov. 25, 1997.
- [Spr15] Vulcan Spring. Conforce constant force springs. <http://www.vulcanspring.com/conforce-constant-force-springs>, 2015. [Online; accessed 01-October-2015].
- [tIDEW15a] WikID, the Industrial Design Engineering Wiki. Function analysis. [http://www.wikid.eu/index.php/Function\\_analysis](http://www.wikid.eu/index.php/Function_analysis), 2015. [Online; accessed 8-September-2015].
- [tIDEW15b] WikID, the Industrial Design Engineering Wiki. Phase model. [http://www.wikid.eu/index.php/Phase\\_model](http://www.wikid.eu/index.php/Phase_model), 2015. [Online; accessed 14-September-2015].
- [Tra50] Gerald O. Transue. *Automatic Injector for Hypodermic Needles*, 1950. US Patent 2,664,086, filed Aug. 15, 1950.
- [VBP<sup>+</sup>11] Michel Vermot, Philippe Bovay, Damien Prongué, Sébastien Dordor, and Vincent Beux. *Traité de construction horlogère*. Presses polytechniques universitaires romandes, 1st edition, 2011.
- [VCFS12] Nicole Viola, Sabrina Corpino, Marco Fioriti, and Fabrizio Stesina. Functional Analysis in Systems Engineering : Methodology and Applications. In Boris Cogan, editor, *Systems Engineering - Practice and Theory*, chapter 3, pages 71–96. InTech, 2012.
- [Wik15] Wikipedia. Quartz clock — wikipedia, the free encyclopedia. [https://en.wikipedia.org/w/index.php?title=Quartz\\_clock&oldid=678920506](https://en.wikipedia.org/w/index.php?title=Quartz_clock&oldid=678920506), 2015. [Online; accessed 3-August-2015].
- [ZC09] Z.Q. Zhu and X. Chen. Analysis of an E-Core Interior Permanent Magnet Linear Oscillating Actuator. *IEEE Transactions on Magnetics*, 45(10):4384–4387, 2009.

- [Zha11] Chunsheng Zhao. *Ultrasonic Motors*. Springer, Berlin Heidelberg, 2011.



# Curriculum Vitae

Romain BESUCHET

Born March 23, 1988

Swiss Citizen

romain.besuchet@alumni.epfl.ch

## Studies and professional experience

- 2011 - 2015 Teaching assistant and PhD student at the Integrated Actuators Laboratory (LAI), École polytechnique fédérale de Lausanne, Switzerland
- 2010 - 2011 Master project, Zhejiang University, Hangzhou, PR China
- 2009 - 2011 Master of Science in Microengineering, École polytechnique fédérale de Lausanne, Switzerland
- 2006 - 2009 Bachelor of Science in Microengineering, École polytechnique fédérale de Lausanne, Switzerland
- 2003 - 2006 Scientific High School, CESSNOV Yverdon-les-Bains, Switzerland

## Patent

- Romain Besuchet, Yves Perriard, and Bernard-Pierre Legrand. *Injection Device*, 2015. US Patent App. 2015/0005708 A1, filed Jan. 1, 2015.

## Publications

- Romain Besuchet, Christophe Auvigne, Dan Shi, Christophe Winter, Yoan Civet, Yves Perriard. Optimisation of an inductive power transfer structure. In *Journal of International Conference on Electrical Machines and Systems (JICEMS)*, Volume 2, Number 3, September 2013.

- Romain Besuchet, Alexandre Gabella, Yves Perriard. Design of a miniature short-stroke constant-force linear actuator. In *Applied Mechanics and Materials (AMM)*, Volume 416-417, September 2013.
- Romain Besuchet, Yoan Civet, and Yves Perriard. Influence of manufacturing tolerances on the performance of an electronically-controlled linear escapement. In *The 10th International Symposium on Linear Drives for Industry Applications (LDIA2015)*, July 2015.
- Romain Besuchet, Yoan Civet, and Yves Perriard. Study of the efficiency of an electronically-controlled linear escapement. In *Advanced Intelligent Mechatronics, IEEE/ASME International Conference on (AIM 2015)*, July 2015.
- Romain Besuchet, Yoan Civet, Yves Perriard. A novel electronically-controlled linear escapement mechanism. In *17<sup>th</sup> International Conference on Electrical Machines and Systems (ICEMS 2014)*, October 2014.
- Romain Besuchet, Yves Perriard. Optimisation of the mover kinetic energy of a miniature linear actuator. In *17<sup>th</sup> International Conference on Electrical Machines and Systems (ICEMS 2014)*, October 2014.
- Dan Shi, Christophe Auvigne, Romain Besuchet, Christophe Winter, Yoan Civet, Yves Perriard. Optimisation of an inductive power transfer structure. In *16<sup>th</sup> International Conference on Electrical Machines and Systems (ICEMS 2013)*, October 2013.
- Romain Besuchet, Alexandre Gabella, Yves Perriard. Design of a miniature short-stroke constant-force linear actuator. In *The 9<sup>th</sup> International Symposium on Linear Drives for Industry Applications (LDIA2013)*, July 2013.

"It works! It works! I finally invented something that works!"

*Emmett Lathrop « Doc » Brown, Ph.D.*